Journal of Ophthalmology

Lymphatic and Blood Vessels in the Eye: Physiology, Health, and Disease

Guest Editors: Yasuaki Hata, Ofra Benny, Claus Cursiefen, and Shintaro Nakao

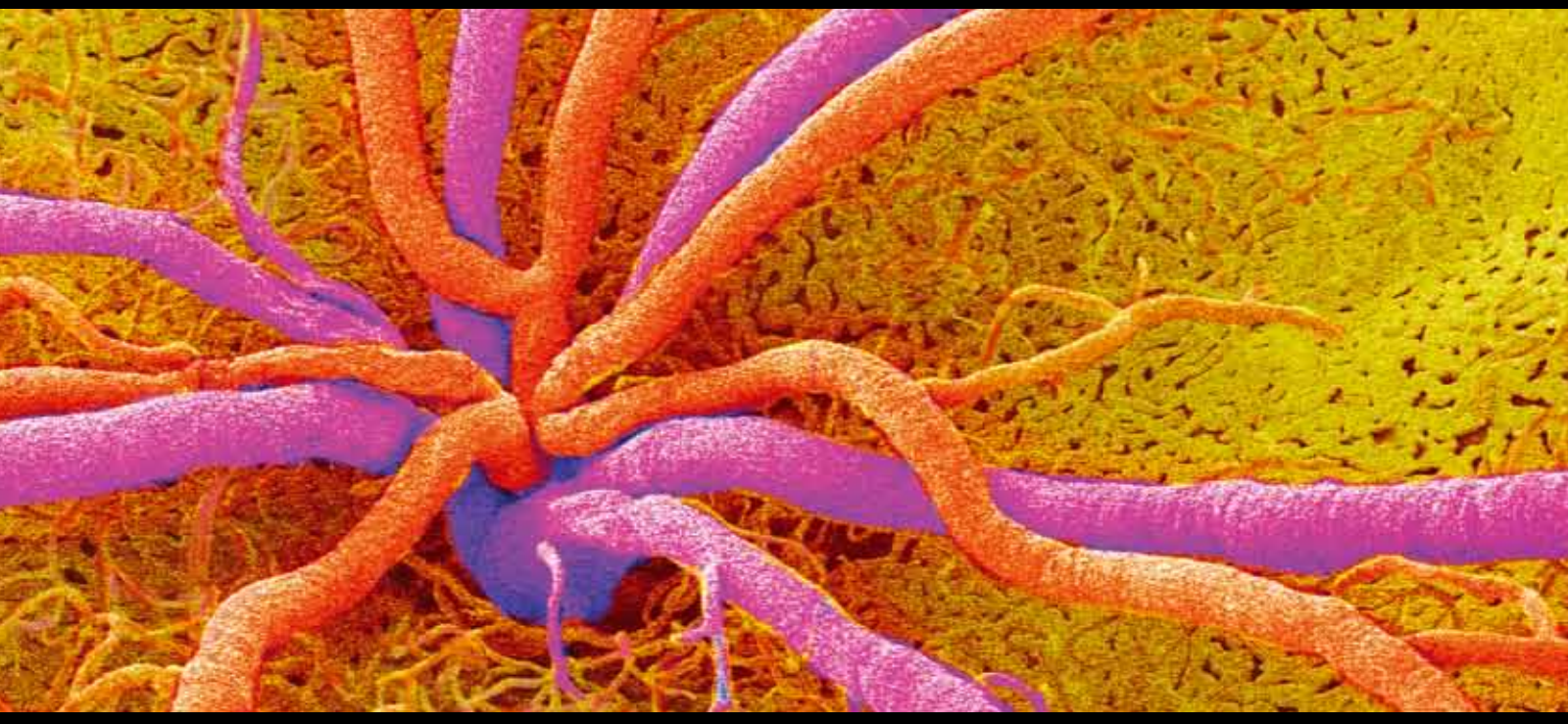

Lymphatic and Blood Vessels in the Eye: Physiology, Health, and Disease

Journal of Ophthalmology

Lymphatic and Blood Vessels in the Eye: Physiology, Health, and Disease

Guest Editors: Yasuaki Hata, Ofra Benny, Claus Cursiefen, and Shintaro Nakao

Editorial Board

Contents

Hindawi Publishing Corporation
Journal of Ophthalmology
Volume 2012, Article ID 953187, 6 pages
doi:10.1155/2012/953187

Research Article

Conjunctival Lymphatic Response to Corneal Inflammation in Mice

Tatiana Ecoiffier, Anna Sadovnikova, Don Yuen, and Lu Chen

Center for Eye Disease and Development, Program in Vision Science, and School of Optometry, University of California, Berkeley, CA 94720, USA

Correspondence should be addressed to Lu Chen, chenlu@berkeley.edu

Received 14 September 2011; Revised 7 November 2011; Accepted 8 November 2011

Academic Editor: Shintaro Nakao

Due to its unique characteristics, the cornea has been widely used for vascular research. However, it has never been studied whether lymphatic vessels in the conjunctiva, its neighboring tissue, are affected by corneal lymphangiogenesis (LG). The purpose of this study was to investigate whether the distribution pattern of conjunctival lymphatic vessels changes during LG using a standardized two-suture placement model. Our data from immunofluorescent microscopic studies demonstrate, for the first time, that conjunctival lymphatic vessels were more distributed in the nasal side under both normal and inflamed conditions. Additionally, under the inflamed condition, conjunctival lymphatic vessels showed a higher density and more branching points, indicating that LG occurs in the conjunctiva in response to corneal inflammation. This study not only provides novel insights into lymphatic events in the ocular surface but also offers new guidelines for developing therapeutic strategies to treat lymphatic diseases at related sites.

1. Introduction

Lymphangiogenesis (LG) has emerged as a new field to understand the fundamental mechanisms of a wide spectrum of physiological and pathological conditions. Lymphatic network penetrates most tissues in the body and plays critical role in many functions, which include immune responses, fat and vitamin absorption, and body fluid regulation. Numerous diseases and conditions are therefore associated with lymphatic dysfunction, such as inflammatory diseases, transplant rejection, cancer metastasis, autoimmune diseases, and lymphedema [1–6]. Unlike blood vessels, lymphatics are not easily visible. However, the recent identification of several lymphatic-specific markers, such as lymphatic vessel endothelial hyaluronan receptor-1 (LYVE-1), vascular endothelial growth factor receptor-3 (VEGFR-3), and Prospero homeobox protein 1 (Prox1) has allowed scientists to further study LG mechanisms [2, 7–9]. The cornea has been a model of choice for LG investigation due to its unique characteristics [10–12]. As the forefront medium in the passage of light to the retina, it is transparent by nature and devoid of any vasculatures. Nevertheless, its neighboring tissue, the conjunctiva, has a rich supply of both blood and lymphatic vessels [12]. As a major component of the immune reflex arc [4], the lymphatic channel facilitates the trafficking of antigen-presenting cells from the peripheral tissue (e.g., ocular surface) to draining lymph nodes. It therefore provides a therapeutic target in immunogenic disorders such as corneal transplant rejection [13–16].

While most of the previous studies on lymphatic research in the ocular surface have focused on the cornea, to date, it still remains largely unknown how conjunctival lymphatic vessels are distributed and whether they respond to pathological stimulations at the cornea. Using a standardized two-suture placement model for corneal inflammation [17], we herein provide the first evidence showing a nasal dominant distribution of lymphatic vessels in the conjunctiva under both normal and inflamed conditions. Moreover, we report a novel finding that corneal inflammation not only induces LG at the site, but also in the neighboring tissue of the conjunctiva. These results offer new insights into ocular surface anatomy and pathogenesis, which are also important

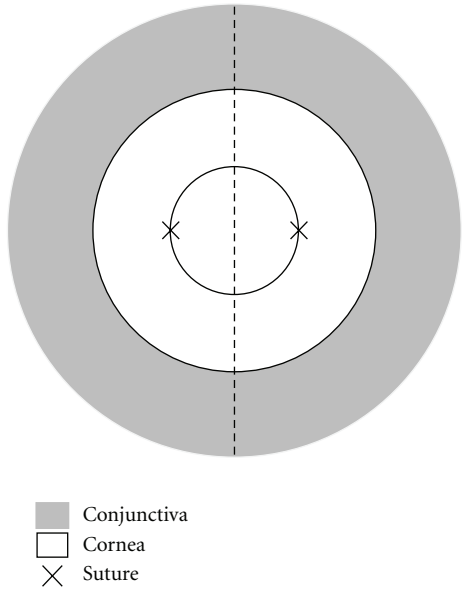

Figure 1: Schematic picture illustrating the suture placement method used to compare the nasal and temporal distributions of vessels. Two sutures were placed at 3 and 9 o'clock of the cornea, respectively. Outer grey area: conjunctiva; Middle white circle: cornea; Inner circle: demarcation of the central cornea with the trephine where sutures were placed. Dashed line: demarcation between the nasal and temporal side.

for developing more effective therapeutic strategies to treat relevant diseases.

2. Methods

2.1. Animal. 6 to 8-week-old male BALB/c (Taconic Farms, Germantown, NY) were used for the experiments. All mice were treated according to ARVO Statement for the Use of Animals in Ophthalmic and Vision Research, and all protocols were approved by the Animal Care and Use Committee, University of California, Berkeley. Mice were anesthetized using a mixture of ketamine, xylazine, and acepromazine (50 mg, 10 mg, and 1 mg/kg body weight, resp.) for each surgical procedure.

2.2. Corneal Suture Placement. Our standard two-suture placement model was used to induce corneal inflammation as described previously [17]. Briefly, to appreciate the nasal versus temporal distributions of the vessels, two diametrically opposed 11–0 nylon sutures (AROSurgical, Newport Beach, CA) were placed at 3 pm and 9 pm of the cornea following a demarcation of a 1.5 mm trephine (Figure 1). Two weeks later, perilimbal bulbar conjunctivae (defined as a ring area 0.8 mm distal to the limbal vasculatures) were collected for immunofluorescent microscopic studies. The experiments were repeated twice with 7 mice in the normal and sutured group, respectively.

2.3. Immunofluorescent Microscopic Studies. The experiments were performed according to our standard protocol [17–20]. Briefly, freshly excised tissues, labeled at 6 pm for orientation, were fixed in acetone for immunofluorescent staining. Nonspecific staining was blocked with 10% donkey serum and 2% BSA. The samples were stained overnight with purified rabbit anti-mouse LYVE-1 antibody (1 : 200 dilution; Abcam, Cambridge, MA). After thorough washings in PBS, samples were incubate with a rhodamine conjugated donkey anti-rabbit secondary antibody (1 : 200 dilution; Jackson ImmunoResearch, West Grove, PA) for 2 hours at room temperature. Samples were covered with Vector Shield mounting medium (Vector Laboratories, Burlingame, CA) and examined by an epifluorescence deconvolution microscope (AxioImager M1, Carl Zeiss AG, Gottingen, Germany).

2.4. Vascular Quantification. Lymphatic density in the perilimbal bulbar conjunctival area was graded and analyzed using the NIH Image J software, as described previously [21]. Basically individual lymphatic vessels in the defined area were highlighted and added together to generate a density score measured in pixels for each sample analyzed. The nasal and temporal sides were divided by a midline across 6 and 12 o'clock (Figure 1).

2.5. Statistical Analysis. Data are expressed as the mean ± SEM. The statistical significance of the difference between each group was evaluated using student t test with GraphPad Prism software (GraphPad Software, Inc., La Jolla, CA). $P < 0.05$ was considered significant.

3. Results

3.1. Conjunctival Lymphatic Vessels Observe a Nasal Dominant Distribution under Normal Condition. We first set to

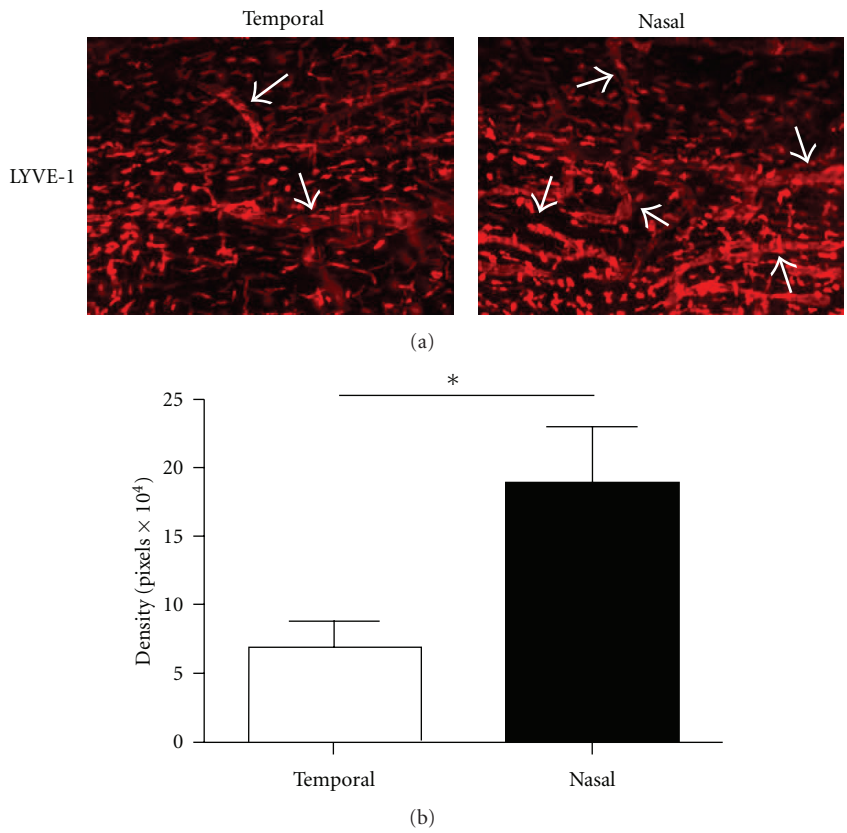

Figure 2: Comparison of lymphatic distribution in the nasal versus temporal side of normal conjunctiva. (a) Representative immunofluorescent micrographs demonstrating that lymphatic vessels were more prominent in the nasal side. LYVE-1: red; Original Magnification: ×50. (b) Summary of repetitive experiments.* $P < 0.05$.

investigate normal distribution of lymphatic vessels in the conjunctiva using a specific antibody against the lymphatic marker LYVE-1. Our results from the immunofluorescent microscopic studies confirmed that in the normal setting, the conjunctiva was endowed with lymphatic vessels. Surprisingly, it was also found that these vessels were not evenly distributed around the clock. As shown in Figure 2(a), conjunctival lymphatic vessels were present more frequently in the nasal side. The results from repetitive studies were summarized in Figure 2(b) ($P < 0.05$).

3.2. Conjunctival Lymphatic Density is Increased during Corneal Inflammation. We next examined whether conjunctival lymphatic vasculatures were affected by corneal inflammation using the two-suture placement model as previously described [17] and further illustrated in Figure 1. This particular model with two equally placed sutures allowed us to perform a precise evaluation between the nasal and temporal sides of the ocular surface. As shown in Figure 3(a), a significant increase of lymphatic vessels was observed in the conjunctiva after the inflammatory stimulation in the cornea. Summarized data from repetitive experiments were presented in Figure 3(b) ($P < 0.05$).

3.3. Conjunctival Lymphatic Vessels Maintain the Nasal Polarity during Corneal Inflammation. As we have observed a nasal dominance in lymphatic vessels distribution in normal conjunctiva, we next determined whether this pattern was preserved during corneal inflammation. As shown in Figure 4(a), this nasal dominant arrangement was still maintained 2 weeks after corneal suture placement. The results from repetitive studies were summarized in Figure 4(b) ($P < 0.05$).

3.4. Conjunctival Lymphatic Vessels Demonstrate More Branching Points in the Nasal Side during Corneal Inflammation. To further characterize the novel findings on increased conjunctival lymphatic density during corneal inflammation, we also examined the number of lymphatic branching points between normal and inflamed condition at both nasal and temporal sides. Our results showed a significant increase of lymphatic branching points in the conjunctiva of the sutured cornea compared to the normal condition. Moreover, it was found that this increase was largely due to an increase of branching points in the nasal than in the temporal side (Figures 5(a) and 5(b), $P < 0.05$).

4. Discussion

In this study, we present novel findings that are important for our understanding of lymphatic vessels in the ocular surface, which include both the cornea and the conjunctiva. Our

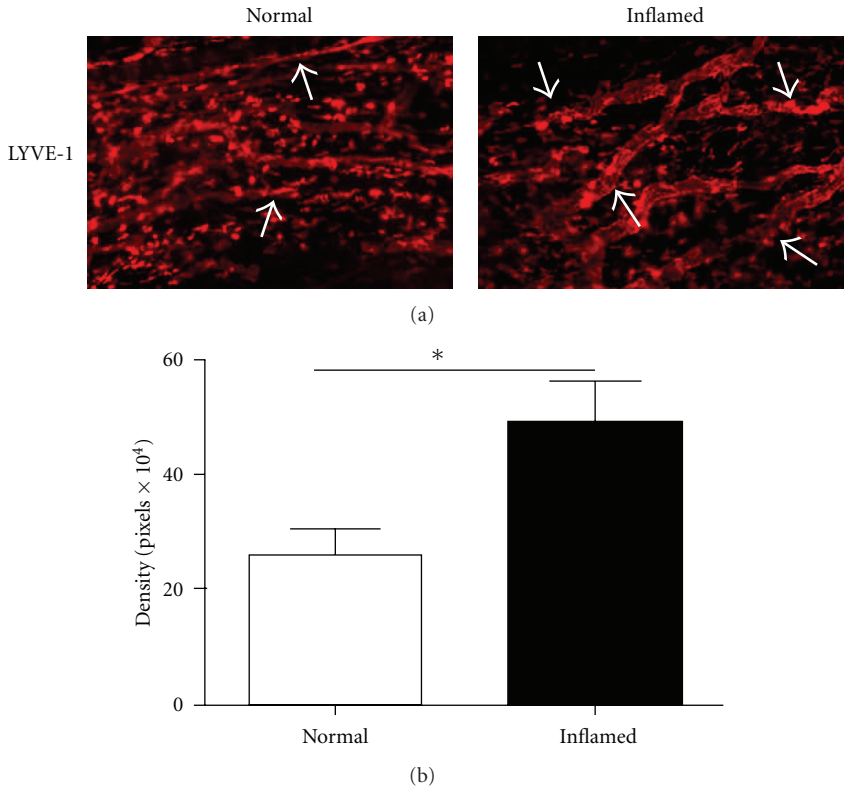

Figure 3: Comparison of lymphatic distribution in the conjunctiva between normal and inflamed conditions. (a) Representative immunofluorescent micrographs illustrating more lymphatic vessels in the conjunctiva of suture-induced inflamed cornea. LYVE-1: red. Original magnification: ×50. (b) Summary of repetitive experiments. $^*P < 0.05$.

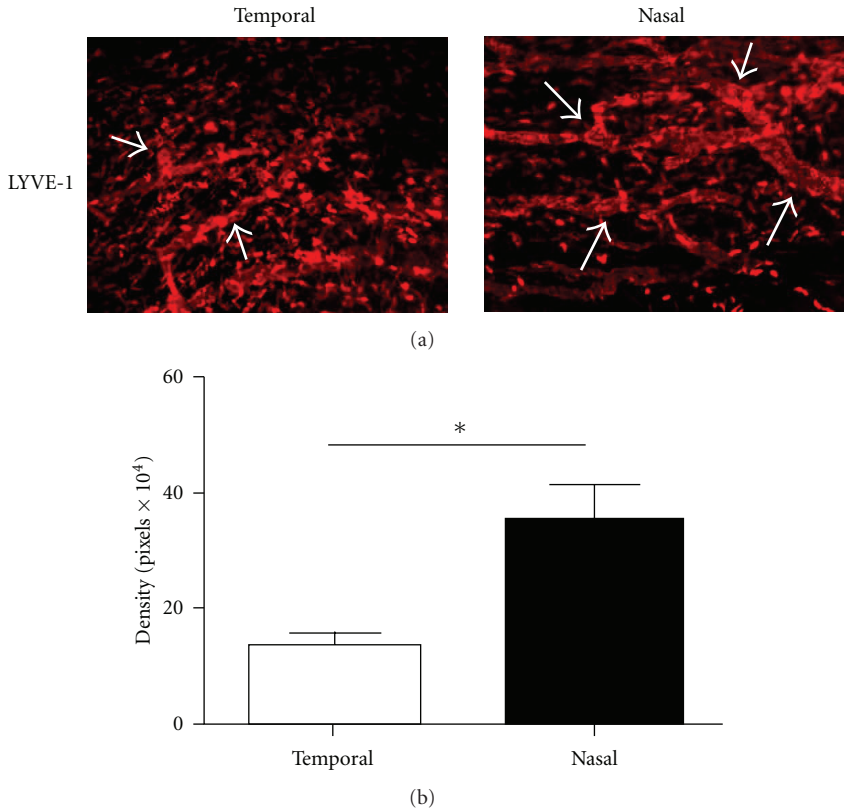

Figure 4: Comparison of conjunctival lymphatic distribution in the nasal versus temporal side of the sutured cornea. (a) Representative immunofluorescent micrographs demonstrating that lymphatic vessels were more prominent in the nasal side. LYVE-1: red; Original Magnification: ×50. (b) Summary of repetitive experiments. $^*P < 0.05$.

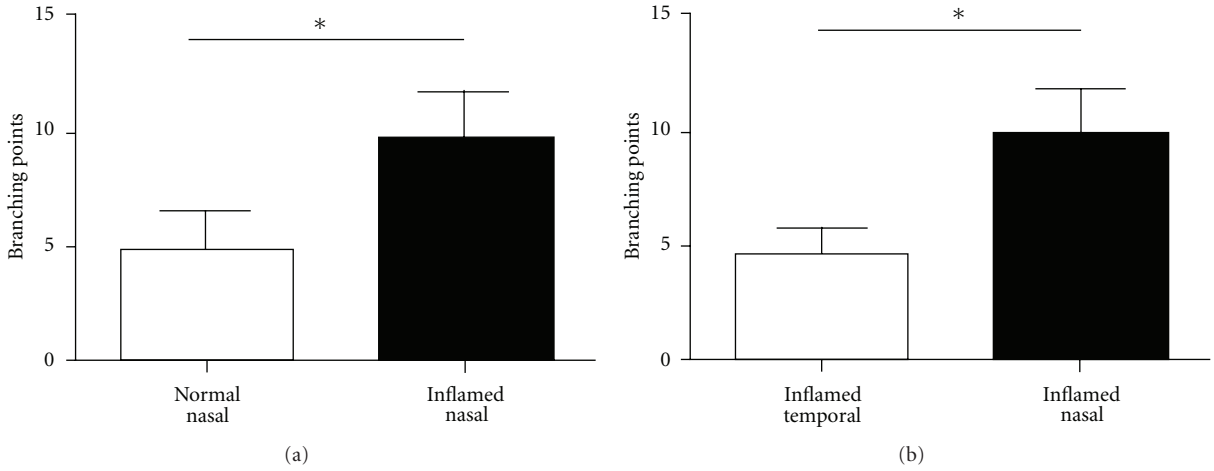

Figure 5: Comparison of branching points in conjunctival lymphatic vessels. (a) Significant difference was found between conjunctival lymphatic vessels under the normal and inflamed conditions at the nasal side $^*P < 0.05$. (b) Significant difference was found in conjunctival lymphatic branching points in the nasal versus temporal side under the inflamed condition. $^*P < 0.05$.

data on the physiological and pathological organization of lymphatic vasculatures in the conjunctiva have shown that conjunctival lymphatic vessels maintain a nasal dominant distribution pattern under both normal and inflamed conditions. This study also defines the conjunctiva as a new site for LG response after an inflammatory stimulation in the ocular surface.

To our knowledge, this is the first study on the disparate distribution of lymphatic vessels in the conjunctiva. Nonetheless our findings are consistent with several previous reports on polarized distribution of ocular tissues. For example, we recently reported a similar nasal dominant distribution of lymphatic vessels in the cornea [17]. The analogous nasal preference pattern has also been observed in antigen-induced conjunctiva-associated lymphoid tissue (CALT) [22, 23], and limbal epithelial crypts [24]. A more recent work byMckenna et al. also highlighted the nasal polarization of eye innervation during embryonic development [25]. Interestingly, dendritic cells of the bulbar conjunctival stroma are more frequently located in the superonasal quadrant [26]. In the clinic, it has been long observed that certain ocular diseases, such as pinguecula and pterygium, predominantly affect the nasal side of the ocular surface. Though the exact mechanisms remain unknown, new evidence have confirmed the presence of lymphatic vessels in human pterygium [27]. Our findings that the nasal side is naturally more endowed with lymphatic vessels may explain partly why this side is more prone to pathological disorders. Additionally, studies suggest that conjunctival defect in dry eye disease (DED) begins in the nasal area and spreads to the temporal area with disease progression [28, 29]. Most recently, corneal LG was found to be critically involved in DED [30]. Taken together, our data may provide a new piece of evidence indicating a correlation between lymphatic response of the nasal side of the ocular surface and DED pathogenesis, which warrants further investigation and is beyond the scope of this study.

In spite of numerous studies on corneal LG with several animal models including suture placement, transplantation, micropocket implantation, herpes simplex virus infection, and chemical burn [10], conjunctival LG has not been yet reported. Our novel finding on conjunctival LG in response to corneal inflammation indicates that lymphatic vessels in the conjunctiva may play a more active role in ocular surface diseases than previously considered. Yet to be examined, conjunctival LG may also occur in other corneal disorders after an infectious, traumatic, or chemical insult. It is therefore important to consider both tissues together when evaluating disease conditions and designing anti-LG treatment regimens.

Finally, a comprehensive description of conjunctival lymphatics may have implication beyond the scope of the eye as well. Unlike the cornea but similar to many other tissues in the body, the conjunctiva has lymphatic supply under normal condition. Results from conjunctival research should therefore be readily applied to the other tissues. Due to its accessible location in the ocular surface, we foresee that further in-depth investigation on conjunctival lymphatics will reveal novel mechanisms and therapies for broad lymphatic diseases occurring both inside and outside the eye.

Acknowledgments

This work is supported in part by research grants from National Institutes of Health, Department of Defense, and the University of California at Berkeley (to L. Chen). Tatiana Ecoiffier is an Ezell Fellow from the American Optometric Foundation.

References

[1] S. Schulte-Merker, A. Sabine, and T. V. Petrova, "Lymphatic vascular morphogenesis in development, physiology, and disease," *Journal of Cell Biology*, vol. 193, no. 4, pp. 607–618, 2011.

[2] T. Tammela and K. Alitalo, "Lymphangiogenesis: molecular mechanisms and future promise," *Cell*, vol. 140, no. 4, pp. 460–476, 2010.

[3] S. G. Rockson, "The broad spectrum of lymphatic health and disease," *Lymphatic Research and Biology*, vol. 8, no. 2, p. 101, 2010.

[4] L. Chen, "Ocular lymphatics: state-of-the-art review," *Lymphology*, vol. 42, no. 2, pp. 66–76, 2009.

[5] M. H. Witte, M. J. Bernas, C. P. Martin, and C. L. Witte, "Lymphangiogenesis and lymphangiodysplasia: from molecular to clinical lymphology," *Microscopy Research and Technique*, vol. 55, no. 2, pp. 122–145, 2001.

[6] G. Oliver and M. Detmar, "The rediscovery of the lymphatic system: old and new insights into the development and biological function of the lymphatic vasculature," *Genes and Development*, vol. 16, no. 7, pp. 773–783, 2002.

[7] S. Banerji, J. Ni, S. X. Wang et al., "LYVE-1, a new homologue of the CD44 glycoprotein, is a lymph-specific receptor for hyaluronan," *Journal of Cell Biology*, vol. 144, no. 4, pp. 789–801, 1999.

[8] A. Kaipainen, J. Korhonen, T. Mustonen et al., "Expression of the fms-like tyrosine kinase 4 gene becomes restricted to lymphatic endothelium during development," *Proceedings of the National Academy of Sciences of the United States of America*, vol. 92, no. 8, pp. 3566–3570, 1995.

[9] J. T. Wigle and G. Oliver, "Prox1 function is required for the development of the murine lymphatic system," *Cell*, vol. 98, no. 6, pp. 769–778, 1999.

[10] L. Chen, B. Hann, and L. Wu, "Experimental models to study lymphatic and blood vascular metastasis," *Journal of Surgical Oncology*, vol. 103, no. 6, pp. 475–483, 2011.

[11] Y. Cao, R. Cao, S. Lim et al., "Mouse corneal lymphangiogenesis model," *Nature Protocols*, vol. 6, no. 6, pp. 817–826, 2011.

[12] H. B. Collin, "Lymphatic drainage of 131-I-albumin from the vascularized cornea," *Investigative Ophthalmology*, vol. 9, no. 2, pp. 146–155, 1970.

[13] H. Zhang, S. Grimaldo, D. Yuen, and L. Chen, "Combined blockade of VEGFR-3 and VLA-1 markedly promotes high-risk corneal transplant survival," *Investigative Ophthalmology and Visual Science*, vol. 52, no. 9, pp. 6529–6535, 2011.

[14] T. Dietrich, F. Bock, D. Yuen et al., "Cutting edge: lymphatic vessels, not blood vessels, primarily mediate immune rejections after transplantation," *Journal of Immunology*, vol. 184, no. 2, pp. 535–539, 2010.

[15] L. Chen, P. Hamrah, C. Cursiefen et al., "Vascular endothelial growth factor receptor-3 mediates induction of corneal alloimmunity," *Nature Medicine*, vol. 10, no. 8, pp. 813–815, 2004.

[16] C. Cursiefen, L. Chen, M. R. Dana, and J. W. Streilein, "Corneal lymphangiogenesis: evidence, mechanisms, and implications for corneal transplant immunology," *Cornea*, vol. 22, no. 3, pp. 273–281, 2003.

[17] T. Ecoiffier, D. Yuen, and L. Chen, "Differential distribution of blood and lymphatic vessels in the murine cornea," *Investigative Ophthalmology and Visual Science*, vol. 51, no. 5, pp. 2436–2440, 2010.

[18] S. Grimaldo, D. Yuen, T. Ecoiffier, and L. Chen, "Very late antigen-1 mediates corneal lymphangiogenesis," *Investigative Ophthalmology and Visual Science*, vol. 52, no. 7, pp. 4808–4812, 2011.

[19] T. Truong, E. Altiok, D. Yuen, T. Ecoiffier, and L. Chen, "Novel characterization of lymphatic valve formation during corneal inflammation," *PLoS ONE*, vol. 6, no. 7, Article ID e21918, 2011.

[20] D. Yuen, B. Pytowski, and L. Chen, "Combined blockade of VEGFR-2 and VEGFR-3 inhibits inflammatory lymphangiogenesis in early and middle stages," *Investigative Ophthalmology and Visual Science*, vol. 52, no. 5, pp. 2593–2597, 2011.

[21] D. Yuen, R. Leu, A. Sadovnikova, and L. Chen, "Increased lymphangiogenesis and hemangiogenesis in infant cornea," *Lymphatic Research and Biology*, vol. 9, no. 2, pp. 109–114, 2011.

[22] T. Sakimoto, J. Shoji, N. Inada, K. Saito, Y. Iwasaki, and M. Sawa, "Histological study of conjunctiva-associated lymphoid tissue in mouse," *Japanese Journal of Ophthalmology*, vol. 46, no. 4, pp. 364–369, 2002.

[23] P. Steven, J. Rupp, G. Hüttmann et al., "Experimental induction and three-dimensional two-photon imaging of conjunctiva-associated lymphoid tissue," *Investigative Ophthalmology and Visual Science*, vol. 49, no. 4, pp. 1512–1517, 2008.

[24] H. S. Dua, V. A. Shanmuganathan, A. O. Powell-Richards, P. J. Tighe, and A. Joseph, "Limbal epithelial crypts: a novel anatomical structure and a putative limbal stem cell niche," *British Journal of Ophthalmology*, vol. 89, no. 5, pp. 529–532, 2005.

[25] C. C. Mckenna and P. Y. Lwigale, "Innervation of the mouse cornea during development," *Investigative Ophthalmology and Visual Science*, vol. 52, no. 1, pp. 30–35, 2011.

[26] T. Hoang-Xuan, C. Baudouin, and C. Creuzot-Garcher, *Inflammatory Disease of the Conjunctiva*, Thieme, 1998.

[27] A. M. Cimpean, M. P. Sava, M. Raica, and D. Ribatti, "Preliminary evidence of the presence of lymphatic vessels immunoreactive for D2-40 and Prox-1 in human pterygium," *Oncology Reports*, vol. 26, no. 5, pp. 1111–1113, 2011.

[28] M. Rolando, S. Barabino, C. Mingari, S. Moretti, S. Giuffrida, and G. Calabria, "Distribution of conjunctival HLA-DR expression and the pathogenesis of damage in early dry eyes," *Cornea*, vol. 24, no. 8, pp. 951–954, 2005.

[29] E. Uchiyama, J. D. Aronowicz, I. A. Butovich, and J. P. McCulley, "Pattern of vital staining and its correlation with aqueous tear deficiency and meibomian gland dropout," *Eye and Contact Lens*, vol. 33, no. 4, pp. 177–179, 2007.

[30] S. Goyal, S. K. Chauhan, J. El Annan, N. Nallasamy, Q. Zhang, and R. Dana, "Evidence of corneal lymphangiogenesis in dry eye disease: a potential link to adaptive immunity?" *Archives of Ophthalmology*, vol. 128, no. 7, pp. 819–824, 2010.

Hindawi Publishing Corporation
Journal of Ophthalmology
Volume 2012, Article ID 783163, 11 pages
doi:10.1155/2012/783163

Review Article

Lymphatics and Lymphangiogenesis in the Eye

Shintaro Nakao,[1] Ali Hafezi-Moghadam,[2] and Tatsuro Ishibashi[1]

[1] *Department of Ophthalmology, Graduate School of Medical Sciences, Kyushu University, 3-1-1 Maidashi, Higashi-Ku, Fukuoka 812-8582, Japan*
[2] *Functional and Molecular Imaging Center and Department of Radiology, Brigham and Women's Hospital, Harvard Medical School, Boston, MA 02115, USA*

Correspondence should be addressed to Shintaro Nakao, snakao@med.kyushu-u.ac.jp

Received 15 August 2011; Revised 20 November 2011; Accepted 21 November 2011

Academic Editor: Claus Cursiefen

Lymphatic is a prerequisite for the maintenance of tissue fluid balance and immunity in the body. A body of evidence also shows that lymphangiogenesis plays important roles in the pathogenesis of diseases such as tumor metastasis and inflammation. The eye was thought to lack lymphatic vessels except for the conjunctiva; however, advances in the field, including the identification of lymphatic endothelial markers (e.g., LYVE-1 or podoplanin) and lymphangiogenic factors (e.g., VEGF-C), have revealed the exsitence and possible roles of lymphatics and lymphangiogenesis in the eye. Recent studies have shown that corneal limbus, ciliary body, lacrimal gland, orbital meninges, and extraocular muscles contain lymphatic vessels and that the choroid might have a lymphatic-like system. There is no known lymphatic outflow from the eye. However, several lymphatic channels including uveolymphatic pathway might serve the ocular fluid homeostasis. Furthermore, lymphangiogenesis plays important roles in pathological conditions in the eye including corneal transplant rejection and ocular tumor progression. Yet, the role of lymphangiogenesis in most eye diseases, especially inflammatory disease or edema, remains unknown. A better understanding of lymphatic and lymphangiogenesis in the eye will open new therapeutic opportunities to prevent vision loss in ocular diseases.

1. Introduction

The lymphatic system in human was first described by Gasper Aselli in 1627 in a paper "De Lacteibus sive Lacteis Venis," Quarto Vasorum Mesarai corum Genere novo invento. Now, it is well known that the lymphatics remove interstitial fluid and macromolecules, including proteins, and transport them to lymph nodes before entering the blood circulation. From the lymphatic capillaries, the lymph is transported via precollectors to collecting lymphatic vessels and is returned through the lymphaticovenous junctions between the thoracic or lymphatic duct and the subclavian veins to the blood circulation [1]. Another role of the lymphatics is to carry immune cells to the lymph nodes and to control the immunity in health and disease.

Although the presence of lymphatics was long known through histology [2], systematic lymphatic research started later than blood vessels because of lack of specific markers. Recent identification of lymphatic endothelial markers facilitated lymphatic research [3, 4]. Furthermore, finding of lymphangiogenic factors reveals various mechanisms of lymphangiogenesis in health and disease. For instance, lymphangiogenesis plays critical roles in various disorders, including cancer metastasis and inflammation [5, 6].

In the past two decades, lymphatics and lymphangiogenesis in the eye and the phenotypes in the various ocular diseases have been investigated. Histological studies show the location and existence of lymphatics in the eye [7]. These studies have revealed that lymphatics contribute to the ocular homeostasis and that ocular lymphangiogenesis may play important roles in eye disorders. This paper reviews current knowledge on lymphatics and lymphangiogenesis in the eye and discusses the possibility of lymphatic-targeting therapy.

2. VEGF/VEGFR System in Lymphangiogenesis

VEGF family is important for vasculogenesis, angiogenesis, and lymphangiogenesis [8]. The mammalian VEGF family

presently contains five members: VEGF-A, placenta growth factor (PlGF), VEGF-B, VEGF-C, and VEGF-D. VEGF-A has important roles in mammalian vascular development and in diseases involving abnormal growth of blood vessels. Recent clinical studies have demonstrated the significance of VEGF-A in ocular neovascularization (e.g., diabetic retinopathy and aged-macular degeneration) with use of VEGF-A neutralizing antibodies [9]. VEGF-C and VEGF-D are main lymphangiogenic factors in both physiological and pathological conditions. The VEGF receptor family contains three members: VEGFR-1 (Flt-1), VEGFR-2 (KDR/Flk-1), and VEGFR-3 (Flt-4). VEGF-A binds and activates two tyrosine kinase receptors: VEGFR-1 and VEGFR-2 [8]. VEGF-A does not show any appreciable binding affinity to VEGFR-3. VEGFR-3 is a ligand for VEGF-C and VEGF-D. Mature form of VEGF-C and human VEGF-D are known to bind and activate VEGFR-2 [10, 11]. Various studies clarify the involvement of VEGF-C and -D/VEGFR-3 system in cancer lymphatic invasion and lymph node metastasis [12, 13]. Furthermore VEGF-C and -D/VEGFR-3 signaling is involved in inflammatory diseases and organ transplantation [6, 14, 15].

3. The Other Lymphangiogenesis-Related Factors

Lymphangiogenic factors include not only VEGF family but also the other growth factors and cytokines such as insulin-like growth factors (IGFs), hepatocyte growth factor (HGF), fibroblast growth factors (FGFs), and interleukins (ILs). These growth factors and cytokines have been well known to be angiogenic. Some of these factors can cause lymphangiogenesis directly and some can induce lymphangiogenesis via VEGF family indirectly. These findings are shown with assays in cornea.

4. Corneal Avascularity and Its Alymphatic Characteristics

The normal cornea, but not the conjunctiva, is devoid of lymphatic vessels as well as blood vessels (Figure 1). The alymphatic mechanism was unknown until recently a study showed that a soluble VEGFR-2 form is secreted by corneal epithelial cells selectively suppressing the physiologic growth of lymphatics [16]. This finding is the first identification of a specific lymphangiogenesis inhibitor.

5. Corneal Lymphangiogenesis Assay

Because of its avascularity, the cornea is widely used to investigate lymphangiogenesis. One of the most reliable methods to examine lymphangiogenesis is corneal inflammation model by suture or alkali burn (NaOH solution) [17, 18] (Figure 2). Another authentic method is cornea micropocket assay, which has been used for estimation of angiogenesis since the 1970s [19, 20] (Figure 2). In both models, lymphangiogenesis occurs from preexisting limbal lymphatics. The cornea micropocket model has revealed that most angiogenic factors also induce lymphangiogenesis (Table 1). This might indicate that the mechanism of lymphangiogenesis is partially similar with angiogenesis. IGF-1 and IGF-2, which significantly stimulates proliferation and migration of lymphatic endothelial cells, can induce corneal lymphangiogenesis. IGF-1-induced lymphangiogenesis is not mediated by VEGFR-3 signaling [21]. A potent angiogenic factor, VEGF-A, is also shown to be a lymphangiogenic factor in mouse cornea [22]. In VEGF-A-induced lymphangiogenesis, there are both mechanisms: VEGFR-3-dependent and VEGFR-3-independent. VEGF-A can induce the proliferation of lymphatic endothelial cells directly, which is not mediated by VEGFR-3 [23]. This lymphangiogenesis is also mediated by macrophage-derived VEGF-C with the inflammatory suture model [24]. The balance between direct and indirect effect in VEGF-A-induced lymphangiogenesis may depend on the situations. VEGF-C, a potent lymphangiogenic factor, was confirmed to induce corneal lymphangiogenesis [25]. VEGF-C156S, which is a specific ligand for VEGFR-3, also causes lymphangiogenesis as well as angiogenesis in the cornea [26]. This VEGFR-3-mediated lymphangiogenesis could be induced by direct effect for lymphatic endothelium as well as macrophage recruitment. Platelet-derived growth factor (PDGF) causes corneal lymphangiogenesis via direct stimulation of lymphatic endothelium [27]. HGF also causes corneal lymphangiogenesis that can be blocked by VEGFR-3 inhibition partially [28]. FGF-2, which is a well-known potent angiogenic factor, could cause lymphangiogenesis with corneal micropocket assay [29]. The FGF-2-induced lymphangiogenesis was blocked by VEGFR-3 inhibition [29]. These investigations suggest that each GF (growth factor) has different dependency on VEGFR-3 signaling in lymphangiogenesis. Some GFs cause proliferation or migration of lymphatic endothelial cells directly, whereas some GFs upregulate VEGF-C/-D to activate VEGFR-3 in lymphangiogenesis. Interestingly, the corneal micropocket assay reveals that low dose of FGF-2 causes selective lymphangiogenesis [30]. This observation provides the evidence that lymphatic growth is possible without angiogenesis. However, the detailed mechanism of FGF-2-mediated lymphangiogenesis has been enigmatic. A recent examination using mouse cornea introduced physiological expression of lymphatics without the presence of blood vessels, which is an indication that angiogenesis and lymphangiogenesis might occur independently [25]. In the study, FGF-2-deficient mice show significantly less preexisting lymphatic sprouts without having an effect on angiogenesis in the cornea compared to their wild-type counterparts [25]. Consequently, this suggests that lymph- and angiogenesis might occur independently.

6. Genetic Heterogeneity of Lymphangiogenesis

Recently two different groups have reported on genetic heterogeneity of corneal lymphangiogenesis in different mouse strains with the corneal suture model and the corneal micropocket model independently [25, 34] (Figure 3). This suggests that heterogeneity of corneal lymphatics shows different inflammatory reactions in patients. In the comparative analysis of lymphatics with various strains, *nu/nu* mice, which have a greatly reduced number of T cells, showed

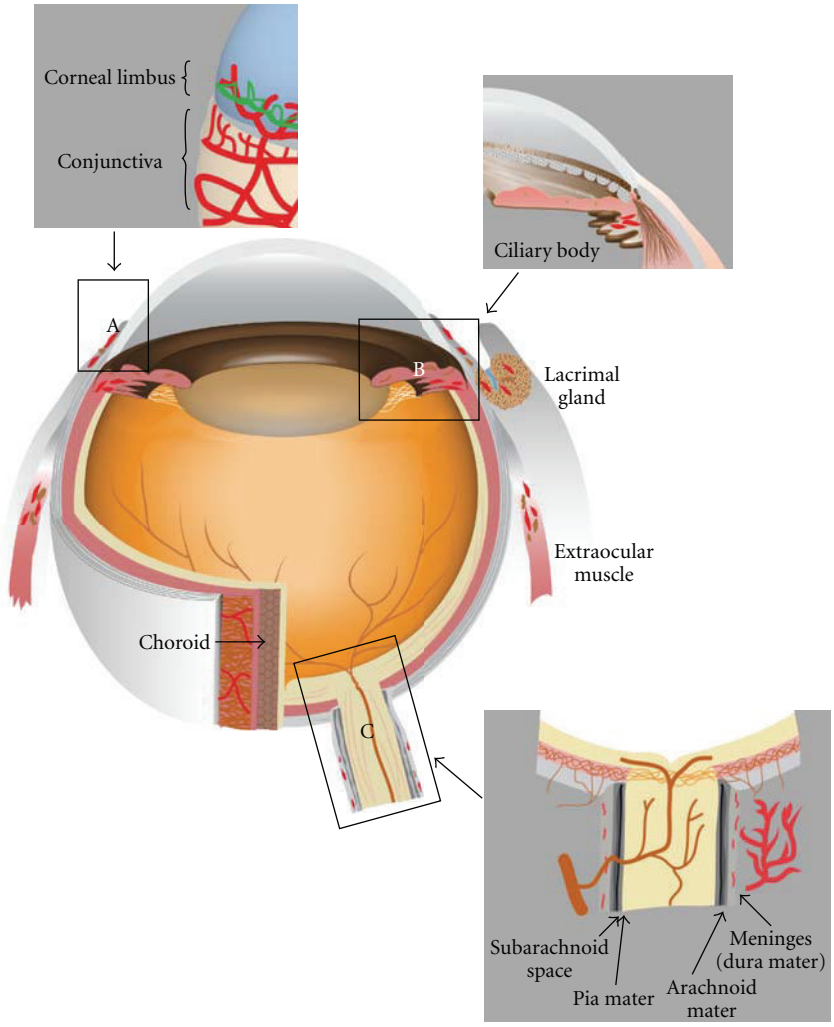

Figure 1: Distribution of lymphatics in the eye. Immunological staining with lymphatic specific markers as well as histological examinations has revealed the distribution of lymphatic vessels in the eye. Conjunctiva is well known to possess lymphatics. Cornea limbus, ciliary body, lacrimal gland, orbital meninges and extraocular muscle also contain lymphatic vessels, and choroid might have lymphatic-like system. Cornea, retina, and optic nerve do not show lymphatics. Intraocular lymphatic can be observed only in the ciliary body. (A), (B), and (C) show the details of corneal limbal area, angulus iridocornealis, and optic nerve, respectively. Red indicates lymphatic vessels.

Table 1: Growth factors and cytokines in corneal lymphangiogenesis assay. Various growth factors or cytokines induce lymphangiogenesis as well as angiogenesis with or without VEGFR-3 activation.

Growth factor/cytokine	Angiogenesis	Lymphangiogenesis	Via VEGFR-3	Reference
VEGF-A (160–200 ng)	++	+/−	Yes/No	[22–24]
VEGF-A (400 ng)	++	+	?	[31]
VEGF-C (160–400 ng)	+	+/++	Yes	[22, 25]
VEGF-C156S (80 ng)	+	+	Yes	[26]
FGF-2 (12.5 ng)	−	+	Yes	[30]
FGF-2 (80–100 ng)	++	++	Yes	[29]
HGF (280 ng)	+	+	Yes	[28]
PDGF-BB (320 ng)	+	+	No	[27]
IGF-1 (1 μg)	+	+	No	[21]
IL-1β (30–50 ng)	+	+	Yes	[32, 33]

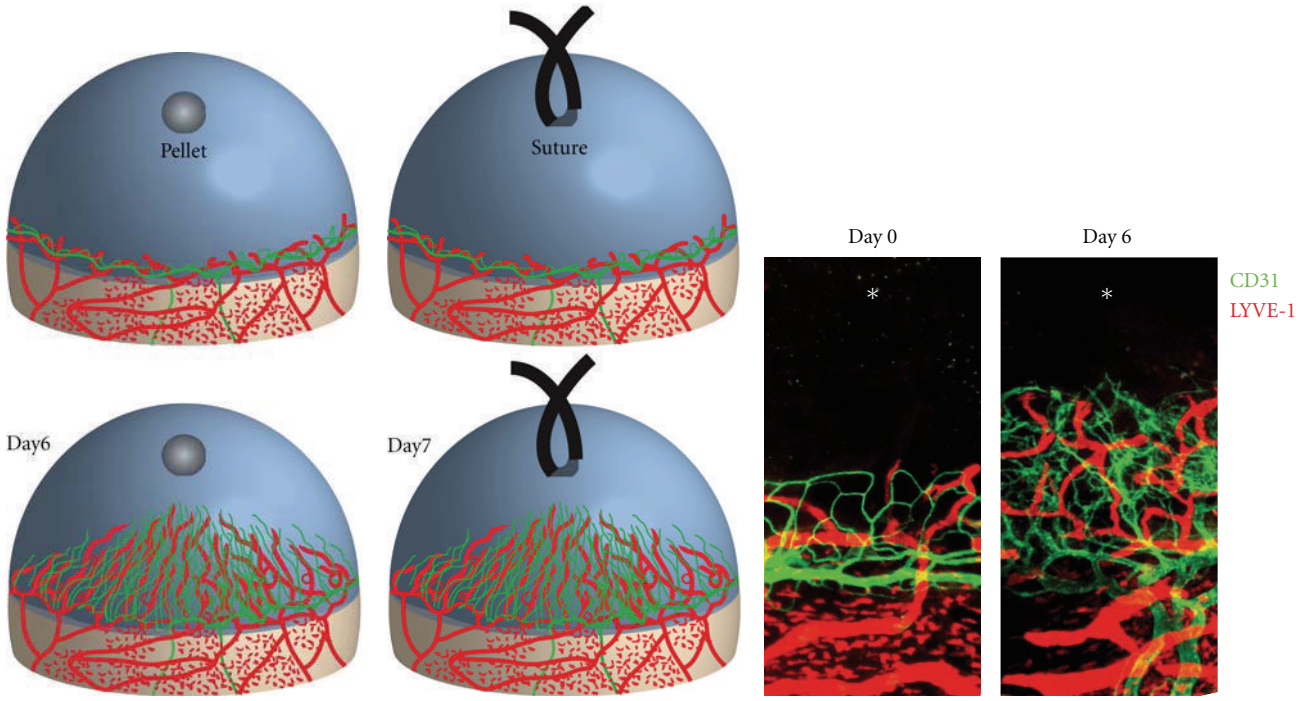

Figure 2: Mouse cornea lymphangiogenesis model. No lymphatic vessels exist in the normal mammalian cornea. Implantation of growth factor or cytokine into a surgically created micropocket in the mouse cornea stroma (a) or corneal injury by suture (b) induces lymphangiogenic response. Corneal lymphangiogenesis as well as angiogenesis can be examined 6 or 7 days after pellet implantation or suture, respectively (a) and (b). Double staining of corneal flat mounts for lymphangiogenic (LYVE-1, red) endothelium and angiogenic (CD31, green) with immunohistochemistry (c).

similar lymphatic development and GF-induced lymphangiogenesis with the other strains, suggesting that T cells might be unnecessary for lymphatic development as well as GF-induced lymphangiogenesis in the cornea [25] (Figure 3). Inflammation model by suture has also revealed various insights of lymphangiogenesis. After corneal inflammation, pathologic corneal lymphangiogenesis can regress earlier than angiogenic vessels [17].

7. The Interplay between Angiogenesis and Lymphangiogenesis

As described above, lymphangiogenesis and angiogenesis occur in concert [6]. However, how blood and lymphatic vessels regulate each other has been unknown. Recently, it was reported that angiogenic vessels delay lymphangiogenesis using corneal micropocket assay [31]. In response to VEGF-A, corneal lymphatics grow with a delay compared to blood vessels. Higher concentrations of VEGF-A are needed for lymphangiogenesis than for angiogenesis. The poised temporal and spatial association of angio- and lymphangiogenesis indicates interdependencies between blood and lymphatic vessels. Proteolytically processed VEGF-C binds to and activates VEGFR-2. Upregulated VEGFR-2 in angiogenic tips could trap VEGF-C, and the trapped VEGF-C could not reach lymphangiogenesis due to the distance apart from the lymphatic vessels [31]. This VEGF-C/VEGFR-2 interaction might regulate the relation between angio- and lymphangiogenesis. Delayed lymphangiogenesis might allow immune cells additional time at the inflammatory sites because immune cells originate from angiogenic vessels and drained through lymphangiogenic vessels [35].

8. Macrophages in Lymphangiogenesis

Macrophages have been well investigated for their role in neovascularization in various ocular diseases including ker atitis [36, 37], retinal angiogenesis [38, 39], and choroidal neovascularization [40, 41]. Macrophages contribute to corneal lymphangiogenesis in two different ways. Maruyama et al. showed that CD11b(+) macrophages infiltrate the inflammatory cornea and transdifferentiate into lymphatic endothelium that contributes to lymphangiogenesis [42]. Another role of macrophages is to provide lymphangiogenic factors. During corneal inflammation, infiltrating macrophage activates the NF-κB signaling and secretes the downstream cytokines (e.g., VEGF-A, -C, and -D) to induce corneal lymphangiogenesis [32]. NF-κB inhibition could block corneal lymphangiogenesis as well as the angiogenesis. A recent paper showed a mechanism for macrophages to infiltrate into the sites of corneal lymphangiogenesis. Vascular adhesion protein-1 (VAP-1) is an endothelial glycoprotein that regulates leukocyte transmigration [43, 44]. VAP-1 inhibition blocks inflammatory corneal lymphangiogenesis by reducing

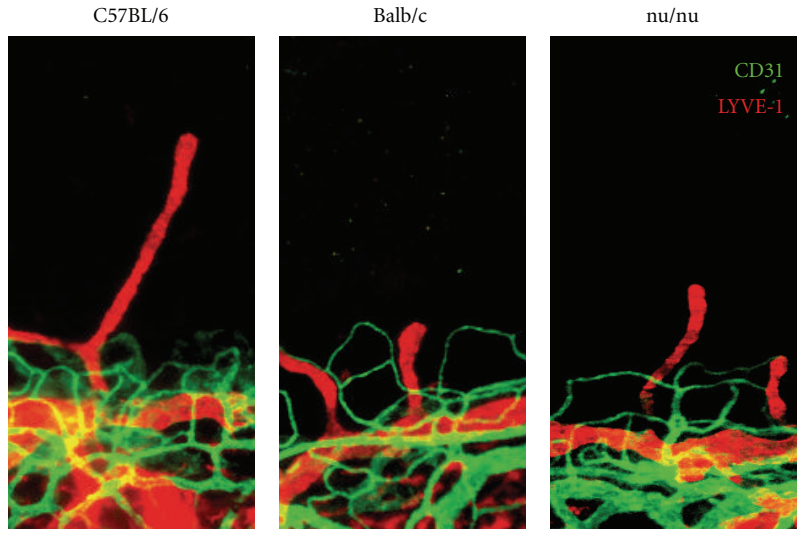

Figure 3: Strain-dependent limbal lymphatics. Genetic background significantly affects corneal preexisting limbal lymphatics. The area of preexisting lymphatics in C57BL/6 mice is significantly larger than that in Balb/c mice. *nu/nu* mice show the intermediate phenotype. Preexisting limbal lymphatics may be heterogenic in patients, causing differences in corneal transplant rejection or keratitis. *nu/nu* mice develop normal lymphatics, suggesting that T cells may not be important for lymphatic development.

Table 2: Lymphatic-associated ocular diseases. The list shows several diseases of the eye that are related to lymphatics or lymphangiogenesis. Further investigation might provide evidence of the contribution of lymphatics or lymphangiogenesis in the other eye diseases.

Eye diseases	Possible role of lymphatics	Reference
Corneal transplant	Lymphatic vessels but not angiogenic vessels are important for the immune rejection	[50]
Dry eye	Dry eye, which is a low-grade corneal inflammatory disorder, induces lymphangiogenesis	[49]
HSV-1 keratitis	Corneal herpes simplex virus-1 infection induces lymphangiogenesis via VEGF-A	[48]
Glaucoma	"Uveolymphatic pathway"; lymphatics exists in the ciliary body	[51]
Intraocular tumors	"Tumor-associated lymphangiogenesis" correlates the malignancy	[52, 53]

macrophage infiltration [33]. Macrophage polarization (M1 classical versus M2 alternatively activated macrophages) was recently discovered to regulate various inflammatory diseases [45]. The number of M2 marker(+) macrophages in inflammatory corneas of VAP-1-inhibitor-treated mice was significantly lower than in vehicle-treated mice [33]. Thus, M2 macrophages might play an important role in corneal lymphangiogenesis. However, further investigation will be necessary to discern the role of macrophage polarization in lymphangiogenesis. VAP-1 may become a therapeutic target for various lymphangiogenesis-related ocular diseases. Furthermore, a recent report showed that the antiangiogenic factor Thrombospondin-1 (TSP-1) is also an endogenous antilymphangiogenic factor [46]. TSP-1 can suppress macrophage-derived VEGF-C and VEGF-D by ligating CD36 on the cells. As a result, TSP-1 can become a therapeutic molecule for corneal lymphangiogenesis.

9. Lymphangiogenesis in Corneal Disorders

Human cornea lacks lymphatic vessels during the development [47]. Vascularization in cornea disturbs visual acuity, whereas corneal lymphangiogenesis cannot. However, lymphangiogenesis in the cornea can modulate corneal immunity or inflammation. Increasing studies on lymphatic and lymphangiogenesis, have shown that lymphatic vessels play an important role for various corneal disorders (Table 2). Herpes simplex virus-1 (HSV-1) infection in the cornea is a leading cause of blindness. Corneal HSV-1 infection induces lymphangiogenesis, and the corneal lymphatics persist past the resolution of infection (Table 2). HSV-1-elicited lymphangiogenesis was reported to be strictly dependent on VEGF-A/VEGFR-2 signaling but not on VEGFR-3 ligands [48]. A recent study also showed that dry eye, a low-grade corneal inflammatory disorder, induces lymphangiogenesis by the upregulation of VEGFs and VEGFRs and CD11b(+) macrophage recruitment. Interestingly, corneal lymphangiogenesis in dry eye does not accompany angiogenesis (Table 2). However, the mechanism is not fully appreciated, and further investigation must include the estimation that lymphangiogenesis can be a therapeutic target for dry eye disease [49].

10. The Role of Lymphangiogenesis in Corneal Graft Rejection

The critical role of lymph nodes in corneal alloimmunization and graft rejection has been well investigated [54]. VEGFR-3 blockade suppressed corneal antigen-presenting cell trafficking to the lymph node and delayed the rejection of corneal

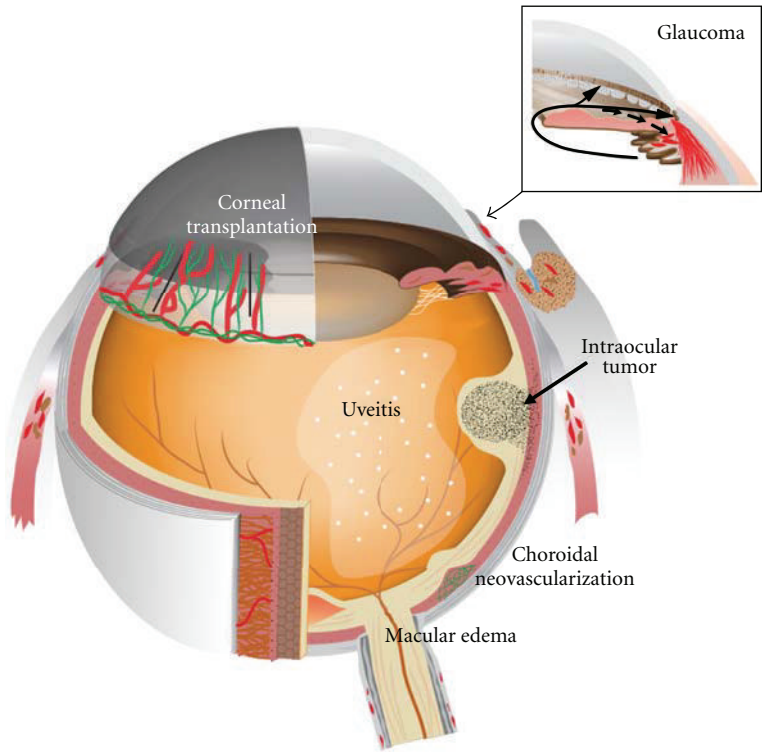

Figure 4: Lymphangiogenesis as a possible therapeutic target for the eye diseases. Corneal transplant, glaucoma, and intraocular tumors were suggested to be related to lymphatics or lymphangiogenesis in the pathogenesis. If choroid has lymphatic function, lymphatics or lymphangiogenesis may be important for the pathology of uveitis, choroidal neovascularization, or macular edema because of the vital role of lymphatics in inflammation or tissue edema. Red: lymphatic vessels. Green: blood vessels.

transplanted graft rejection [55]. Lymphatic vessels, but not angiogenic vessels, could be important for immune rejection after corneal transplantation [50] (Table 2). Lymphatics and lymphangiogenesis-related factor would be a therapeutic target for corneal graft rejection (Figure 4).

11. Conjunctival Lymphatics in Glaucoma Surgery

Conjunctiva is the most lymphatic-developed tissue in the eye. A surgeon incidentally fills anesthetic solution into the lymphatics of a patient's conjunctiva during an operation. The doctor routinely visualizes conjunctival lymphatic vessels with a dye to decide where to make scleral filter to lower intraocular pressure (IOP) in glaucoma patients. Interestingly, he suggests that a healthy lymphatic system in the conjunctiva may decide the outcome of lowering IOP surgery and alerts that mitomycin or cauterization can cause damage to the lymphatic structures [56].

12. Lymphangiogenesis in Conjunctivitis

Various studies with LYVE-1 or podoplanin antibody confirmed that lymphatic vessels exist in conjunctiva in various species. Corneal lymphangiogenesis is sprouted from limbal lymphatics that connect to conjunctival lymphatic [57]. The removal of conjunctiva could not affect GF-induced corneal lymphangiogenesis, suggesting that the conjunctiva, including its LYVE-1(+) lymphatics and cells, may not be necessary for corneal lymphangiogenesis [25]. However, lymphatics might play an important role to heal conjunctivitis or conjunctival chemosis, or probably corneal edema. Furthermore, a group reported that injected tracers in the anterior chamber or the vitreous utilize conjunctival lymphatics to reach the lymph nodes [58, 59]. These data alert that intraocular drug injection affects the immunity.

13. The Possibility of Lymphatic-Targeting Therapy in Retinal Disorders

Retina is part of the central nervous system (CNS) that is vascularized and has been thought not to have lymphatics as well as other parts of the CNS like the brain [60]. In addition to severe vision loss, macular edema is commonly associated with many retinal diseases including diabetic macular edema and retinal vein occlusion [61]. It is believed to be caused by hyperpermeability of the retinal vessels and/or decreased efflux of fluid across the retinal pigment epithelium, which can be induced by outer/inner blood retinal barrier dysfunction. In the past decade, there were advances in therapy for macular edema. Administration of steroid or VEGF neutralizing antibodies or vitrectomy can reduce macular edema significantly in patients [62]. However, these treatments may cause adverse effects including an increased incidence of IOP

elevation or tractional retinal detachment [63, 64]. These pharmacological mechanisms to reduce macular edema must be caused by the blockade of leakage from retinal vessels [65–67]. However, the mechanism to absorb leaked interstitial fluid in macular edema is unclear. A recent paper suggested that drainage from the vitreous might exist via conjunctival lymphatics [59]. Furthermore, as described below, choroid might have lymphatic-like system. It has been reported that the dysfunction of lymphatic vessels causes lymphedema or tissue edema in various diseases and that lymphatic normalization or newly lymphatic vessels reduce tissue edema in the skin [68]. Further investigations of the lymphatic role of the posterior eye segment may reveal novel ways to manage macular edema (Figure 4).

Recently podoplanin is shown to be expressed in retinal pigment epithelium (RPE) [69]. Podoplanin depletion with siRNA reduces cell aggregation, proliferation, and the tight junction. RPE regulates outer blood-retinal barrier, which is broken down in various retinal diseases. Further research is required to reveal how podoplanin in RPE contributes to the pathogenesis of retinal disorders.

14. Choroidal Lymphatics: A Controversial Point

The choroid, which forms the uvea with the ciliary body and the iris, is one of the most highly vascularized tissue in the body. The choroid provides oxygen and nourishment to the outer layers of the retina. Before the discoveries of lymphatic specific markers, various histological examinations of animal choroid have shown the existence of lymphatic vessels in the choroid (Figure 1). In 1997, a paper on the avian eye proposed that the lacunae of the choroid represented a system with short lymphatic vessels that reached the choriocapillaris [70]. The authors proposed that the system might drain intraocular fluids directly into the eye venous system. In 1998, W. krebs ad I. P. krebs showed evidence of choroidal lymphatic vessels in the monkey by using electron microscopy [71]. In this paper, their observation with lymphatic specific features, including the lack of a continuous external basement lamina and the presence of anchoring filaments, supported their conclusion. Another study examined whether lymphatic vessels existed in monkey choroid [72]. This electron microscopic study observed the lymphatic sinus-like structures in the outer choroid. The lymphatic sinus-like structures were lined with fibroblast-like cells with large intercellular gaps and contained amorphous material, which was probably tissue fluid. Furthermore, this study indicated that the cells lining the lymphatic sinus-like structures put out valve-like cytoplasmic processes into the lumen. However, this study also pointed out that the ultrastructure in the outer choroid differed from typical lymphatics in the point of the discontinuous cell lining with large gaps.

Lymphatic vessel endothelial hyaluronic acid receptor (LYVE-1) is widely accepted as the most reliable lymphatic marker that is also expressed by a subpopulation of macrophages [4, 42]. A recent paper on human choroid checked for lymphatic vessels with immunohistochemistry of LYVE-1 and podoplanin. LYVE-1(+) podoplanin(+) lymphatic vessel could not be observed and all LYVE-1(+) cells were expressed macrophage markers in human choroid [73]. These findings can support observation that the choroid contains some LYVE-1(+) macrophages and no lymphatics [74]. In corneal inflammation, LYVE-1(+) macrophages transdifferentiate and contribute to lymphangiogenesis [42]. However, the role of LYVE-1(+) macrophages has not been examined. It is unknown whether LYVE-1(+) macrophages are vital for choroidal homeostasis or how these cells conduct themselves in the pathological condition. Because the outer choroid is recognized as an unconventional route of aqueous humor outflow, choroid may have lymphatic-like system despite the lack of authentic lymphatic vessels in human.

15. Lymphatic-Targeting Therapy in Choroidal/Uveal Disorders

Choroidal neovascularization (CNV), which involves abnormal growth of blood vessels in the back of the eyes, is a hallmark of age-related macular degeneration (AMD). A paper reported that both VEGF-C and VEGF-D were markedly expressed in the retinal pigment epithelium (RPE) in a surgically removed subretinal vascular membrane of AMD patients [75]. Because VEGF-C and VEGF-D show angiogenic potential, they may contribute to CNV formation. Further investigation is necessary to estimate the contribution to AMD pathogenesis (Figure 4).

Uveitis in humans is an inflammatory and immune disease in the eye that causes severe vision loss [76]. The eye is thought to have no lymphatic drainage, and the uvea may act as an accessory lymph node during the immune response. However, the role of lymphatic system in uveitis is unclear (Figure 4). Because lymphatic system contributes to the pathogenesis of immune diseases, lymphatic-targeting drug may provide agents for uveitis treatment.

16. Ocular Tumor-Associated Lymphangiogenesis

Lymphangiogenesis is observed in many types of solid tumors [77]. Human cancers express various lymphangiogenic factors including VEGF-C. Furthermore, many clinical studies showed positive correlation between VEGF-C, lymphatic invasion, lymph node metastasis, and poor patient survival. What about ocular tumors? A paper by Heindl et al. analyzed the correlation of tumor-associated lymphangiogenesis and malignancy in conjunctival squamous cell carcinoma (SCC) [52] (Table 2, Figure 4). They observed that the development of conjunctival SCC from premalignant stage was accompanied by conjunctival lymphangiogenesis. The study also noticed that the lymphangiogenesis in tumor was associated with an increased risk of local recurrence in patients with SCC. Another study evaluated whether lymphangiogenesis could contribute to the prognosis of ciliary body melanoma with extraocular extension [53]. Intraocular lymphatic vessels were found in 60% of the melanoma with extraocular extension and the lymphangiogenesis is associated with an increased mortality risk. However, uveal melanoma does not

include lymphangiogenesis despite expressions of VEGF-C and its receptor VEGFR-2 and VEGFR-3 [78]. The tumor location, tumor type, or tumor malignancy can be a contributing factor to this variation. The contribution of VEGF-C to tumor progression remains unclear. Lymphangiogenesis in some ocular tumors may play an important role for the tumor progression. In the future, it will be possible that antilymphangiogenic treatment will lower metastasis rate of ocular tumor and mortality.

17. Ocular Drainage System

A recent paper shows that various lymphatic markers are expressed in the human anterior segment [79]. Podoplanin is widely accepted as a reliable lymphatic marker, because of its continuous expression in lymphatic endothelium [80]. The immunohistochemical examination for podoplanin and other lymphatic markers reveals that the anterior eye segment does not have lymphatic vessels. Interestingly podoplanin can be expressed on almost all cells of the trabecular meshwork, endothelial cells of Schlemm's canal, and cells of anterior ciliary muscle tips despite the lack of lymphatics. This suggests that the aqueous humor outflow tissues have similar characteristics of lymphatic vessels (e.g., immune cell way to lymph node). Intracameral injected fluorescent antigens can be observed in the ipsilateral lymph node of the head and neck within 24 hours, suggesting that the antigen in the anterior chamber reaches the lymphoid organ [58]. This route to travel to the lymph node must be via conjunctival lymphatic and blood circulation. Furthermore, an alternative pathway via trabecular meshwork may exist. Lymphatic-related molecular or cellular targeting strategies will offer novel approaches in the treatment of inflammatory or immunological disorders in anterior ocular segments. Aqueous humor drainage from the eye is known to travel via two pathways: conventional pathway (trabecular meshwork) and alternative pathway (uveoscleral outflow) (Figure 4). Impaired aqueous humor drainage elevates intraocular pressure and results in glaucoma. A lymphatic outflow from the eye has been considered to be absent [81]. Interestingly, a third pathway was recently reported, "uveolymphatic pathway" [51] (Figure 4, Table 2). Immunogold stain as well as immunohistochemistry with podoplanin or LYVE-1 antibody showed lymphatic vessels in the human ciliary body (Figure 1). Furthermore, intracamerally injected tracer could be detected in several lymph nodes (e.g., cervical lymph node). The uveolymphatic pathway may be a novel therapeutic target for glaucoma patients.

In 1989, McGetrick et al. searched for lymphatic drainage from monkey orbit. They injected colloid solution, or India ink, into the retrobulbar space and examined if they could reach the lymphatic vessels or the lymph node. However, no lymphatic vessels could be identified in the orbit and these tracers left the posterior orbit. This paper concluded that the posterior pathway did not lead to the lymphatic vessels or the lymph node [82]. From these observations, the human orbit has been thought to lack lymphatic vessels in a long time [83]. However, in 1993, a paper using an enzymatic method in monkey demonstrated the presence of lymphatic vessels in the orbital arachnoid, lacrimal gland, extraocular muscle, and connective tissue at the orbital apex [84] (Figure 1). In 1999, an electron microscopic study with India ink showed that human optic nerve meninges have lymphatic vessels [85]. These studies suggested new evidence that cerebrospinal fluid drained into lymphatics within the meninges of the intraorbital part of the optic nerve. However, it is unclear how lymphatics within the meninges can affect ocular disorders including glaucoma, optic neuritis, or optic neuropathy.

18. Conclusion

Increasing evidence shows that lymphangiogenesis, as well as angiogenesis, has a key role in ocular physiology and pathology (Table 2). Recently antiangiogenic therapy (e.g., bevacizumab) is widely used for various ocular diseases. However, various ocular disorders including edema or inflammation still remain as a cause of visual loss. Better understanding of lymphatics and lymphangiogenesis in the eye will provide a basis for the development of novel therapeutic strategies for incurable ocular diseases (Figure 4).

Conflict of Interests

The authors declare no competing financial interests.

Acknowledgments

This work was supported by an overseas Research Fellowship Award from Bausch & Lomb, a Fellowship Award from the Japan Eye Bank Association and Tear Film and Ocular Surface Society, and Young Investigator Fellowship (to S. Nakao).

References

[1] C. Norrmén, T. Tammela, T. V. Petrova, and K. Alitalo, "Biological basis of therapeutic lymphangiogenesis," *Circulation*, vol. 123, no. 12, pp. 1335–1351, 2011.

[2] F. Sabin, "On the origin of the lymphatic system from the veins and the development of the lymphatic hearts and thoracic duct in the pig," *American Journal of Anatomy*, vol. 1, pp. 367–391, 1902.

[3] S. Breiteneder-Geleff, A. Soleiman, H. Kowalski et al., "Angiosarcomas express mixed endothelial phenotypes of blood and lymphatic capillaries: podoplanin as a specific marker for lymphatic endothelium," *American Journal of Pathology*, vol. 154, no. 2, pp. 385–394, 1999.

[4] S. Banerji, J. Ni, S. X. Wang et al., "LYVE-1, a new homologue of the CD44 glycoprotein, is a lymph-specific receptor for hyaluronan," *Journal of Cell Biology*, vol. 144, no. 4, pp. 789–801, 1999.

[5] M. Skobe, T. Hawighorst, D. G. Jackson et al., "Induction of tumor lymphangiogenesis by VEGF-C promotes breast cancer metastasis," *Nature Medicine*, vol. 7, no. 2, pp. 192–198, 2001.

[6] P. Baluk, T. Tammela, E. Ator et al., "Pathogenesis of persistent lymphatic vessel hyperplasia in chronic airway inflammation," *Journal of Clinical Investigation*, vol. 115, no. 2, pp. 247–257, 2005.

[7] R. E. Gausas, R. S. Gonnering, B. N. Lemke, R. K. Dortzbach, and D. D. Sherman, "Identification of human orbital lymphatics," *Ophthalmic Plastic and Reconstructive Surgery*, vol. 15, no. 4, pp. 252–259, 1999.

[8] M. Shibuya and L. Claesson-Welsh, "Signal transduction by VEGF receptors in regulation of angiogenesis and lymphangiogenesis," *Experimental Cell Research*, vol. 312, no. 5, pp. 549–560, 2006.

[9] S. Wolf, "Current status of anti-vascular endothelial growth factor therapy in Europe," *Japanese Journal of Ophthalmology*, vol. 52, no. 6, pp. 433–439, 2008.

[10] V. Joukov, T. Sorsa, V. Kumar et al., "Proteolytic processing regulates receptor specificity and activity of VEGF-C," *EMBO Journal*, vol. 16, no. 13, pp. 3898–3911, 1997.

[11] S. A. Stacker, K. Stenvers, C. Caesar et al., "Biosynthesis of vascular endothelial growth factor-D involves proteolytic processing which generates non-covalent homodimers," *Journal of Biological Chemistry*, vol. 274, no. 45, pp. 32127–32136, 1999.

[12] Y. He, I. Rajantie, K. Pajusola et al., "Vascular endothelial cell growth factor receptor 3-mediated activation of lymphatic endothelium is crucial for tumor cell entry and spread via lymphatic vessels," *Cancer Research*, vol. 65, no. 11, pp. 4739–4746, 2005.

[13] K. Shimizu, H. Kubo, K. Yamaguchi et al., "Suppression of VEGFR-3 signaling inhibits lymph node metastasis in gastric cancer," *Cancer Science*, vol. 95, no. 4, pp. 328–333, 2004.

[14] K. Kajiya and M. Detmar, "An important role of lymphatic vessels in the control of UVB-induced edema formation and inflammation," *Journal of Investigative Dermatology*, vol. 126, no. 4, pp. 919–921, 2006.

[15] D. Kerjaschki, N. Huttary, I. Raab et al., "Lymphatic endothelial progenitor cells contribute to de novo lymphangiogenesis in human renal transplants," *Nature Medicine*, vol. 12, no. 2, pp. 230–234, 2006.

[16] R. J. Albuquerque, T. Hayashi, W. G. Cho et al., "Alternatively spliced vascular endothelial growth factor receptor-2 is an essential endogenous inhibitor of lymphatic vessel growth," *Nature Medicine*, vol. 15, no. 9, pp. 1023–1030, 2009.

[17] C. Cursiefen, K. Maruyama, D. G. Jackson, J. W. Streilein, and F. E. Kruse, "Time course of angiogenesis and lymphangiogenesis after brief corneal inflammation," *Cornea*, vol. 25, no. 4, pp. 443–447, 2006.

[18] S. Ling, H. Lin, L. Liang et al., "Development of new lymphatic vessels in alkali-burned corneas," *Acta Ophthalmologica*, vol. 87, no. 3, pp. 315–322, 2009.

[19] M. A. Gimbrone Jr., R. S. Cotran, S. B. Leapman, and J. Folkman, "Tumor growth and neovascularization: an experimental model using the rabbit cornea," *Journal of the National Cancer Institute*, vol. 52, no. 2, pp. 413–427, 1974.

[20] Y. Cao, S. Lim, H. Ji et al., "Mouse corneal lymphangiogenesis model," *Nature Protocols*, vol. 6, no. 6, pp. 817–826, 2011.

[21] M. Björndahl, R. Cao, L. J. Nissen et al., "Insulin-like growth factors 1 and 2 induce lymphangiogenesis in vivo," *Proceedings of the National Academy of Sciences of the United States of America*, vol. 102, no. 43, pp. 15593–15598, 2005.

[22] M. A. Björndahl, R. Cao, J. B. Burton et al., "Vascular endothelial growth factor-a promotes peritumoral lymphangiogenesis and lymphatic metastasis," *Cancer Research*, vol. 65, no. 20, pp. 9261–9268, 2005.

[23] F. Bock, J. Onderka, T. Dietrich et al., "Bevacizumab as a potent inhibitor of inflammatory corneal angiogenesis and lymphangiogenesis," *Investigative Ophthalmology and Visual Science*, vol. 48, no. 6, pp. 2545–2552, 2007.

[24] C. Cursiefen, L. Chen, L. P. Borges et al., "VEGF-A stimulates lymphangiogenesis and hemangiogenesis in inflammatory neovascularization via macrophage recruitment," *Journal of Clinical Investigation*, vol. 113, no. 7, pp. 1040–1050, 2004.

[25] S. Nakao, K. Maruyama, S. Zandi et al., "Lymphangiogenesis and angiogenesis: concurrence and/or dependence? Studies in inbred mouse strains," *The FASEB Journal*, vol. 24, no. 2, pp. 504–513, 2010.

[26] E. S. Chung, S. K. Chauhan, Y. Jin et al., "Contribution of macrophages to angiogenesis induced by vascular endothelial growth factor receptor-3-specific ligands," *American Journal of Pathology*, vol. 175, no. 5, pp. 1984–1992, 2009.

[27] R. Cao, M. A. Björndahl, P. Religa et al., "PDGF-BB induces intratumoral lymphangiogenesis and promotes lymphatic metastasis," *Cancer Cell*, vol. 6, no. 4, pp. 333–345, 2006.

[28] R. Cao, M. A. Björndahl, M. I. Gallego et al., "Hepatocyte growth factor is a lymphangiogenic factor with an indirect mechanism of action," *Blood*, vol. 107, no. 9, pp. 3531–3536, 2006.

[29] H. Kubo, R. Cao, E. Bräkenhielm, T. Mäkinen, Y. Cao, and K. Alitalo, "Blockade of vascular endothelial growth factor receptor-3 signaling inhibits fibroblast growth factor-2-induced lymphangiogenesis in mouse cornea," *Proceedings of the National Academy of Sciences of the United States of America*, vol. 99, no. 13, pp. 8868–8873, 2002.

[30] L. K. Chang, G. Garcia-Cardeña, F. Farnebo et al., "Dose-dependent response of FGF-2 for lymphangiogenesis," *Proceedings of the National Academy of Sciences of the United States of America*, vol. 101, no. 32, pp. 11658–11663, 2004.

[31] S. Nakao, S. Zandi, Y. Hata et al., "Blood vessel endothelial vegfr-2 delays lymphangiogenesis: an endogenous trapping mechanism links lymph- and angiogenesis," *Blood*, vol. 117, no. 3, pp. 1081–1090, 2011.

[32] K. Watari, S. Nakao, A. Fotovati et al., "Role of macrophages in inflammatory lymphangiogenesis: enhanced production of vascular endothelial growth factor C and D through NF-κB activation," *Biochemical and Biophysical Research Communications*, vol. 377, no. 3, pp. 826–831, 2008.

[33] S. Nakao, K. Noda, S. Zandi et al., "VAP-1-mediated M2 macrophage infiltration underlies IL-1beta- but not VEGF-A-induced lymph- and angiogenesis," *The American Journal of Pathology*, vol. 178, pp. 1913–1921, 2011.

[34] B. Regenfuß, J. Onderka, F. Bock, D. Hos, K. Maruyama, and C. Cursiefen, "Genetic heterogeneity of lymphangiogenesis in different mouse strains," *American Journal of Pathology*, vol. 177, no. 1, pp. 501–510, 2010.

[35] S. Nakao, S. Zandi, S. Faez, R. I. Kohno, and A. Hafezi-Moghadam, "Discontinuous LYVE-1 expression in corneal limbal lymphatics: dual function as microvalves and immunological hot spots," *The FASEB Journal*, vol. 26, no. 2, pp. 808–817, 2012.

[36] S. Nakao, T. Kuwano, C. Tsutsumi-Miyahara et al., "Infiltration of COX-2-expressing macrophages is a prerequisite for IL-1β-induced neovascularization and tumor growth," *Journal of Clinical Investigation*, vol. 115, no. 11, pp. 2979–2991, 2005.

[37] S. Nakao, Y. Hata, M. Miura et al., "Dexamethasone inhibits interleukin-1β-induced corneal neovascularization: role of nuclear factor-κB-activated stromal cells in inflammatory angiogenesis," *American Journal of Pathology*, vol. 171, no. 3, pp. 1058–1065, 2007.

[38] S. Yoshida, A. Yoshida, T. Ishibashi, S. G. Elner, and V. M. Elner, "Role of MCP-1 and MIP-1α in retinal neovascularization during postischemic inflammation in a mouse model of retinal neovascularization," *Journal of Leukocyte Biology*, vol. 73, no. 1, pp. 137–144, 2003.

[39] S. Ishida, T. Usui, K. Yamashiro et al., "VEGF164-mediated inflammation is required for pathological, but not physiological, ischemia-induced retinal neovascularization," *Journal of Experimental Medicine*, vol. 198, no. 3, pp. 483–489, 2003.

[40] C. Tsutsumi, K. H. Sonoda, K. Egashira et al., "The critical role of ocular-infiltrating macrophages in the development of choroidal neovascularization," *Journal of Leukocyte Biology*, vol. 74, no. 1, pp. 25–32, 2003.

[41] E. Sakurai, A. Anand, B. K. Ambati, N. van Rooijen, and J. Ambati, "Macrophage depletion inhibits experimental choroidal neovascularization," *Investigative Ophthalmology and Visual Science*, vol. 44, no. 8, pp. 3578–3585, 2003.

[42] K. Maruyama, M. Ii, C. Cursiefen et al., "Inflammation-induced lymphangiogenesis in the cornea arises from CD11b-positive macrophages," *Journal of Clinical Investigation*, vol. 115, no. 9, pp. 2363–2372, 2005.

[43] S. Jalkanen and M. Salmi, "VAP-1 and CD73, endothelial cell surface enzymes in leukocyte extravasation," *Arteriosclerosis, Thrombosis, and Vascular Biology*, vol. 28, no. 1, pp. 18–26, 2008.

[44] K. Noda, S. Nakao, S. Zandi, V. Engelstädter, Y. Mashima, and A. Hafezi-Moghadam, "Vascular adhesion protein-1 regulates leukocyte transmigration rate in the retina during diabetes," *Experimental Eye Research*, vol. 89, no. 5, pp. 774–781, 2009.

[45] A. Sica, P. Allavena, and A. Mantovani, "Cancer related inflammation: the macrophage connection," *Cancer Letters*, vol. 267, no. 2, pp. 204–215, 2008.

[46] C. Cursiefen, K. Maruyama, F. Bock et al., "Thrombospondin 1 inhibits inflammatory lymphangiogenesis by CD36 ligation on monocytes," *Journal of Experimental Medicine*, vol. 208, no. 5, pp. 1083–1092, 2011.

[47] C. Cursiefen, C. Rummelt, A. Jünemann et al., "Absence of blood and lymphatic vessels in the developing human cornea," *Cornea*, vol. 25, no. 6, pp. 722–726, 2006.

[48] T. R. Wuest and D. J. Carr, "VEGF-A expression by HSV-1-infected cells drives corneal lymphangiogenesis," *Journal of Experimental Medicine*, vol. 207, no. 1, pp. 101–115, 2010.

[49] S. Goyal, S. K. Chauhan, J. El Annan, N. Nallasamy, Q. Zhang, and R. Dana, "Evidence of corneal lymphangiogenesis in dry eye disease: a potential link to adaptive immunity?" *Archives of Ophthalmology*, vol. 128, no. 7, pp. 819–824, 2010.

[50] T. Dietrich, F. Bock, D. Yuen et al., "Cutting edge: lymphatic vessels, not blood vessels, primarily mediate immune rejections after transplantation," *Journal of Immunology*, vol. 184, no. 2, pp. 535–539, 2010.

[51] Y. H. Yucel, M. G. Johnston, T. Ly et al., "Identification of lymphatics in the ciliary body of the human eye: a novel "uveolymphatic" outflow pathway," *Experimental Eye Research*, vol. 89, no. 5, pp. 810–819, 2009.

[52] L. M. Heindl, C. Hofmann-Rummelt, W. Adler et al., "Tumor-associated lymphangiogenesis in the development of conjunctival squamous cell carcinoma," *Ophthalmology*, vol. 117, no. 4, pp. 649–658, 2010.

[53] L. M. Heindl, T. N. Hofmann, W. Adler et al., "Intraocular tumor-associated lymphangiogenesis a novel prognostic factor for ciliary body melanomas with extraocular extension?" *Ophthalmology*, vol. 117, no. 2, pp. 334–342, 2010.

[54] S. Yamagami and M. R. Dana, "The critical role of lymph nodes in corneal alloimmunization and graft rejection," *Investigative Ophthalmology and Visual Science*, vol. 42, no. 6, pp. 1293–1298, 2001.

[55] L. Chen, P. Hamrah, C. Cursiefen et al., "Vascular endothelial growth factor receptor-3 mediates induction of corneal alloimmunity," *Nature Medicine*, vol. 10, pp. 813–815, 2004.

[56] D. Singh, "Conjunctival lymphatic system," *Journal of Cataract and Refractive Surgery*, vol. 29, no. 4, pp. 632–633, 2003.

[57] H. B. Collin, "Endothelial cell lined lymphatics in the vascularized rabbit cornea," *Investigative Ophthalmology*, vol. 5, no. 4, pp. 337–354, 1966.

[58] S. Camelo, J. Kezic, A. Shanley, P. Rigby, and P. G. McMenamin, "Antigen from the anterior chamber of the eye travels in a soluble form to secondary lymphoid organs via lymphatic and vascular routes," *Investigative Ophthalmology and Visual Science*, vol. 47, no. 3, pp. 1039–1046, 2006.

[59] S. Camelo, L. Lajavardi, A. Bochot et al., "Drainage of fluorescent liposomes from the vitreous to cervical lymph nodes via conjunctival lymphatics," *Ophthalmic Research*, vol. 40, no. 3-4, pp. 145–150, 2008.

[60] T. Karpanen and K. Alitalo, "Molecular biology and pathology of lymphangiogenesis," *Annual Review of Pathology: Mechanisms of Disease*, vol. 3, pp. 367–397, 2008.

[61] R. Klein, B. E. K. Klein, and S. E. Moss, "The wisconsin epidemiologic study of diabetic retinopathy. IV. Diabetic macular edema," *Ophthalmology*, vol. 91, no. 12, pp. 1464–1474, 1984.

[62] A. Gandorfer, E. M. Messmer, M. W. Ulbig, and A. Kampik, "Resolution of diabetic macular edema after surgical removal of the posterior hyaloid and the inner limiting membrane," *Retina*, vol. 20, no. 2, pp. 126–133, 2000.

[63] J. F. Arevalo, M. Maia, H. W. Flynn Jr. et al., "Tractional retinal detachment following intravitreal bevacizumab (Avastin) in patients with severe proliferative diabetic retinopathy," *British Journal of Ophthalmology*, vol. 92, no. 2, pp. 213–216, 2008.

[64] J. B. Jonas, I. Kreissig, A. Sofker, and R. F. Degenring, "Intravitreal injection of triamcinolone for diffuse diabetic macular edema," *Archives of Ophthalmology*, vol. 121, no. 1, pp. 57–61, 2003.

[65] C. A. Wilson, B. A. Berkowitz, Y. Sato, N. Ando, J. T. Handa, and E. De Juan, "Treatment with intravitreal steroid reduces blood-retinal barrier breakdown due to retinal photocoagulation," *Archives of Ophthalmology*, vol. 110, no. 8, pp. 1155–1159, 1992.

[66] Q. D. Nguyen, S. Tatlipinar, S. M. Shah et al., "Vascular endothelial growth factor is a critical stimulus for diabetic macular edema," *American Journal of Ophthalmology*, vol. 142, no. 6, pp. 961–e4, 2006.

[67] T. Sakamoto, M. Miyazaki, T. Hisatomi et al., "Triamcinolone-assisted pars plana vitrectomy improves the surgical procedures and decreases the postoperative blood-ocular barrier breakdown," *Graefe's Archive for Clinical and Experimental Ophthalmology*, vol. 240, no. 6, pp. 423–429, 2002.

[68] Y. S. Yoon, T. Murayama, E. Gravereaux et al., "VEGF-C gene therapy augments postnatal lymphangiogenesis and ameliorates secondary lymphedema," *Journal of Clinical Investigation*, vol. 111, no. 5, pp. 717–725, 2003.

[69] S. Grimaldo, M. Garcia, H. Zhang, and L. Chen, "Specific role of lymphatic marker podoplanin in retinal pigment epithelial cells," *Lymphology*, vol. 43, no. 3, pp. 128–134, 2010.

[70] M. E. De Stefano and E. Mugnaini, "Fine structure of the choroidal coat of the avian eye: lymphatic vessels," *Investigative Ophthalmology and Visual Science*, vol. 38, no. 6, pp. 1241–1260, 1997.

[71] W. Krebs and I. P. Krebs, "Ultrastructural evidence for lymphatic capillaries in the primate choroid," *Archives of Ophthalmology*, vol. 106, no. 11, pp. 1615–1616, 1988.

[72] A. Sugita and T. Inokuchi, "Lymphatic sinus-like structures in choroid," *Japanese Journal of Ophthalmology*, vol. 36, no. 4, pp. 436–442, 1992.

[73] F. Schroedl, A. Brehmer, W. L. Neuhuber, F. E. Kruse, C. A. May, and C. Cursiefen, "The normal human choroid is endowed with a significant number of lymphatic vessel endothelial hyaluronate receptor 1 (LYVE-1)—positive macrophages," *Investigative Ophthalmology and Visual Science*, vol. 49, no. 12, pp. 5222–5229, 2008.

[74] H. Xu, M. Chen, D. M. Reid, and J. V. Forrester, "LYVE-1-positive macrophages are present in normal murine eyes," *Investigative Ophthalmology and Visual Science*, vol. 48, no. 5, pp. 2162–2171, 2007.

[75] Y. Ikeda, Y. Yonemitsu, M. Onimaru et al., "The regulation of vascular endothelial growth factors (VEGF-A, -C, and -D) expression in the retinal pigment epithelium," *Experimental Eye Research*, vol. 83, no. 5, pp. 1031–1040, 2006.

[76] J. W. Streilein, "Ocular immune privilege: the eye takes a dim but practical view of immunity and inflammation," *Journal of Leukocyte Biology*, vol. 74, no. 2, pp. 179–185, 2003.

[77] S. A. Stacker, M. E. Baldwin, and M. G. Achen, "The role of tumor lymphangiogenesis in metastatic spread," *The FASEB Journal*, vol. 16, no. 9, pp. 922–934, 2002.

[78] R. Clarijs, L. Schalkwijk, D. J. Ruiter, and R. M. de Waal, "Lack of lymphangiogenesis despite coexpression of VEGF-C and its receptor Flt-4 in uveal melanoma," *Investigative Ophthalmology and Visual Science*, vol. 42, no. 7, pp. 1422–1428, 2001.

[79] K. Birke, E. Lütjen-Drecoll, D. Kerjaschki, and M. T. Birke, "Expression of podoplanin and other lymphatic markers in the human anterior eye segment," *Investigative Ophthalmology and Visual Science*, vol. 51, no. 1, pp. 344–354, 2010.

[80] S. Breiteneder-Geleff, K. Matsui, A. Soleiman et al., "Podoplanin, novel 43-kd membrane protein of glomerular epithelial cells, is down-regulated in puromycin nephrosis," *American Journal of Pathology*, vol. 151, no. 4, pp. 1141–1152, 1997.

[81] A. Bill, "Blood circulation and fluid dynamics in the eye," *Physiological Reviews*, vol. 55, no. 3, pp. 383–417, 1975.

[82] J. J. McGetrick, D. G. Wilson, R. K. Dortzbach, P. L. Kaufman, and B. N. Lemke, "A search for lymphatic drainage of the monkey orbit," *Archives of Ophthalmology*, vol. 107, no. 2, pp. 255–260, 1989.

[83] A. J. Dickinson and R. E. Gausas, "Orbital lymphatics: do they exist?" *Eye*, vol. 20, no. 10, pp. 1145–1148, 2006.

[84] D. D. Sherman, R. S. Gonnering, I. H. Wallow et al., "Identification of orbital lymphatics: enzyme histochemical light microscopic and electron microscopic studies," *Ophthalmic Plastic and Reconstructive Surgery*, vol. 9, no. 3, pp. 153–169, 1993.

[85] H. E. Killer, H. R. Laeng, and P. Groscurth, "Lymphatic capillaries in the meninges of the human optic nerve," *Journal of Neuro-Ophthalmology*, vol. 19, no. 4, pp. 222–228, 1999.

Hindawi Publishing Corporation
Journal of Ophthalmology
Volume 2012, Article ID 498565, 6 pages
doi:10.1155/2012/498565

Research Article

Modulation of Vasomotive Activity in Rabbit External Ophthalmic Artery by Neuropeptides

Esmeralda Sofia Costa Delgado,[1] Carlos Marques-Neves,[2] Maria Isabel Sousa Rocha,[2] José Paulo Pacheco Sales-Luís,[1] and Luís Filipe Silva-Carvalho[2]

[1] *Clinical Department, CIISA, Faculty of Veterinary Medicine, Technical University of Lisbon, Alameda da Universidade Técnica, 1300-477 Lisbon, Portugal*
[2] *Instituto de Medicina Molecular and Instituto de Fisiologia, Faculdade de Medicina, Universidade de Lisboa, Avenida Professor Egas Moniz, 1649-028 Lisbon, Portugal*

Correspondence should be addressed to Esmeralda Sofia Costa Delgado, esmeralda@fmv.utl.pt

Received 8 August 2011; Revised 1 November 2011; Accepted 3 November 2011

Academic Editor: Shintaro Nakao

Purpose. To investigate the vasomotive activity upon the external ophthalmic artery of vasointestinal peptide (VIP) and neuropeptide Y (NPY) using a previously developed model. *Methods*. Isolated rabbit eyes ($n = 12$) were perfused *in situ* with tyrode through the external ophthalmic artery. Effects of intra-arterial injections of NPY 200 μg/ml (Group A; $n = 6$) and VIP 200 μg/ml (Group B; $n = 6$) on the recorded pressure were obtained. For statistical analysis, Student's paired t-test and Fast Fourier Transform were used. *Results*. Spontaneous oscillations were observed before any drug administration in the 12 rabbit models. NPY produced an increase in total vascular resistance and a higher frequency and amplitude of oscillations, while VIP evoked the opposite effects. *Conclusions*. This study provides evidence of vasomotion in basal conditions in rabbit external ophthalmic artery. Concerning drug effects, NPY increased arterial resistance and enhanced vasomotion while VIP produced opposite effects which demonstrates their profound influence in arterial vasomotion.

1. Introduction

Disturbances of ocular blood flow are involved in many ophthalmic diseases and therefore are of the utmost clinical relevance. The eye is one of the best perfused organs in the body. In humans and in experimental animals, the eye has two separate systems of blood vessels, which anatomically and physiologically differ: the retinal vessels, which supply part of the retina, and the uveal or ciliary blood vessels, which supply the rest of the eye. There is autonomic innervation of the extraocular vessels as well as of choroidal vessels [1, 2]. In primates, innervation of the central artery occurs as far as to the lamina cribrosa. There is no innervation of vessels of the retina although alpha, beta-adrenergic and cholinergic receptors are present [3, 4]. There are studies describing some innervation of the optic nerve head [5].

Besides there is mounting evidence that the retinal blood vessels have receptors for and sensitivity to neurotransmitters and neurohormones, including biologically active peptides [6, 7]. NPY and VIP are two neuropeptides that occur in peripheral nerves supplying both the eye and blood vessels to the brain [7, 8].

Vasoactive intestinal peptide (VIP) is a peptide hormone containing 28 amino acid residues produced in many areas of the human body including the gut, pancreas, and suprachiasmatic nuclei of the hypothalamus in the brain and is neuroprotective [9].

Neuropeptide Y (NPY) is a 36-amino acid peptide neurotransmitter found in the brain and autonomous nervous system, secreted by the hypothalamus, and it has been associated with several physiologic processes in the brain, blocking nociceptive signals and augmenting the vasoconstrictor effects of noradrenergic neurons [10].

They are both vasoactive, VIP nerve fibers are parasympathetic causing vasodilation, and NPY is generally associated with the sympathetics, although it is also found in

some parasympathetic neurons supplying the eye, suggesting a mixed autonomic origin [7]. In several organs, VIP seems to be colocalized with neuronal NOS and the same holds true for nitrergic choroidal innervation [11].

In this work, we used an isolated model of rabbit eye previously developed [12] to study the evoked vasomotor responses with NPY and VIP intra-arterial administration upon perfusion pressure and periodic oscillations at the rabbit external ophthalmic artery *in vitro*.

2. Methods

2.1. Anaesthesia and Surgical Procedures. Twelve hybrid NewZealand rabbits of either sex were used, weighing between 2,10 Kg and 3,90 Kg, mean 3,20 ± 0.157 Kg, anaesthetized with pentobarbital sodium (40 mg/Kg body weight iv, Eutasil, Sanofi, Portugal), supplemented as necessary, tracheostomised and artificially ventilated with O_2-enriched air applied using a positive pressure ventilator (Harvard Apparatus Ltd, UK). Body temperature was monitored and maintained constant (38-39°C) by using a servocontrolled heating blanket (Harvard Apparatus Ltd, UK). The external carotid artery and jugular vein were cannulated for the administration of drugs and bleeding, respectively. During the surgical procedures, arterial pressure (Neurolog System, Digitimer, UK), respiratory rate, and ECG (Neurolog System, Digitimer, UK) were monitored to assess the depth of anaesthesia. Heparin (1000 UI/Kg) was perfused through the external carotid artery, and a waiting time of 20 min was respected. After that euthanasia was performed with an overdose of pentobarbital sodium, the head was sectioned at cervical level and perfusion was commenced at the external carotid artery. Encephalon and intact cranial nerves were mechanically destroyed using a scalpel blade that entered the cranium through the foramen magnum, to ensure that the interference of stimuli originating outside the ocular globe in the central nervous system and the autonomous nervous system was abolished. The protocols and procedures were approved by the University Ethics Committee and conformed to the Helsinki Declaration.

2.2. Isolated Eye Model. External ophthalmic arteries were exposed, and a 0,6 mm outside diameter polypropylene tube was placed in the vessels with the aid of a surgical microscope (Shin Nippon, Japan). The three-way catheter was further connected to a continuous intravenous infusion apparatus (Semat, series 81706, UK) and to a pressure transducer (Neurolog System, Digitimer, UK). The effect of intraluminal pressure as a measure of total vascular resistance was assessed. The head was maintained immerse in a glass chamber containing O_2-enriched tyrode at a constant temperature of 38°C and controlled pH. Continuous infusion was commenced at a flow rate of 135 μL/min.

There was a period between the death of the animal and the beginning of the experiment that corresponded to 40.6 ± 0.93 minutes in Group A and 39.4 ± 0.93 minutes in Group B ($n = 12, P = 0.387$). Once perfusion commenced, an equilibration period was respected that corresponded to 16.0 ± 0.71 minutes in Group A and 15.4 ± 0.51 minutes in Group B ($n = 12, P = 0.511$). On what concerns the total time of an experiment, from the euthanasia of the animal until the end of the experiment, it was 110.4 ± 2.42 minutes in Group A and 109,2 ± 2,13 minutes in Group B ($n = 12, P = 0.719$). Since P values were greater than 0.05, differences were considered not significant, that is, the difference between means is not significantly greater than expected by chance.

2.3. Drug Injections. In group A ($n = 6$), response curves to three injections of NPY in a concentration of 200 μg/mL [13] were obtained. In group B ($n = 6$), response curves to three injections of VIP [13] in a concentration of 200 μg/mL were obtained. Injections were given intra-arterially in a volume of 0.1 mL in a system derivation, with a 20-minute interval and the waiting time respected intended to allow the pressure to return to a stable baseline. In the end, the pressure was calibrated to a value of 40 mm Hg to adjust pressure values obtained. Finally, methylene blue dye was injected through the ophthalmic artery to confirm eye perfusion by blue staining.

2.4. Drugs and Solutions. Tyrode solution comprises NaCl (137 mM), KCl (2.7 mM), $CaCl_2$ (1.8 mM), $MgCl_2$ (0.49 mM), NaH_2PO_4 (0.36 mM), $NaHCO_3$ (11.9 mM), glucose (5.6 mM), and distilled water (1 L). NPY (N9409) and VIP (V6130) both from Sigma Aldrich Chemie Gmbh P. O. 1120, 89552 Steinheim, Germany, were diluted in distilled water and freshly prepared.

2.5. Data Analysis. For the variables recorded, the baseline values were taken immediately before the beginning of the injection and compared with the ones obtained in the peak of the response. Perfusion pressure, frequency, and amplitude of the oscillations were evaluated before and after the drug injections. All recorded variables were digitised (Instrutech VR100B, Digitimer Ltd, UK) and recorded on videotape. Off-line analysis was done using a computer A/D system with data capture and analysis software (Chart for Windows, 5.0, USA). Data were analysed with GraphPad (InStat, version 3.00 for Windows 95, GraphPad Software, San Diego California USA) and are reported as mean ± standard error. Student's t-test for paired comparisons were performed to compare values obtained before and after the drug injections for perfusion pressure, frequency, and amplitude of the oscillations with $P < 0.05$ testing for significance. Data were tested for normal distribution with the Kolmogoroff-Smirnoff test.

Episodes of vasomotion were recorded, and the amplitudes and frequencies of the oscillations were characterized by fast fourier analysis. The frequency spectra of the oscillations are expressed in Hertz (Hz).

3. Results

3.1. Spontaneous Oscillations. Without any drug administration, spontaneous myogenic responses were observed in the 12 rabbit models showing oscillations of a medium frequency

Table 1: PP: Perfusion Pressure (mm Hg); Freq: Frequency of oscillations (number oscillations/min); Ampl: Amplitude of oscillations (mm Hg); NPY = Neuropeptide Y.

	Group A								
	Basal	First NPY	*P*	Basal	Second NPY	*P*	Basal	Third NPY	*P*
PP	9.1 ± 1.67	19.2 ± 3.49	<0.015	11.9 ± 1.66	15.9 ± 2.49	<0.008	10.7 ± 1.29	16.5 ± 2.23	<0.015
Freq	10.4 ± 5.00	19.2 ± 9.27	<0.002	7.2 ± 4.35	17.7 ± 8.83	0.034	5.7 ± 3.54	13.5 ± 7.38	0.011
Ampl	1.4 ± 0.73	2.7 ± 1.17	<0.021	0.7 ± 0.26	1.9 ± 0.71	<0.01	0.3 ± 0.06	0.7 ± 0.12	<0.01

Table 2: PP: Perfusion Pressure (mm Hg); Freq: Frequency of oscillations (number oscillations/min); Ampl: Amplitude of oscillations (mm Hg); VIP: Vasointestinal Peptide.

	Group B								
	Basal	First VIP	*P*	Basal	Second VIP	*P*	Basal	Third VIP	*P*
PP	23.9 ± 6.98	15.4 ± 4.31	<0.006	20.8 ± 5.40	12.9 ± 3.14	<0.004	18.6 ± 4.32	12.2 ± 3.37	0.001
Freq	13.6 ± 7.14	8.3 ± 5.00	0.001	9.8 ± 5.18	5.9 ± 3.80	0.015	7.8 ± 4.06	3.7 ± 2.16	0.004
Amp	2.7 ± 1.53	1.9 ± 1.17	0.050	2.4 ± 1.39	1.7 ± 1.11	<0.032	2.0 ± 1.23	1.5 ± 1.13	0.004

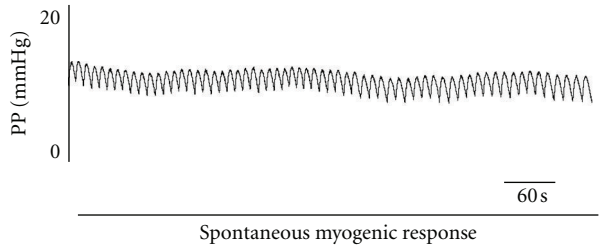

Figure 1: Example of basal periodic oscillations in vascular tone observed before any drug administration. On the *x* axis, the perfusion pressure recorded at the rabbit external ophthalmic artery is represented in mm Hg. In the *y* axis, we represent the time in seconds.

of 7.7 ± 1.71 oscillations per minute and a medium amplitude value of 2.1 ± 1.13 mm Hg (Figure 1).

3.2. NPY and VIP Effects on Perfusion Pressure. In Group A ($n = 6$) of experiments we observed that the intra-arterial delivered NPY elicited vasoconstriction. The first intra-arterial injection of 0.1 mL of NPY 200 μg/mL evoked an increase of 41%, the second intra-arterial injection elicited an increase of 25%, and the third registered an increase of 35% (Table 1). In Group B ($n = 6$), the arteries dilated in response to VIP. With the first intra-arterial injection, we registered a decrease of 29%, with the second administration a decrease of 29%, and the third evoked a decrease of 27% (Table 2).

3.3. NPY and VIP Effects on the Frequency of Periodic Oscillations. In Group A, with NPY, the frequency of the oscillations increased. The first injection resulted in increase of 36%, the second produced an increase of 47%, and the third an increase of 40% (Table 1). In Group B, with VIP, the frequency of the oscillations decreased. With the first intra-arterial injection, we registered a frequency decrease of 35%, with the second a decrease of 46%, and with the third administration a decrease of 45% (Table 2).

3.4. NPY and VIP Effects on the Amplitude of Periodic Oscillations. In Group A, with NPY, the amplitude of the oscillations increased. With the first injection, we registered an increase of 48%, with the second an increase of 63% and with the third an increase of 57% (Table 1). In Group B there was a decrease in the amplitude of the oscillations. The first injection of VIP made the amplitude of the oscillations decrease 30%, the second elicited a decrease of 29%, and the third a decrease of 25%($P = 0.004$) (Table 2, Figure 2).

3.5. Fast Fourier Analysis. As a result of the mathematical analysis with Fast Fourier Transform, a power spectrum density (PSD) was built for each rabbit. The most prominent frequency was considered as the principal frequency and was used to characterize the vasomotion pattern. The frequency spectrums illustrated the results displayed in Figure 3, although we could see the presence of several superimposed frequencies. So there was a marked increase in the frequency of the oscillations with NPY and a decrease following VIP administration (Figure 3).

4. Discussion

In this study, we characterized the reactivity of rabbit ocular vasculature to intraluminal pressure by perfusing the feeding external ophthalmic artery in a head-mounted preparation. This, thus, ruled out a central nervous system (CNS) mediation and led the authors to postulate that this *in vitro* model abolished the interference of stimuli originating outside the ocular globe, through the CNS, therefore proved that the spontaneous oscillations observed in basal conditions were independent of central regulation, being interpreted as vasomotion [12].

However, one cannot interpret this ex vivo model as representing a purely vasomotor paradigm devoid of any autonomic innervation. There are some 20 intrinsic choroidal neurons in the rabbit eye [11], and the sphenopalatine ganglion still intact in this preparation may receive trigeminal peptidergic collaterals also in the rabbit as it does in the rat.

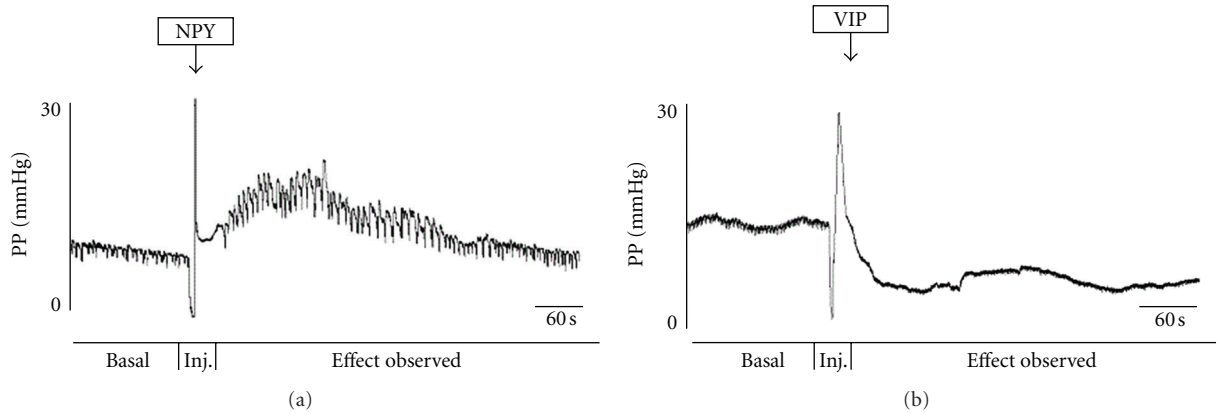

Figure 2: Example of changes in vascular tone observed after an intra-arterial injection of NPY in group A, causing vasoconstriction and increase in frequency and amplitude of the oscillations. We can see an example of an effect of an intra-arterial injection of VIP in perfusion pressure, producing vasodilation and decrease in frequency and amplitude of the oscillations. On the x axis, the perfusion pressure recorded at the rabbit external ophthalmic artery is represented in mm Hg. In the y axis, we represent the time in seconds.

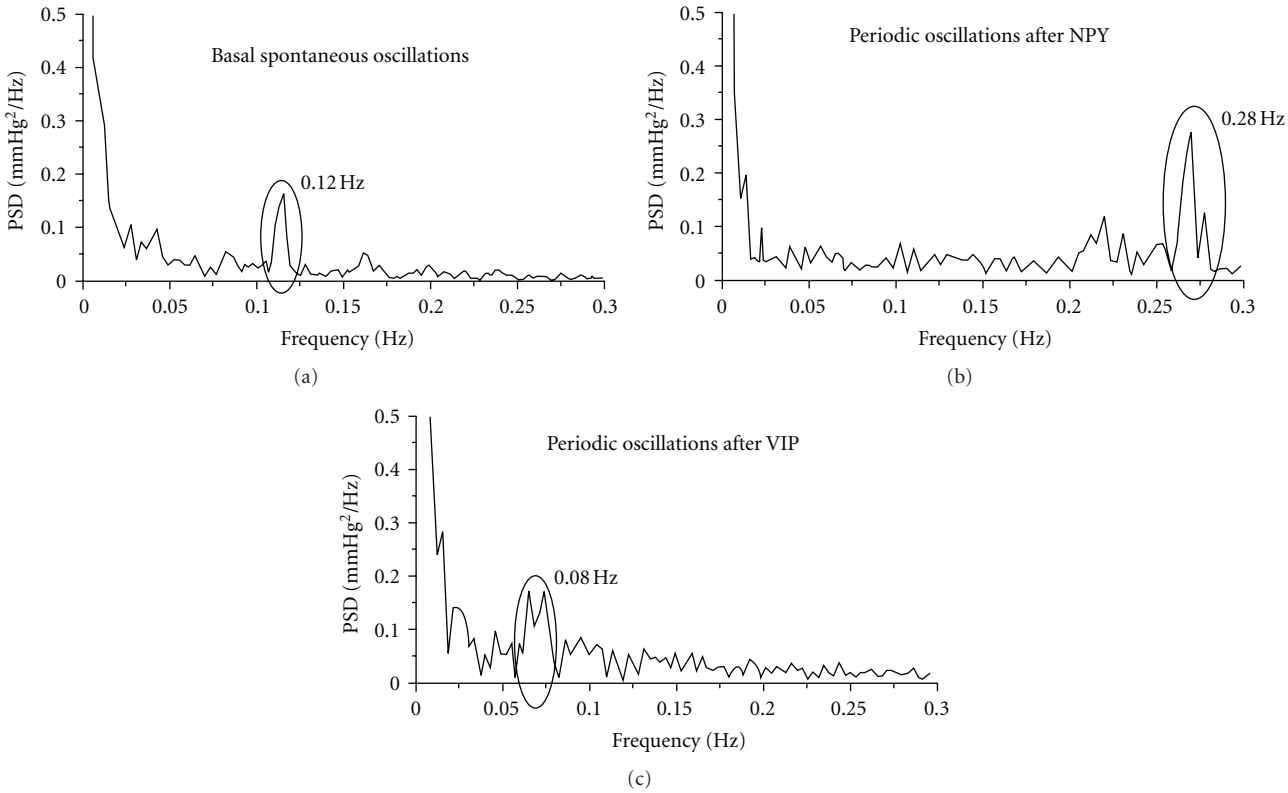

Figure 3: In the upper panel, the power spectrum density (PSD) of basal spontaneous oscillations obtained as a result of mathematical analysis with the Fast Fourier algorithm shows a major band at 0.12 Hz. In the middle panel, the power spectrum density obtained after Fourier analysis of the oscillations after NPY injection shows a major band around 0.28 Hz which results in an increase in the frequency of the oscillations, so there was a marked increase in the frequency of the spontaneous oscillations. In the lower panel, the power spectrum density obtained after VIP injection shows a peak frequency of 0.08 Hz, so there was a decrease in the frequency of the spontaneous oscillations.

The brain vasculature was shown to be one target structure for the innervated principal cells in the sphenopalatine ganglion [14], so ocular vasculature could be another target. Thus, peripheral "pre-central" neuronal reflexes may superimpose on vasomotor activity in the ocular vasculature.

Vasomotion is periodic oscillations in the tone of arterioles resulting in an intermittent supply of blood to individual microcirculatory units, facilitating oxygenation of tissues near prevenular capillaries [15]. The phenomenon is therefore assumed to play an important role in microcirculation.

In retinal microcirculation [16] and in isolated bovine [17] and porcine [18] retinal arterioles, the presence of vasomotion has been demonstrated. Recently, it has been proposed that disturbances in vasomotion might be important factors in the development of retinal lesions in diabetic maculopathy [19]. Therefore, a further characterization of vasomotion in ocular arteries is pertinent.

Although, in our study, the experimental design cannot determine the arterial segment responsible for the vasomotion observed, external ophthalmic artery/choroid/retina, clinical studies use ophthalmic artery haemodynamics as a measure of the overall function of the ophthalmic circulation [20].

We also quantified the responses to NPY and VIP, two neuropeptides that occur in peripheral nerves supplying the eye [7], by monitoring the perfusion pressure near the entry point to the eye as a measure of total vascular resistance.

Concerning the effects on vasoreactivity of intra-arterial administration, NPY and VIP showed opposite effects: NPY elicited a vasoconstrictor response, and VIP produced vasodilation of the external ophthalmic artery and its collaterals. These results show that, under *in vitro* perfusion, eye arteries present similar responses to NPY and VIP than those observed in *in vivo* models [21].

Yet previous studies have shown that VIP receptors and VIP-containing neurons are not uniformly distributed in the arterial vasculature and that VIP may have selective vasodilatory effects [22].

On what regards the effects on vasomotion, NPY produced an increase in total vascular resistance and vasomotion became more evident, exhibiting a higher frequency and amplitude of oscillations. The evoked vasomotor responses with VIP were vasodilation and decrease of the frequency and amplitude of the oscillations of myogenic tone, which is in favour of a functional role of perivascular peptides in the control of ocular circulation.

Being so, the results of this investigation have shown that neuropeptidergic innervation of the rabbit eye has a profound influence in arterial vasomotion, which might be important in diagnosis or therapeutics of ocular ischemic diseases.

Acknowledgment

This work was supported by CIISA (Centro de Investigação Interdisciplinar em Sanidade Animal). There are no financial interests in the equipment or methods described.

References

[1] A. Bill and G. O. Sperber, "Control of retinal and choroidal blood flow," *Eye*, vol. 4, no. 2, pp. 319–325, 1990.

[2] J. W. Kiel, "Choroidal myogenic autoregulation and intraocular pressure," *Experimental Eye Research*, vol. 58, no. 5, pp. 529–543, 1994.

[3] R. M. Mann, C. E. Riva, R. A. Stone, G. E. Barnes, and S. D. Cranstoun, "Nitric oxide and choroidal blood flow regulation," *Investigative Ophthalmology and Visual Science*, vol. 36, no. 5, pp. 925–930, 1995.

[4] J. J. Steinle, D. Krizsan-Agbas, and P. G. Smith, "Regional regulation of choroidal blood flow by autonomic innervation in the rat," *American Journal of Physiology*, vol. 279, no. 1, pp. R202–R209, 2000.

[5] A. Bergua, F. Schrödl, and W. L. Neuhuber, "Vasoactive intestinal and calcitonin gene-related peptides, tyrosine hydroxylase and nitrergic markers in the innervation of the rat central retinal artery," *Experimental Eye Research*, vol. 77, no. 3, pp. 367–374, 2003.

[6] A. M. Hoste, P. J. Boels, D. L. Brutsaert, and J. J. De Laey, "Effect of alpha-1 and beta agonists on contraction of bovine retinal resistance arteries *in vitro*," *Investigative Ophthalmology and Visual Science*, vol. 30, no. 1, pp. 44–50, 1989.

[7] X. Ye, A. M. Laties, and R. A. Stone, "Peptidergic innervation of the retinal vasculature and optic nerve head," *Investigative Ophthalmology and Visual Science*, vol. 31, no. 9, pp. 1731–1737, 1990.

[8] L. Edvinsson, "Functional role of perivascular peptides in the control of cerebral circulation," *Trends in Neurosciences*, vol. 8, no. 3, pp. 126–131, 1985.

[9] J. Fahrenkrug and P. C. Emson, "Vasoactive intestinal polypeptide: functional aspects," *British Medical Bulletin*, vol. 38, no. 3, pp. 265–270, 1982.

[10] W. F. Colmers and B. El Bahn, "Neuropeptide Y and Epilepsy," *Epilepsy Currents/American Epilepsy Society*, vol. 2, no. 3, pp. 53–58, 2003.

[11] C. Flügel, E. R. Tamm, B. Mayer, and E. Lutjen-Drecoll, "Species differences in choroidal vasodilative innervation: evidence for specific intrinsic nitrergic and VIP-positive neurons in the human eye," *Investigative Ophthalmology and Visual Science*, vol. 35, no. 2, pp. 592–599, 1994.

[12] E. Delgado, C. Marques-Neves, I. Rocha, J. Sales-Luís, and L. Silva-Carvalho, "Intrinsic vasomotricity and adrenergic effects in a model of isolated rabbit eye," *Acta Ophthalmologica*, vol. 87, no. 4, pp. 443–449, 2009.

[13] W. Yao, S. P. Sheikh, B. Ottesen, and J. C. Jorgensen, "The effect of neuropeptides on vessel tone and cAMP production," *Annals of the New York Academy of Sciences*, vol. 805, pp. 784–788, 1996.

[14] N. Suzuki, J. E. Hardebo, C. Owman et al., "Trigeminal fibre collaterals storing substance P and calcitonin gene-related peptide associate with ganglion cells containing choline acetyltransferase and vasoactive intestinal polypeptide in the sphenopalatine ganglion of the rat. An axon reflex modulating parasympathetic ganglionic activity?" *Neuroscience*, vol. 30, no. 3, pp. 595–604, 1989.

[15] A. G. Tsai and M. Intaglietta, "Evidence of flowmotion induced changes in local tissue oxygenation," *International Journal of Microcirculation*, vol. 12, no. 1, pp. 75–88, 1993.

[16] R. D. Braun, R. A. Linsenmeier, and C. M. Yancey, "Spontaneous fluctuations in oxygen tension in the cat retina," *Microvascular Research*, vol. 44, no. 1, pp. 73–84, 1992.

[17] C. Delaey and J. Van de Voorde, "Pressure-induced myogenic responses in isolated bovine retinal arteries," *Investigative Ophthalmology and Visual Science*, vol. 41, no. 7, pp. 1871–1875, 2000.

[18] P. Jeppesen, C. Aalkjær, and T. Bek, "Myogenic response in isolated porcine retinal arterioles," *Current Eye Research*, vol. 27, no. 4, pp. 217–222, 2003.

[19] T. Bek, "Diabetic maculopathy caused by disturbances in retinal vasomotion. A new hypothesis," *Acta Ophthalmologica Scandinavica*, vol. 77, no. 4, pp. 376–380, 1999.

[20] D. Y. Yu, E. N. Su, S. J. Cringle, and P. K. Yu, "Isolated preparations of ocular vasculature and their applications in

ophthalmic research," *Progress in Retinal and Eye Research*, vol. 22, no. 2, pp. 135–169, 2003.

[21] E. Lütjen-Drecoll, "Choroidal innervation in primate eyes," *Experimental Eye Research*, vol. 82, no. 3, pp. 357–361, 2006.

[22] A. N. Sidawy, H. Sayadi, J. W. Harmon et al., "Distribution of vasoactive intestinal peptide and its receptors in the arteries of the rabbit," *Journal of Surgical Research*, vol. 47, no. 2, pp. 105–111, 1989.

Hindawi Publishing Corporation
Journal of Ophthalmology
Volume 2012, Article ID 956705, 15 pages
doi:10.1155/2012/956705

Research Article

Refractive Development in the "ROP Rat"

Toco Y. P. Chui,[1] David Bissig,[2] Bruce A. Berkowitz,[2,3] and James D. Akula[1]

[1] *Department of Ophthalmology, Children's Hospital Boston and Harvard Medical School, 300 Longwood Avenue, Fegan 4, Boston, MA 02115, USA*
[2] *Department of Anatomy and Cell Biology, Wayne State University School of Medicine, Detroit, MI 48201, USA*
[3] *Department of Ophthalmology, Wayne State University School of Medicine, Detroit, MI 48201, USA*

Correspondence should be addressed to James D. Akula, ximtc@yahoo.com

Received 6 September 2011; Accepted 8 October 2011

Academic Editor: Shintaro Nakao

Although retinopathy of prematurity (ROP) is clinically characterized by abnormal retinal vessels at the posterior pole of the eye, it is also commonly characterized by vascular abnormalities in the anterior segment, visual dysfunction which is based in retinal dysfunction, and, most commonly of all, arrested eye growth and high refractive error, particularly (and paradoxically) myopia. The oxygen-induced retinopathy rat model of ROP presents neurovascular outcomes similar to the human disease, although it is not yet known if the "ROP rat" also models the small-eyed myopia characteristic of ROP. In this study, magnetic resonance images (MRIs) of albino (Sprague-Dawley) and pigmented (Long-Evans) ROP rat eyes, and age- and strain-matched room-air-reared (RAR) controls, were examined. The positions and curvatures of the various optical media were measured and the refractive state (R_x) of each eye estimated based on a previously published model. Even in adulthood (postnatal day 50), Sprague-Dawley and Long-Evans ROP rats were significantly myopic compared to strain-matched controls. The myopia in the Long-Evans ROP rats was more severe than in the Sprague-Dawley ROP rats, which also had significantly shorter axial lengths. These data reveal the ROP rat to be a novel and potentially informative approach to investigating physiological mechanisms in myopia in general and the myopia peculiar to ROP in particular.

1. Introduction

Retinopathy of prematurity (ROP) presents as abnormal retinal blood vessels in an ophthalmoscopic exam of the premature infant. Evidence indicates that the appearance of the abnormal retinal blood vessels in ROP is instigated by changes in the neural retina [1, 2]. In addition, infants born prematurely are at increased risk for developing a range of structural ophthalmic sequelae including impaired ocular growth and increased incidence and magnitude of refractive error, particularly myopia [3, 4]. Myopia is a mismatch between the light-focusing power of the anterior segment and the axial length of the eye in which the visual image comes to a focus in front of the retina. Myopia is therefore typically associated with longer-than-average eyes [5]. Paradoxically, in ROP myopia the eye is usually small [3, 4, 6–14]. These common, clinically important ROP outcomes—vascular, neurologic, and structural—are likely interrelated.

Visual impairment, with a basis in the neural retina, is commonly found in subjects with a history of ROP, even when the vasculopathy was mild [15–20]. Specifically, psychophysical dark-adapted and increment threshold functions obtained in ROP subjects show higher *eigengrau* (optic nerve signaling in darkness [21]) values [22, 23], likely a consequence of disorganized [24] or fewer photoreceptors [25]; subtle differences in the vascular supply may also be at play [25]. Notably, the psychophysical changes are most marked in ROP subjects with high myopia while such abnormalities are *not* found in similarly myopic control subjects [26]. Electroretinographic (ERG) studies of retinal function also reveal deficits that are significantly associated with early myopia [27]. Defects in "ON signals" are associated with anomalous eye growth [28] and are abnormal in the ERGs of eyes with a history of ROP [26, 29]. For instance, there is evidence of a depressed postreceptor ON signal in the multifocal ERG (mfERG) responses of myopic children with a history of mild ROP that is not found in myopes

with no ROP [29]. Taken together, the psychophysical and ERG data from ROP and control subjects with and without myopia imply that deficits in retinal function in ROP are not explained by myopia alone [27]. Despite refractive errors being collectively the most common sequela of ROP and therefore of high clinical importance, the mechanisms underlying the altered eye growth remain poorly understood. No doubt this is partly for lack of a relevant animal model.

The retina controls eye growth and refractive development [30, 31]. Evidence from simian eyes [32, 33] strongly indicates that it is the peripheral retina, in particular, which is most important to these processes (although the evidence in humans is weaker [34]). Notably, the peripheral retina is avascular in ROP. The avascular peripheral retina must have altered function, and thus it should not be surprising that the vasculopathy which clinically characterizes ROP is also strongly associated with altered eye growth and ametropia [8–11, 35, 36].

Rat pups exposed to a clinically relevant [37] alternation of relatively high and low oxygen during the first weeks after birth develop a retinopathy that models human ROP [37, 38]. This oxygen-induced retinopathy (OIR) represents a convenient *in vivo* model in which to study ROP that has been widely adopted, the so-called "ROP rat." The ROP rat's vascular abnormalities include an avascular peripheral retina and neovascularization [39–41], as in human ROP [42]. Also as in human ROP, retinal function is persistently abnormal [43–52]. Ocular structures have been studied in normal rats but have received only limited attention in ROP rats. Whether or not the ROP rat mimics the ametropias common to human ROP remains to be determined, although, in a histological study of young ROP rats with active disease, the OIR eye was found to be smaller with a relatively shorter anterior segment than the room-air-reared (RAR) rat's eye [53], as is again the case in human ROP [3, 4].

Manganese-enhanced magnetic resonance imaging (MRI) of the retina in RAR rats finds that it thins following a posterior-to-periphery gradient; in contrast, ROP rats' retinae are more uniform in thickness [47, 52]. As the eye grows, the peripheral retina, posterior to the iris and anterior to the equator (where the ocular muscles attach), may "stretch" to pave a larger area. A failure of the eye to grow in this fashion would be reflected in the more uniform retinal thickness of the ROP rat. Calcium channel activity in the postreceptor retina is supernormal during active disease in ROP rats and decreases as the vasculature matures [47, 52]. Likewise, relative to posterior retina (and to any region of normal retina), oxygen tension is lower in the avascular periphery of OIR eyes [54]. Changes in autoregulation of retinal oxygenation persist long after active disease has resolved [55]. That the retina and its circulation are rendered persistently dysfunctional in ROP rats might limit its ability to mediate emmetropization by regulating the growth of the sclera.

To be both small and myopic, the anterior segment of an eye must be of substantially higher-than-normal dioptric power. The hyaloidal vasculature that supplies the developing lens is present in the prematurely born infant [56, 57] and persists, much engorged, in ROP [57, 58]. MRI reveals that the same is true in the ROP rat [59]. Furthermore, in the RAR rat, the regression of the hyaloid is well coordinated with the development of other ocular structures, such as the vitreous chamber and crystalline lens; in the ROP rat, growth of ocular structures and hyaloidal regression proceed in a less-coordinated fashion [59]. Prolonged hyperemia of the anterior segment might lead to changes in the shape and thickness of the lens and cornea that, combined with a shorter anterior segment length, would lead to increased refractive power. Thus, it is plausible that the ROP rat models the peculiar ametropia common to ROP: small-eyed myopia.

In summary, the refractive state of the eye depends upon the refractive indices and curvatures of its various media and their spatial relationships to each other and the retina, and there is plentiful reason to suspect that the development of the optic media is altered in ROP. Assessing the refractive state of small eyes using traditional approaches such as retinoscopy is notoriously difficult. Further, the so-called "small-eye artifact" is well documented [60] but remains problematic and poorly specified [61]. Some modern approaches, like wavefront sensing and automated photorefracting [28, 62], are less variable but are not immune to the artifactual distortion of small-eye refractions. Furthermore, those methods do not provide details about the relative contributions of the cornea and lens or their relative positions. Advanced imaging techniques like MRI permit inspection of these surfaces noninvasively and, importantly, in their intact state (something that cannot be achieved *ex vivo*) and do so *simultaneously*. They are also theoretically immune to artifacts of eye size wherein the retinal origin of reflections is problematic [63]. Other approaches, such as high-frequency ultrasound, optical coherence tomography, and multiple-wavelength interferometry may (especially in the future) be able to produce biometry of resolution comparable to today's MRI. A high-quality schematic eye for the adult rat is available [64] that provides the refractive indices of the cornea and lens. Allowing for a number of assumptions (detailed below), the schematic eye provides a framework from which the refractive status of *any* rat eye can be estimated from an MRI of the globe. In this study, structural measurements were obtained from MRIs of immature and adult ROP and RAR rat eyes and referenced to the previously published schematic eye to calculate refractive state (R_x). The calculations suggest that the adult ROP rat is, indeed, characterized by small-eyed myopia. A comparison between albino (Sprague-Dawley) and pigmented (Long-Evans) strains is also included.

The ROP rat can provide insights into refractive development that cannot be observed from traditional myopia models (e.g., form deprivation [5, 65]) wherein the eye is large and can provide a basis for biochemical (genetic, protein, etc.) investigations into the most common and least studied clinical sequela of ROP: refractive error.

2. Materials and Methods

2.1. Subjects. Sprague-Dawley albino and Long-Evans hooded rats were studied. As described elsewhere in detail [46], OIR was induced in ROP rats by placing pups and dams

in an OxyCycler (Biospherix Ltd., Lacona, NY, USA) and exposing them to alternating 24-hour periods of 50% and 10% oxygen from postnatal day (P) 0, the day of birth, to P14 [39]. This "50/10 model" reliably produces peripheral neovascularization and increased tortuosity of the posterior retinal arterioles [39, 44, 46, 47, 66]. RAR rats served as controls. The Sprague-Dawley 50/10 model rat is considered the canonical 50/10 model [41].

2.2. Magnetic Resonance Imaging. The present images were previously collected and analyzed as part of our ongoing MRI studies of the neural retina. Most of these images were used to generate previous reports (summarized in Berkowitz and Roberts, 2010, [51] and Berkowitz et al., 2011 [52]). The imaging methods, briefly described here, are detailed therein and elsewhere: after rats were anesthetized with freshly prepared 36% urethane IP (~0.083 mL/20 g; Sigma-Aldrich, Milwaukee, WI, USA), T_1-weighted spin-echo images were obtained on either a 4.7 T Bruker Avance system (repetition time, TR = 350 s; echo time, TE = 16.7 ms; Sprague-Dawley images) or a 7 T Bruker ClinScan system (TR = 1 s; TE = 13 ms; Long-Evans images) using a 1 cm diameter surface coil placed around the left eye. A cross-sectional image of the left eye was collected as a single, 600 μm thick slice passing through the optic nerve head and pupil center. To be deemed suitable for analysis, both the pupil and optic nerve needed to be clearly visible in all images, indicating negligible deviation from the central axis of the eye. In-plane axial spatial resolution (i.e., along a line passing though the cornea, pupil, lens, and central retina) was always $\leq$25 μm/pixel width.

2.3. Image Analyses. All images were analyzed using a custom-developed MATLAB (The Mathworks, Inc., Natick, MA, USA) program. First, each MR image was rotated so that the plane of the *ora serrata* was parallel with the horizontal axis. Two intensity plots were then obtained along the lines passing (a) through the pupil center and the optic nerve head (ONH) and (b) through the plane of the *ora serrata*. Then, each image was thresholded into a binary (black and white) image for segmentation of the ocular structures from the fluid bodies (e.g., air and aqueous and vitreous humors). From the intensity plots and segmented images, the positions of the ocular media and their curvatures were, respectively, determined.

2.3.1. Positions of the Ocular Media. Measures of ocular dimensions were determined from the peaks and troughs on the first derivative of the intensity plots assuming that the edges of the ocular surfaces corresponded to the most rapid changes in intensity. The following biometric parameters, based upon Robb's [67], were thus obtained (Figure 1): (1) the "diameter" between the apex of the cornea and the posterior pole of the retina (axial length, *d*), (2) the portion of the axial length from the apex of the cornea to the plane of the *ora serrata* (anterior segment length, *c*), (3) the remaining distance from the *ora serrata* to the posterior pole (posterior segment length, *h*), (4) the diameter of the eye along the plane of the *ora serrata* (equatorial diameter, *e*), (5) lens thickness (LT), and (6) equatorial diameter (LE).

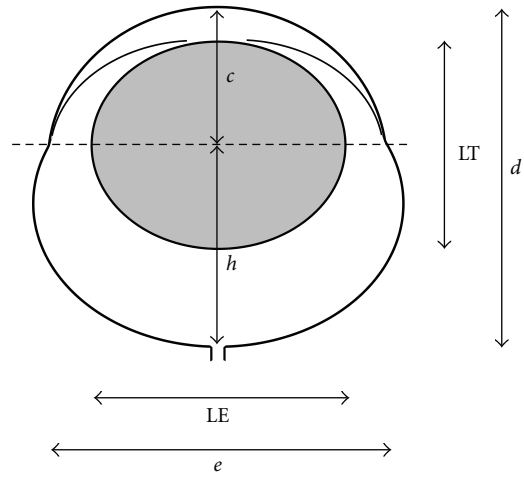

Figure 1: Schematic diagram showing the ocular dimensions obtained from the MRI. *d:* axial length; *c:* anterior segment length; *h:* posterior segment length; *e:* equatorial diameter at the plane of the *ora serrata* (*dashed line*); LT: lens axial thickness; LE: lens equatorial diameter.

2.3.2. Measurements of Curvature. Edge detection on the binary image was performed using the Canny method available in MATLAB. The subset of edge data from the relevant ocular surfaces (cornea, lens, and retina) was selected by the operator (TYPC) on the MR image from the superset of detected edges (Figure 2(b)). Occasionally, edge detection on the full anterior lens surface was hindered by the iris; in these cases the operator added edge data by tracing the obscured region of the surface manually and removed the iridic edge from further analysis. Following segmentation, the anterior cornea surface, anterior lens surface, and posterior lens surface were identified by the operator and circles were fitted through the respective edge data using a least-squares approach (Figures 2(c) and 2(d)), providing radius of curvature parameters for the optical media. These measurements were validated by a second reviewer (DB) for a large subset of images using a less-automated approach, developed in R [68], which yielded nearly identical results (not shown).

2.4. Calculation of Refractive State. The refractive state of the rat eye was computed based on the ocular dimensions and the curvatures of its various refractive surfaces measured from the MR images using either the core lens model (Figure 3) of Hughes (1979) [64] or assuming a homogeneous lens. Refractive indices of all ocular media were adopted from Hughes as constants [64]. The parameters used and the values employed, or that they were directly measured or derived, are given in Table 1 (parameters not used in the homogeneous lens model are marked as "not applicable" by "NA").

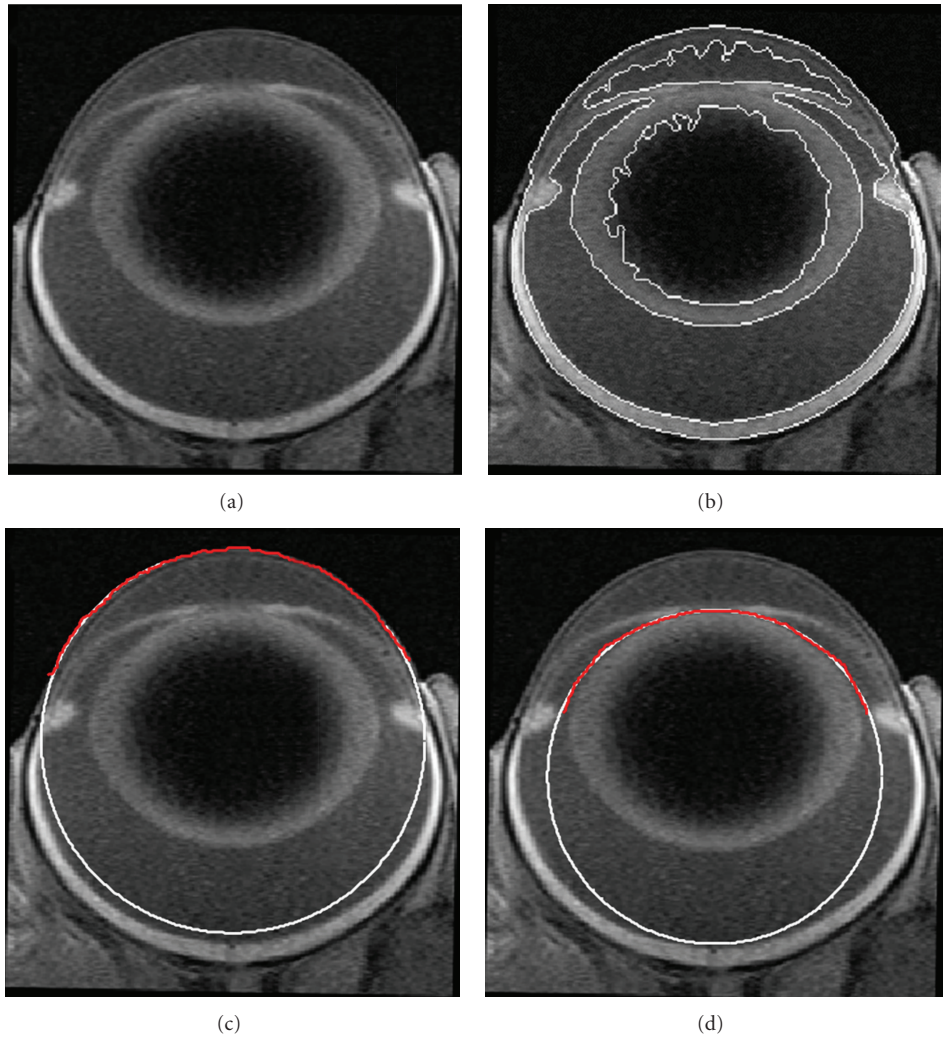

Figure 2: (a) MR image of a Long-Evans control rat P50. (b) The same image with the detected edges. (c) Circle (*white*) fit to the edge data of the anterior cornea surface (*red*). (d) Circle (*white*) fit to the edge data of the anterior lens surface (*red*).

The curvature of the anterior corneal surface (rC1) was measured as described above. However, edge detection of the posterior corneal surface proved unsatisfactory. Thus, in the final analysis, measurements of the corneal thickness (A2 − A1) and the curvature of the posterior corneal surface (rC2) were not made but were instead derived for each MR image based on the ratio of (A2 − A1)/(A7 − A1) and rC1/rC2 obtained from Hughes' [64] study, respectively. The whole lens thickness (LT = A6 − A3) and curvatures of the anterior and posterior lens surfaces (rL1, rL2) were measured directly in the study. However, for the core lens model, the core lens thickness (A5 − A4) was scaled linearly for each MR image based on the measured LT, and the ratio of core thickness to lens thickness, (A5 − A4)/LT, described by Hughes. Since the lens core of this model is spherical [64], the radii of curvature for the anterior and posterior core lens surfaces (rLC1, rLC2) were, respectively, computed as plus and minus half of the derived core lens thickness.

The refractive state of the eye was derived by calculating and combining the dioptric powers and the principal points of the cornea and lens components following the method of Southall [69] and the notation in Hughes [64]. The complete formulae needed to satisfy (1) through (4), below, are given in the Appendix.

The power of the cornea (FC) was calculated as

$$\mathrm{FC} = \mathrm{F1} + \mathrm{F2} - \mathrm{c1} \cdot \mathrm{F1} \cdot \mathrm{F2}, \tag{1}$$

where F1 and F2 are the respective powers (D) of the anterior and posterior surface of the cornea, and c1 is the reduced interval (m) between them.

The power of the lens was calculated in two ways, assuming either a homogenous lens ($\mathrm{FL}_{\mathrm{hmgns}}$) or using the core lens model ($\mathrm{FL}_{\mathrm{core}}$) of Hughes [64]. For the core lens model,

$$\mathrm{FL} = \mathrm{F}(3,4) + \mathrm{F}(5,6) - \mathrm{s} \cdot \mathrm{F}(3,4) \cdot \mathrm{F}(5,6), \tag{2}$$

where F(3,4) and F(5,6) are the respective powers of the anterior and posterior lens system, including half of the core in each, and s is the reduced interval between the anterior

Table 1: Parameters for refractive state estimation in rat eye.

Category	Parameters	Symbol	Homogeneous lens model	Core lens model
Refractive indices*	Air	n1	1.000	1.000
	Cornea	n2	1.380	1.380
	Aqueous and vitreous humors	n3, n7	1.337	1.337
	Lens cortex	n4, n6	NA	1.390
	Lens core	n5	1.683	1.500
Axial positions (m)	Anterior cornea surface	A1	Measured from MRI	Measured from MRI
	Posterior cornea surface	A2	Scaled†	Scaled†
	Anterior lens surface	A3	Measured from MRI	Measured from MRI
	Anterior core lens surface	A4	NA	Scaled†
	Posterior core lens surface	A5	NA	Scaled†
	Posterior lens surface	A6	Measured from MRI	Measured from MRI
	Retina	A7	Measured from MRI + 130 μm	Measured from MRI + 130 μm
Radii of curvature (m)	Anterior cornea surface	rC1	Measured from MRI	Measured from MRI
	Posterior cornea surface	rC2	Scaled†	Scaled†
	Anterior lens surface	rL1	Measured from MRI	Measured from MRI
	Anterior core lens surface	rLC1	NA	(A5 − A4)/2
	Posterior core lens surface	rLC2	NA	(A5 − A4)/2
	Posterior lens surface	rL2	Measured from MRI	Measured from MRI
Dioptric powers (D)	Cornea	FC	Equation (1)	Equation (1)
	Lens	FL	Reduced equation (2) (FL_{hmgns})	Equation (2) (FL_{core})
	Whole eye	FE	Equation (3) (FE_{hmgns})	Equation (3) (FE_{core})
	Refractive state	R	Equation (4) (R_{hmgns})	Equation (4) (R_{core})

* Refractive indices are adopted from Hughes (1979).
† Parameters were obtained by scaling linearly to the values obtained from Hughes' study.

and posterior lens system. When the homogenous lens was assumed, the terms relating to the core lens (F4 and F5) were omitted and the equation for FL_{hmgns} adjusted accordingly (including changing the reduced interval to be that between the anterior and posterior lens surface; see the appendices).

Hughes' [64] formula was used in the final determination of R. First, the refracting power of the whole eye was derived, for both the homogeneous (FE_{hmgns}) and core lens (FE_{core}) models, as

$$FE = FC + FL - cE \cdot FC \cdot FL, \quad (3)$$

where cE is the reduced interval between the cornea and lens components (FC, FL). Second, R was derived (for both lens models) by

$$R = \frac{n7}{(A7 - A1) - A1H'} - FE. \quad (4)$$

In (4), A1H′ is the distance (m) between the anterior cornea surface (A1) and the second principal point of the eye (H′).

2.5. Data Analyses. R was evaluated by analysis of variance (ANOVA). Because significant changes in R were detected between levels of factors, the sources of the changes were explored by evaluating the dioptric powers of the cornea (FC_{core}) and lens (FL_{core}) in a second ANOVA and the ratio of anterior to posterior depth (c/h) in a third ANOVA. To determine if axial length was affected by ROP, d was evaluated in a fourth ANOVA. To detect changes in the gross shape of the eye and lens, the ratio of axial length to equatorial diameter (d/e) and lens thickness and diameter (LT/LE) were also, respectively, evaluated in a fifth and sixth ANOVA. *Post hoc* testing was performed using t-tests corrected by the Bonferroni method. The acceptable type-1 error rate (α) for all tests was 5%, but because the parameters of the multiple analyses were not likely independent, significance for each ANOVA was set to a more conservative $P \leq 0.01$.

3. Results and Discussion

Ninety images were suitable for analysis, 56 from Sprague-Dawley rats (24 RAR, 32 ROP) and 34 from Long-Evans rats (17 RAR, 17 ROP). R was estimated for each animal, and the results are plotted in Figures 4(a) and 4(b). As shown therein, data were collected at approximately postnatal day (P) 14 (at the end of the induction of retinopathy [39]), at ~P20 (when the disease is active and neovascularization is present [44, 46, 51, 54, 55]), and at ~P50 (an "adult" eye [70–73] with "normal" vasculature [53]). Analysis of these R data by lens model × age × group × strain repeated measures (lens model) ANOVA revealed significant main effects for all factors and several significant interaction effects, as discussed below.

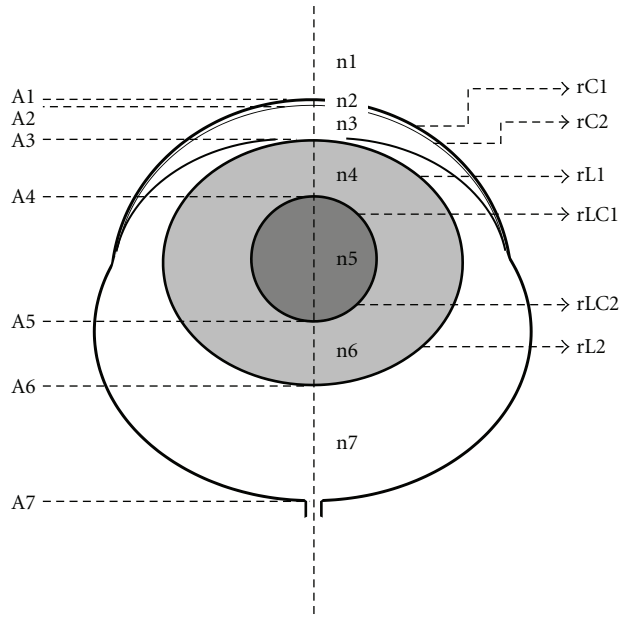

Figure 3: Schematic rat eye model with main parameters needed for refractive state estimation (see Table 1). A1 (corneal surface) through A7 (vitreoretinal border) are distances along the horizontal dashed line; 130 μm was added to A7 to approximately account for the postreceptor retina contribution. If A1 is set to 0 mm from corneal surface and numbers increase from top to bottom, then rC1, rC2, rL1, and rLC1 are positive, while rLC2 and rL2 are negative.

3.1. Core versus Homogenous Lens Model. The R& results obtained using the core (Figure 4(a)) and homogenous (Figure 4(b)) lens models were highly correlated ($r = 0.94$). As shown in Figure 4(c), which plots respective R& means (±SEM) for ROP and RAR Sprague-Dawley and Long-Evans rats from the ~P50 data, the homogenous model tended to yield relatively less myopic "refractions" (F(model) = 59.8, df = 1,78, $P < 10^{-10}$): in every case the homogenous lens model predicted less average myopia (although not always so in individual rats). There was not, however, a significant model × group interaction (F(model × group) = 2.55, df = 1,78, $P = 0.114$), so that interpretation of the ROP *versus* RAR data does not depend significantly upon the lens model selected. Hughes preferred the core lens model since it produced refractive estimates closer to his (roughly emmetropic) assessments of the refractive state of the adult rat eye [74]; in the present study, however, it is the homogenous lens model that produced R& estimates closest to emmetropia. Careful reevaluation of Hughes' values (his Table 2 [64]) using his core lens model yields slightly hyperopic refractive estimates for his rats. Therefore, the discrepancy between Hughes' data and the data in the present study may be due to the age of the rats, which were 115 to 130 days old in that study. Furthermore, advances in noninvasive imaging techniques may soon permit analysis of the lens gradient in the rat *in vivo* [75], improving estimates of refractive state. In any event, it is likely that the normal rat is approximately emmetropic throughout its adult life [61, 76].

3.2. Emmetropization. There was strong evidence of emmetropization (Figures 4(a) and 4(b)) in RAR and ROP Sprague-Dawley rats (*dashed light blue and light red lines*) as well as ROP Long-Evans rats (*dark red lines*) resulting in a highly significant effect of age (F(age) = 32.6, df = 2,78, $P < 10^{-10}$). On the other hand, the change in R& in normal Long-Evans rats (*dark blue lines*), who were relatively emmetropic at ~P14 and ~P20, and remained similarly myopic ~P50, was significantly less (F(age × group) = 12.2, df = 2,78, $P < 10^{-4}$). Two interesting elements of the emmetropization process revealed in these data are discussed below.

First, in the R& data of normal, RAR rats, the young Sprague-Dawley rats appeared highly myopic and became relatively less so over time. In this respect, the Sprague-Dawley rats differed significantly from the Long-Evans rats (F(strain) = 12.0, df = 1,78, $P = 0.001$). Retinoscopic measurements of refractive development in the pigmented (Brown Norway) rat have not shown systematic changes with age [77], consistent with the data from the pigmented rats herein, but no attempt has (to the authors' knowledge) been made to monitor the refractive development in the albino rats' eye. Nevertheless, the standard process of emmetropization—progression from hyperopia to emmetropia [78]—is the obverse of the progression found herein in the RAR Sprague-Dawley rats.

Second, *post hoc* testing revealed that in the adult animals (~P50), ROP rats were significantly more myopic than RAR controls ($P = 0.007$). This was despite the fact that the Sprague-Dawley ROP rats were *less* myopic at ~P14 than the RAR rats of the same strain. That is, regardless the amount of ametropia in each group at ~P14, emmetropization left both the Sprague-Dawley and Long-Evans ROP rats myopic at ~P50, relative to strain-matched RAR controls (F(age × strain × group) = 11.7, df = 2,78, $P < 10^{-4}$).

3.3. Severity of Ametropia and Strain. By retinoscopy, many (if not all) strains of rats appear hyperopic [77, 79]. Hooded-rats, like the Long-Evans, appear approximately 5–15 D more hyperopic than Sprague-Dawley rats. Estimates of refractive state by visually evoked potential (VEP) found rats are, in fact, more emmetropic than retinoscopy indicates [61]. Nevertheless, in the data from the adult rats in the present study, R& was correspondingly more relatively myopic in the Sprague-Dawley than Long-Evans rats (Figure 4(c)). Indeed, the magnitude of ametropia in RAR Long-Evans rats was similar to that in the ROP Sprague-Dawley animals (i.e., the second and third sets of columns in Figure 4(c) appear comparable).

Thus, by retinoscopy and now by MRI "refractions," the albino strain appears more emmetropic than the pigmented one. However, caution in interpretation of this finding is urged because the *direction* of the pigmented rats' measured ametropia is opposite using each approach: more hyperopic by retinoscopy and more myopic herein. Since the rat eye is so powerful, tiny errors, such as those from rounding, in the refractive indices used in the calculations of R& would result in large changes in the estimate of the refractive power of the eye. Indeed, it is quite plausible that pink- and black-eyed animals' optical media would refract light somewhat

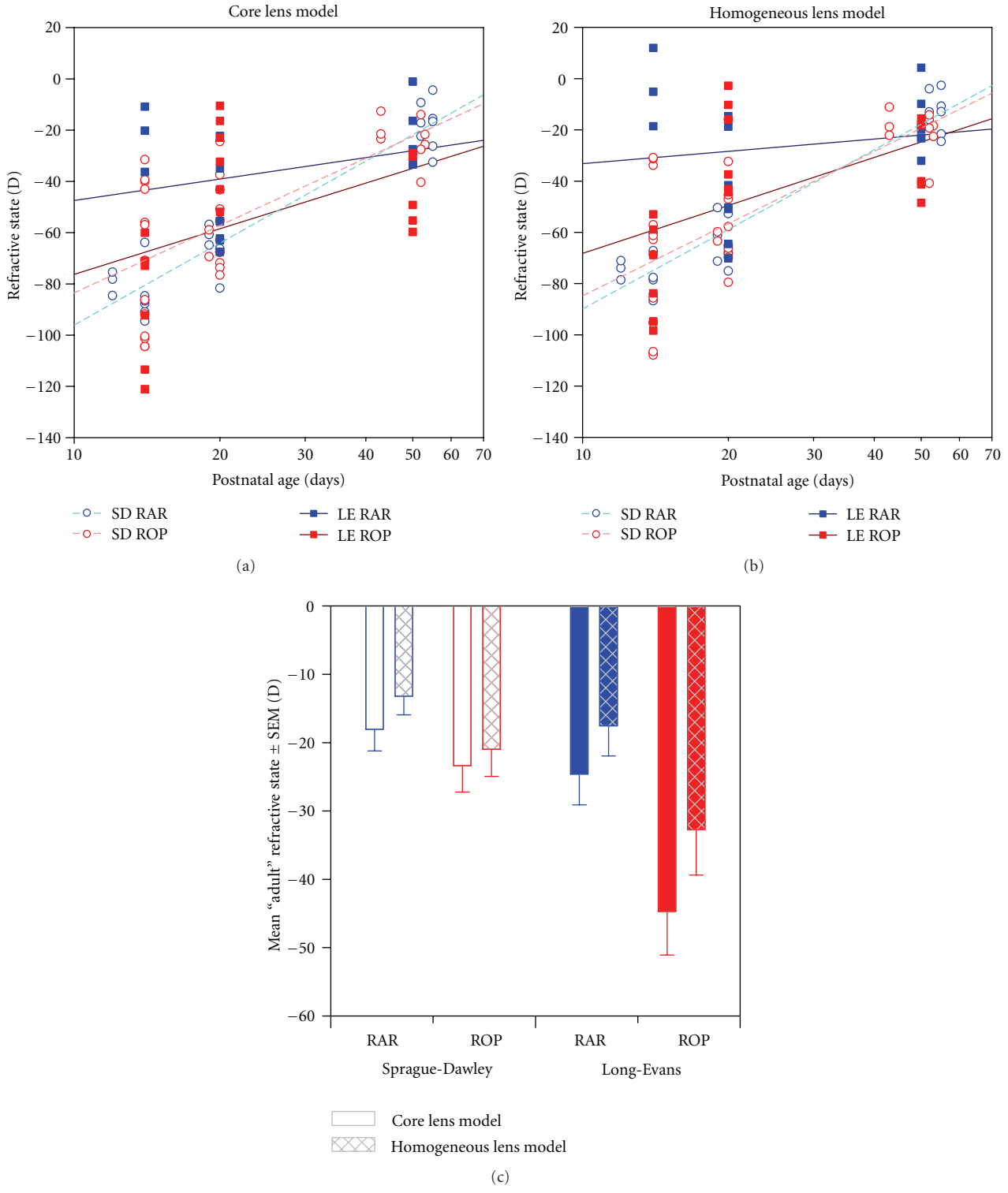

FIGURE 4: Measurements of refractive state, ℞. (a) ℞ measured using the core lens model ($℞_{core}$). Lines are log-linear regressions through Sprague-Dawley (*light dashed*) and Long-Evans (*dark solid*) ROP (*red*) and RAR (*blue*) rats' data. (b) ℞ measured using the homogeneous lens model ($℞_{hmgns}$). Lines as in (a). (c) ℞ at ~P50, an "adult" age.

differently [80]. For these reasons, comparisons of strain-matched experimental groups may prove most reliable in future studies. Nevertheless, in the present dataset, OIR caused a larger shift toward myopia—across every age—in Long-Evans than Sprague-Dawey rats (F(group × strain) = 11.1, df = 1,78, P = 0.001).

3.4. Biometric Bases of ROP Myopia. Human myopia of prematurity, exacerbated by ROP, persists into adulthood. On average, relative to myopic adults born full term, adults with the same degree of myopia and a history of ROP have eyes with shorter axial length, increased corneal curvature, increased lens thickness, and shallow anterior chamber depth. Amongst these features, the increased corneal curvature is most responsible for the myopia [13]. In the human eye, despite the fact that the lens is a more powerful convergent surface than the cornea, the cornea contributes approximately two-thirds of the total refracting power to the eye (~43 D) because the gelatinous aqueous humor provides a weaker index of refraction than air [81]. As shown in Figure 5(a), which plots the contributions of the cornea (FC) and lens (FL_{core}) in the ~P50 ROP and RAR Sprague-Dawley and Long-Evans rats, the proportion is reversed: the rat cornea contributes only about a third of the total refracting power to the eye. Thus, changes to the lens might be very important in ROP rat myopia.

Indeed, the results of media × group × strain repeated measures ANOVA (media: cornea *versus* lens) in ~P50 rats revealed that the cornea contributed significantly less power to the eye than the lens (F(media) = 6,930, df = 1,24, $P < 10^{-31}$). In ROP rats, the total dioptric power of the cornea (FC) and lens (FL_{core}) was higher than that in RAR controls (F(group) = 22.1, df = 1,24, $P < 10^{-5}$). The Sprague-Dawley rats had less powerful media than the Long-Evans rats (F(strain) = 23.1, df = 1,24, $P < 10^{-5}$). And indeed, the increase in the power of the lens in ROP was greater than that in the cornea (F(media × group) = 8.19, df = 1,24, P = 0.009); in the Long-Evans rats, in fact, corneal power did not change at all in ROP (P = 0.91).

3.5. Paradoxical Myopia? As stated earlier, the myopia characteristic of prematurity and ROP is a peculiar one in that a history of ROP is also associated with short axial length. The axial length data (d) were analyzed at ~P50 by group × strain ANOVA. As shown in Figure 5(b), short axial length is also a feature of the ROP rat (F(group) = 9.34, df = 1,24, P = 0.005) but only the albino (F(group × strain) = 20.2, df = 1,24, $P < 10^{-4}$) which normally had a larger eye (F(strain) = 8.31, df = 1,24, P = 0.008).

Furthermore, as indicated in Figure 5(c) and confirmed by group × strain ANOVA, the ratio of anterior-to-posterior segment depth (c/h) was significantly reduced at ~P50 in both the Spague-Dawley and Long-Evans ROP rats (F(group) = 10.3, df = 1,24, P = 0.004), as it is in human ROP myopia [3, 4].

3.6. Changes in Eye Shape. The subjective appearance of the ROP eyes was occasionally heteroclitic beyond just the noted changes to the refractive surfaces of the eye and their spatial interrelations (Figure 6). This might be the case if the ROP eyes' failure to elongate along the visual axis was not matched by an equivalent failure to expand along the perpendicular axis, thus creating a "fatter" eye. To test for changes in the proportions of the eye, the ratio of axial length over equatorial diameter at the plane of the *ora serrata* (d/e) at ~P50 was evaluated in a group × strain ANOVA. No significant effect of group was found. In addition, test of the ratio of lens thickness over lens equatorial diameter (LT/LE) likewise detected no significant effect of OIR.

3.7. Methodological Limitations. The absolute refractive measurements based on MRI appear reasonable (*e.g.*, in adults) but are, of course, limited by the modeling assumptions. That is, an MRI "refraction" of *plano* R_x does not necessarily indicate a truly emmetropic eye. That said, comparison of refractive state estimates by retinoscopy and VEP [61] indicate that it is the outer-middle retina that accounts for the retinoscopy reflex and not the inner limiting membrane (ILM) as has often been suggested [60]. The measurement of retinal position (A7; Table 1) in the present study was at the vitreoretinal boundary; therefore, 130 μm was added to A7 to make these MRI "refractions" more comparable to those obtained by retinoscopy. To estimate R_x ILM from these data, it is therefore necessary to add ~10 D (i.e., *less* myopia) to the results shown in Figure 4. As earlier discussed, the normal rat is probably close to emmetropic [76] (although slightly hyperopic [61] and slightly myopic [82] measures have both been reported for the murine eye) in adulthood. Thus, this roughly 10 D correction *may* better align estimates of refractive state obtained *via* this MRI procedure with those obtained by other techniques.

Note that neither errors in the refractive indices used herein nor the particular selection of retinal position in the calculation of R_x should impact much the *relative* relationships between the refractive states derived for the rats in this study: the calculations in all animals would be similarly impacted by such systematic errors. Future comparisons between this method and other techniques (retinoscopy, photorefraction, wavefront sensing, electrophysiology, etc.) may reveal what the necessary correction is (if any) to reach agreement between sundry techniques.

3.8. Relationship to Human ROP. The induction of experimental ROP lasts through the first 14 days of the rat's life, and a 50-day-old rat may be roughly equated to an adolescent or young-adult human. The equivalent disturbance in the human would last at most a couple of months. Thus, the time to recover from the original, oxygen-induced insult to the eye would be only about two-thirds or three-quarters of the lifetime (to date) for the rats at ~P50, but ~99% of the lifetime for the equivalent young-adult human, perhaps an important difference. However, to achieve parity in this respect, the rat would need to be tested more than 1,000 days after the induction of retinopathy, a span longer than the typical life of a lab rat. Evaluation of refractive state in rats older than P50 might nevertheless provide valuable information. That said, to date the ROP rat has been mostly considered a model of retinal neovascularization. At least

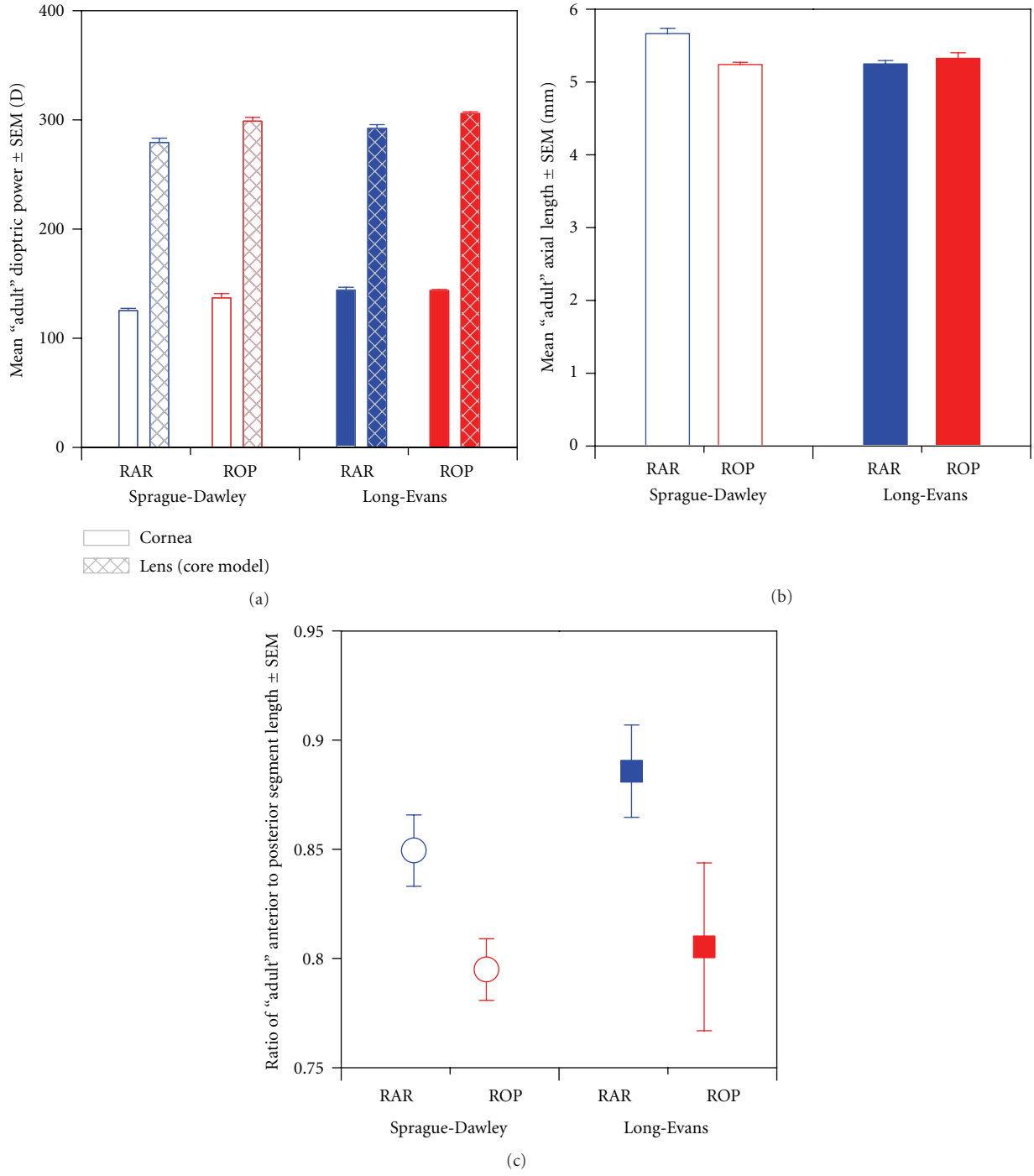

Figure 5: Biometric bases of Rx at ~P50. (a) Dioptric power of the cornea and lens. (b) Axial length (*d*). (c) Quotient of anterior segment length (*c*) divided by posterior segment length (*h*).

over the timeframe included in this study, the ROP rat seems also to be a novel model of myopia.

A further difficulty is that the OIR consistently models a moderate ROP, neither particularly severe (retinal detachments are not noted in the literature on this ROP rat model, although they are in others [83, 84]) nor particularly mild (marked NV occurs in 100% of animals). As detailed in the Introduction section, in human ROP the severity of the vasculopathy is related to the severity of ametropia but leads to greater incidences of both myopia *and* hyperopia, with myopia predominating. The range of disease severity in human eyes is much broader than in the model and, in the most severe cases, is generally treated using laser ablative therapy. The consequences of treatment on the present outcomes in the ROP rat were not investigated. Nevertheless, two multicenter trials for the treatment of severe ROP,

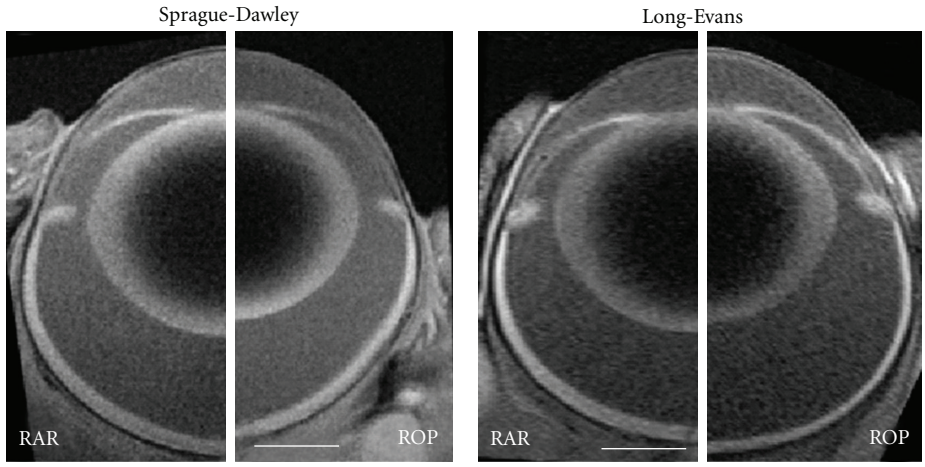

Figure 6: MR images obtained in ~P50 Sprague-Dawley RAR (a) and ROP (b) rats and Long-Evans RAR (c) and ROP (d) rats. All images are displayed at the same magnification (scale bars are 1 mm). The ROP rat images (b, d) are mirrored to eliminate nasal-temporal asymmetries, if any. Note that the ROP rat eyes are characterized by steeper corneae and relatively reduced anterior segment depths. Note also that the Sprague-Dawley ROP rat has a short axial length.

CRYO-ROP and ETROP, concluded that ROP treatment does not itself influence refractive outcomes [85, 86]. That said, in addition to ROP severity, birth weight and degree of prematurity may be additional, independent risk factors for myopia [35, 36], neither of which are factors accounted for in the rat model. Slow postnatal weight gain, which is increasingly recognized as an important prognostic of ROP severity in both human ROP [87, 88] and rodent OIR models [89, 90], *was* controlled for in large part by supplementing litter sizes to 12–15 pups; these "expanded litters" (typical litter size is 10–12) increase competition for milk supply [91] and express more severe retinopathy [89]. Note that even after matching litter size, ROP rats weigh approximately half as much as age-matched RAR rats at the conclusion of the oxygen exposure regimen, a gap they reduce but never close.

3.9. Final Thoughts. The ROP rat models well the myopia peculiar to premature birth and which is exacerbated by ROP: short axial length, increased corneal power and lens power, and proportionally shallow anterior segment. The albino Sprague-Dawley strain, in particular, appears to model *all* of these characteristics, while the hooded Long-Evans strain suffers from a more exaggerated ametropia but no change in axial length. Several developmental features of the ROP rat's eye may underpin these phenomena: First, the decreased axial length may be a consequence of an (especially) dysfunctional peripheral retina consequent to prolonged hypoxic ischemia from a failure of normal peripheral vascularization. Second, the much increased lens power may be consequent to prolonged hyperemia of the anterior segment mediated by a persistent, engorged, and unregulated hyaloid. Third, the normally exquisite mediation of emmetropization may be lacking due to retinal dysfunction as well as a poorly regulated ionic retinal *milieu* [92], an imbalance [51] of which perhaps travels the uvea or vitreous from the retina to anterior segment [93]. Fourth, alterations in retinal, vitreal, or uveal levels of other paracrine signaling molecules, such as dopamine or nitric oxide, are also plausible [5, 94–96]. Further experiments are needed to ascertain if these and other factors are indeed at play in this sight-threatening condition.

Regardless of the underlying mechanisms, the short-eyed myopia found in the present study is distinct from other myopia models in that it accurately models the clinical myopia of prematurity. Study of the ROP rat may therefore provide insights into ocular development difficult or impossible to obtain using traditional models such as the chick or monkey with occluded vision. Furthermore, the correlation between optical and neurovascular abnormalities implies that treatments that result in less severe myopia will also be beneficial to the underlying retinal pathology. The method described in this paper, specifically the use of the noninvasive MRI, makes for ready translation from animal models to human patients.

Appendices

The following formulae provide for all calculations needed to satisfy (1)–(4) in the text, also reprinted below. They are derived from Southall [69], wherein fuller explanations can be found. Parameter values were either taken from Hughes [64] or were measured in the MR images, as indicated in Table 1.

A. The Cornea

Refracting power of the anterior cornea surface

$$\mathrm{F1} = \frac{\mathrm{n2} - \mathrm{n1}}{\mathrm{rC1}}. \tag{A.1}$$

Refracting power of the posterior cornea surface

$$F2 = \frac{n3 - n2}{rC2}. \quad (A.2)$$

Reduced interval between the two surfaces

$$c1 = \frac{A2 - A1}{n2}. \quad (A.3)$$

Refracting power of the cornea system (FC) is as shown in (1).

B. The Lens

(B.1) The Anterior Lens System. Refracting power of the anterior lens surface

$$F3 = \frac{n4 - n3}{rL1}. \quad (B.1)$$

Refracting power of the anterior core lens surface

$$F4 = \frac{n5 - n4}{rLC1}. \quad (B.2)$$

Reduced interval between the two surfaces

$$c3 = \frac{A4 - A3}{n4}. \quad (B.3)$$

Refracting power of the anterior lens system

$$F(3,4) = F3 + F4 - c3 \cdot F3 \cdot F4. \quad (B.4)$$

(B.2) The Posterior Lens System. Refracting power of the posterior core lens surface

$$F5 = \frac{n6 - n5}{rLC2}. \quad (B.5)$$

Refracting power of the posterior lens surface

$$F6 = \frac{n7 - n6}{rL2}. \quad (B.6)$$

Reduced interval between the two surfaces

$$c5 = \frac{A6 - A5}{n6}. \quad (B.7)$$

Refracting power of the posterior lens system

$$F(5,6) = F5 + F6 - c5 \cdot F5 \cdot F6. \quad (B.8)$$

(B.3) Combining the Anterior and Posterior of the Lens. The refracting power of the lens system (FL) is as shown in (2) where

$$s = \frac{H(3,4)H'(5,6)}{n5}. \quad (B.9)$$

C. The Refractive State of the Eye

The refracting power of the whole eye as (FE) is as shown in (3) where

$$cE = \frac{H'(1,2)H(3,6)}{n3}. \quad (C.1)$$

The refractive state of the eye (Ɍ) is as shown in (4).

Note. In the MR image analysis, A7 was measured at the vitreoretinal border; a 130 μm correction for the thickness of the retina was included *ad hoc* to extend the plane of focus approximately to the middle of the photoreceptor layer, as indicated in Table 1 and described by Hughes [64].

D. Calculating the Principal Points of the Eye

To successfully combine the several optical systems of the eye and account for their spatial relations, it is necessary to derive the principal points (H and H′) of each refractive element: cornea, lens (anterior *and* posterior, if using core model), and their combination.

(D.1) The Cornea System. The positions of the principal points A1H(1, 2) and A2H′(1, 2) of the cornea are given by

$$\frac{A1H(1,2)}{n1} = \frac{c1 \cdot F2}{FC}, \qquad \frac{A2H'(1,2)}{n3} = -\frac{c1 \cdot F1}{FC} \quad (D.1)$$

and though the first principle point is already referenced to the position of the corneal surface, the second point is referenced to the corneal surface (A1) by

$$A1H'(1,2) = A1A2 + A2H'(1,2). \quad (D.2)$$

(D.2) The Anterior Lens System. The positions of the principal points A3H(3,4) and A4H′(3,4) of the anterior lens surfaces are given by

$$\frac{A3H(3,4)}{n3} = \frac{c3 \cdot F4}{F(3,4)}, \qquad \frac{A4H'(3,4)}{n5} = -\frac{c3 \cdot F3}{F(3,4)} \quad (D.3)$$

and when referencing the principal points to the anterior corneal surface (A1),

$$\begin{aligned} A1H(3,4) &= A1A3 + A3H(3,4), \\ A1H'(3,4) &= A1A4 + A4H'(3,4). \end{aligned} \quad (D.4)$$

(D.3) The Posterior Lens System. The positions of the principal points A5H(5,6) and A6H′(5,6) of the posterior lens surfaces are given by

$$\frac{A5H(5,6)}{n5} = \frac{c5 \cdot F6}{F(5,6)}, \qquad \frac{A6H'(5,6)}{n7} = -\frac{c5 \cdot F5}{F(5,6)} \quad (D.5)$$

and when referencing the principal points to the anterior corneal surface (A1),

$$\begin{aligned} A1H(5,6) &= A1A5 + A5H(5,6), \\ A1H'(5,6) &= A1A6 + A6H'(5,6). \end{aligned} \quad (D.6)$$

(D.4) The Anterior and Posterior Lens Systems. After combining the anterior and posterior lens systems (when using the core lens model), the positions of the principal points H(3, 4)H(3, 6) and H′(5, 6)H′(3, 6) of the whole lens system are given by

$$\frac{\mathrm{H}(3,4)\mathrm{H}(3,6)}{\mathrm{n3}} = \frac{\mathrm{s}\cdot\mathrm{F}(5,6)}{\mathrm{FL}},$$
$$\frac{\mathrm{H}'(5,6)\mathrm{H}'(3,6)}{\mathrm{n7}} = -\frac{\mathrm{s}\cdot\mathrm{F}(3,4)}{\mathrm{FL}} \quad \text{(D.7)}$$

and when referencing the principal points to the anterior corneal surface (A1),

$$\mathrm{A1H}(3,6) = \mathrm{A1H}(3,4) + \mathrm{H}(3,4)\mathrm{H}(3,6),$$
$$\mathrm{A1H}'(3,6) = \mathrm{A1H}'(5,6) + \mathrm{H}'(5,6)\mathrm{H}'(3,6). \quad \text{(D.8)}$$

(D.5) The Whole Eye System. Combining the cornea and lens, the positions of the principal points H(1, 2)H and H′(3, 6)H′ of the whole eye system are given by

$$\frac{\mathrm{H}(1,2)\mathrm{H}}{\mathrm{n1}} = \frac{\mathrm{cE}\cdot\mathrm{FL}}{\mathrm{FE}}, \qquad \frac{\mathrm{H}'(3,6)\mathrm{H}'}{\mathrm{n7}} = -\frac{\mathrm{cE}\cdot\mathrm{FC}}{\mathrm{FE}} \quad \text{(D.9)}$$

and when referencing the principal points to the anterior corneal surface (A1),

$$\mathrm{A1H} = \mathrm{A1H}(1,2) + \mathrm{H}(1,2)\mathrm{H},$$
$$\mathrm{A1H}' = \mathrm{A1H}'(3,6) + \mathrm{H}'(3,6)\mathrm{H}'. \quad \text{(D.10)}$$

Authors' Contribution

T. Y. P. Chui and D. Bissig contributed equally to the work.

Acknowledgments

This work was supported by NIH EY020308 (J. D. Akula), NIH EY018109 and Juvenile Diabetes Research Foundation (B. A. Berkowitz), NIH AG034752 and Wayne State University School of Medicine MD/PhD Program (D. Bissig), and an unrestricted grant from the Research to Prevent Blindness (Kresge Eye Institute). The authors thank Drs. Anne Fulton and Anne Moskowitz for their careful reading of and comments on the paper.

References

[1] A. B. Fulton, J. D. Akula, J. A. Mocko et al., "Retinal degenerative and hypoxic ischemic disease," *Documenta Ophthalmologica*, vol. 118, no. 1, pp. 55–61, 2009.

[2] J.-S. Joyal, N. Sitaras, F. Binet et al., "Ischemic neurons prevent vascular regeneration of neural tissue by secreting semaphorin 3A," *Blood*, vol. 117, no. 22, pp. 6024–6035, 2011.

[3] H. C. Fledelius, "Pre-term delivery and the growth of the eye. An oculometric study of eye size around term-time," *Acta Ophthalmologica Supplement*, no. 204, pp. 10–15, 1992.

[4] H. C. Fledelius, "Pre-term delivery and subsequent ocular development. A 7-10 year follow-up of children screened 1982-84 for ROP. 4) Oculometric—and other metric considerations," *Acta Ophthalmologica Scandinavica*, vol. 74, no. 3, pp. 301–305, 1996.

[5] I. G. Morgan, "The biological basis of myopic refractive error," *Clinical and Experimental Optometry*, vol. 86, no. 5, pp. 276–288, 2003.

[6] A. R. Fielder and G. E. Quinn, "Myopia of prematurity: nature, nurture, or disease?" *British Journal of Ophthalmology*, vol. 81, no. 1, pp. 2–3, 1997.

[7] A. R. Fielder, "Retinopathy of prematurity," in *Pediatric Ophthalmology and Strabismus*, D. Taylor and C. S. Hoyt, Eds., pp. 537–556, Elsevier Saunders, Philadelphia, Pa, USA, 1997.

[8] A. R. O'Connor, T. Stephenson, A. Johnson et al., "Long-term ophthalmic outcome of low birth weight children with and without retinopathy of prematurity," *Pediatrics*, vol. 109, no. 1, pp. 12–18, 2002.

[9] A. R. O'Connor, T. J. Stephenson, A. Johnson, M. J. Tobin, S. Ratib, and A. R. Fielder, "Change of refractive state and eye size in children of birth weight less than 1701 g," *British Journal of Ophthalmology*, vol. 90, no. 4, pp. 456–460, 2006.

[10] A. Cook, S. White, M. Batterbury, and D. Clark, "Ocular growth and refractive error development in premature infants without retinopathy of prematurity," *Investigative Ophthalmology and Visual Science*, vol. 44, no. 3, pp. 953–960, 2003.

[11] A. Cook, S. White, M. Batterbury, and D. Clark, "Ocular growth and refractive error development in premature infants with or without retinopathy of prematurity," *Investigative Ophthalmology and Visual Science*, vol. 49, no. 12, pp. 5199–5207, 2008.

[12] M. Snir, R. Friling, D. Weinberger, I. Sherf, and R. Axer-Siegel, "Refraction and keratometry in 40 week old premature (corrected age) and term infants," *British Journal of Ophthalmology*, vol. 88, no. 7, pp. 900–904, 2004.

[13] P. S. Baker and W. Tasman, "Myopia in adults with retinopathy of prematurity," *American Journal of Ophthalmology*, vol. 145, no. 6, pp. 1090–1094, 2008.

[14] H. Mactier, S. Maroo, M. Bradnam, and R. Hamilton, "Ocular biometry in preterm infants: implications for estimation of retinal illuminance," *Investigative Ophthalmology and Visual Science*, vol. 49, no. 1, pp. 453–457, 2008.

[15] E. E. Birch and R. Spencer, "Visual outcome in infants with cicatricial retinopathy of prematurity," *Investigative Ophthalmology and Visual Science*, vol. 32, no. 2, pp. 410–415, 1991.

[16] R. Robinson and M. O'Keefe, "Follow-up study on premature infants with and without retinopathy of prematurity," *British Journal of Ophthalmology*, vol. 77, no. 2, pp. 91–94, 1993.

[17] V. Dobson, G. E. Quinn, C. G. Summers et al., "Effect of acute-phase retinopathy of prematurity on grating acuity development in the very low birth weight infant," *Investigative Ophthalmology and Visual Science*, vol. 35, no. 13, pp. 4236–4244, 1994.

[18] A. R. O'Connor, T. J. Stephenson, A. Johnson et al., "Visual function in low birthweight children," *British Journal of Ophthalmology*, vol. 88, no. 9, pp. 1149–1153, 2004.

[19] E. A. Palmer, R. J. Hardy, V. Dobson et al., "15-Year outcomes following threshold retinopathy of prematurity: final results from the Multicenter Trial of Cryotherapy for Retinopathy of Prematurity," *Archives of Ophthalmology*, vol. 123, no. 3, pp. 311–318, 2005.

[20] R. Spencer, "Long-term visual outcomes in extremely low-birth-weight children (An American Ophthalmological Society Thesis)," *Transactions of the American Ophthalmological Society*, vol. 104, pp. 493–516, 2006.

[21] R. M. Hansen and A. B. Fulton, "Rod-mediated increment threshold functions in infants," *Investigative Ophthalmology and Visual Science*, vol. 41, no. 13, pp. 4347–4352, 2000.

[22] R. M. Hansen and A. B. Fulton, "Background adaptation in children with a history of mild retinopathy of prematurity," *Investigative Ophthalmology and Visual Science*, vol. 41, no. 1, pp. 320–324, 2000.

[23] A. M. Barnaby, R. M. Hansen, A. Moskowitz, and A. B. Fulton, "Development of scotopic visual thresholds in retinopathy of prematurity," *Investigative Ophthalmology and Visual Science*, vol. 48, no. 10, pp. 4854–4860, 2007.

[24] A. B. Fulton, X. Reynaud, R. M. Hansen, C. A. Lemere, C. Parker, and T. P. Williams, "Rod photoreceptors in infant rats with a history of oxygen exposure," *Investigative Ophthalmology and Visual Science*, vol. 40, no. 1, pp. 168–174, 1999.

[25] D. X. Hammer, N. V. Iftimia, R. Daniel Ferguson et al., "Foveal fine structure in retinopathy of prematurity: an adaptive optics fourier domain optical coherence tomography study," *Investigative Ophthalmology and Visual Science*, vol. 49, no. 5, pp. 2061–2070, 2008.

[26] A. B. Fulton, R. M. Hansen, A. Moskowitz, and J. D. Akula, "The neurovascular retina in retinopathy of prematurity," *Progress in Retinal and Eye Research*, vol. 28, no. 6, pp. 452–482, 2009.

[27] A. Moskowitz, R. Hansen, and A. Fulton, "Early ametropia and rod photoreceptor function in retinopathy of prematurity," *Optometry and Vision Science*, vol. 82, no. 4, pp. 307–317, 2005.

[28] M. T. Pardue, A. E. Faulkner, A. Fernandes et al., "High susceptibility to experimental myopia in a mouse model with a retinal on pathway defect," *Investigative Ophthalmology and Visual Science*, vol. 49, no. 2, pp. 706–712, 2008.

[29] C. D. Luu, A. H. C. Koh, and Y. Ling, "The ON/OFF-response in retinopathy of prematurity subjects with myopia," *Documenta Ophthalmologica*, vol. 110, no. 2-3, pp. 155–161, 2005.

[30] D. Troilo, "Neonatal eye growth and emmetriopisation—a literature review," *Eye*, vol. 6, no. 2, pp. 154–160, 1992.

[31] J. Wallman, "Retinal control of eye growth and refraction," *Progress in Retinal Research*, vol. 12, pp. 133–153, 1993.

[32] E. L. Smith, C. S. Kee, R. Ramamirtham, Y. Qiao-Grider, and L. F. Hung, "Peripheral vision can influence eye growth and refractive development in infant monkeys," *Investigative Ophthalmology and Visual Science*, vol. 46, no. 11, pp. 3965–3972, 2005.

[33] E. L. Smith, R. Ramamirtham, Y. Qiao-Grider et al., "Effects of foveal ablation on emmetropization and form-deprivation myopia," *Investigative Ophthalmology and Visual Science*, vol. 48, no. 9, pp. 3914–3922, 2007.

[34] D. O. Mutti, L. T. Sinnott, G. L. Mitchell et al., "Relative peripheral refractive error and the risk of onset and progression of myopia in children," *Investigative Ophthalmology and Visual Science*, vol. 52, no. 1, pp. 199–205, 2011.

[35] G. E. Quinn, V. Dobson, M. X. Repka et al., "Development of myopia in infants with birth weights less than 1251 grams," *Ophthalmology*, vol. 99, no. 3, pp. 329–340, 1992.

[36] G. E. Quinn, V. Dobson, J. Kivlin et al., "Prevalence of myopia between 3 months and 5 1/4 years in preterm infants with and without retinopathy of prematurity," *Ophthalmology*, vol. 105, no. 7, pp. 1292–1300, 1998.

[37] S. Cunningham, B. W. Fleck, R. A. Elton, and N. Mclntosh, "Transcutaneous oxygen levels in retinopathy of prematurity," *The Lancet*, vol. 346, no. 8988, pp. 1464–1465, 1995.

[38] J. S. Penn, B. L. Tolman, and L. A. Lowery, "Variable oxygen exposure causes preretinal neovascularization in the newborn rat," *Investigative Ophthalmology and Visual Science*, vol. 34, no. 3, pp. 576–585, 1993.

[39] J. S. Penn, M. M. Henry, and B. L. Tolman, "Exposure to alternating hypoxia and hyperoxia causes severe proliferative retinopathy in the newborn rat," *Pediatric Research*, vol. 36, no. 6, pp. 724–731, 1994.

[40] J. S. Penn, M. M. Henry, P. T. Wall, and B. L. Tolman, "The range of PaO2 variation determines the severity of oxygen-induced retinopathy in newborn rats," *Investigative Ophthalmology and Visual Science*, vol. 36, no. 10, pp. 2063–2070, 1995.

[41] J. M. Barnett, S. E. Yanni, and J. S. Penn, "The development of the rat model of retinopathy of prematurity," *Documenta Ophthalmologica*, vol. 120, no. 1, pp. 3–12, 2010.

[42] D. Lepore, F. Molle, M. M. Pagliara et al., "Atlas of fluorescein angiographic findings in eyes undergoing laser for retinopathy of prematurity," *Ophthalmology*, vol. 118, no. 1, pp. 168–175, 2011.

[43] O. Dembinska, L. M. Rojas, S. Chemtob, and P. Lachapelle, "Evidence for a brief period of enhanced oxygen susceptibility in the rat model of oxygen-induced retinopathy," *Investigative Ophthalmology and Visual Science*, vol. 43, no. 7, pp. 2481–2490, 2002.

[44] K. Liu, J. D. Akula, C. Falk, R. M. Hansen, and A. B. Fulton, "The retinal vasculature and function of the neural retina in a rat model of retinopathy of prematurity," *Investigative Ophthalmology and Visual Science*, vol. 47, no. 6, pp. 2639–2647, 2006.

[45] K. Liu, J. D. Akula, R. M. Hansen, A. Moskowitz, M. S. Kleinman, and A. B. Fulton, "Development of the electroretinographic oscillatory potentials in normal and ROP rate," *Investigative Ophthalmology and Visual Science*, vol. 47, no. 12, pp. 5447–5452, 2006.

[46] J. D. Akula, R. M. Hansen, M. E. Martinez-Perez, and A. B. Fulton, "Rod photoreceptor function predicts blood vessel abnormality in retinopathy of prematurity," *Investigative Ophthalmology and Visual Science*, vol. 48, no. 9, pp. 4351–4359, 2007.

[47] B. A. Berkowitz, R. Roberts, J. S. Penn, and M. Gradianu, "High-resolution manganese-enhanced MRI of experimental retinopathy of prematurity," *Investigative Ophthalmology and Visual Science*, vol. 48, no. 10, pp. 4733–4740, 2007.

[48] J. D. Akula, J. A. Mocko, A. Moskowitz, R. M. Hansen, and A. B. Fulton, "The oscillatory potentials of the dark-adapted electroretinogram in retinopathy of prematurity," *Investigative Ophthalmology and Visual Science*, vol. 48, no. 12, pp. 5788–5797, 2007.

[49] A. Dorfman, O. Dembinska, S. Chemtob, and P. Lachapelle, "Early manifestations of postnatal hyperoxia on the retinal structure and function of the neonatal rat," *Investigative Ophthalmology and Visual Science*, vol. 49, no. 1, pp. 458–466, 2008.

[50] J. D. Akula, J. A. Mocko, I. Y. Benador et al., "The neurovascular relation in oxygen-induced retinopathy," *Molecular Vision*, vol. 14, pp. 2499–2508, 2008.

[51] B. A. Berkowitz and R. Roberts, "Evidence for a critical role of panretinal pathophysiology in experimental ROP," *Documenta Ophthalmologica*, vol. 120, no. 1, pp. 13–24, 2010.

[52] B. A. Berkowitz et al., "Intraretinal calcium channels and retinal morbidity in experimental retinopathy of prematurity," *Molecular Vision*, vol. 17, pp. 2516–2526, 2011.

[53] J. D. Akula, T. L. Favazza, J. A. Mocko et al., "The anatomy of the rat eye with oxygen-induced retinopathy," *Documenta Ophthalmologica*, vol. 120, no. 1, pp. 41–50, 2010.

[54] R. Roberts, W. Zbang, Y. Ito, and B. A. Berkowitz, "Spatial pattern and temporal evolution of retinal oxygenation response in

oxygen-induced retinopathy," *Investigative Ophthalmology and Visual Science*, vol. 44, no. 12, pp. 5315–5320, 2003.

[55] W. Zhang, Y. Ito, E. Berlin, R. Roberts, H. Luan, and B. A. Berkowitz, "Specificity of subnormal ΔPO2 for retinal neovascularization in experimental retinopathy of prematurity," *Investigative Ophthalmology and Visual Science*, vol. 44, no. 8, pp. 3551–3555, 2003.

[56] T. L. Terry, "Fibroblastic overgrowth of persistent tunica vasculosa lentis in infants born prematurely: II. Report of cases-clinical aspects," *Transactions of the American Ophthalmological Society*, vol. 40, pp. 262–284, 1942.

[57] Y. Soh, T. Fujino, and Y. Hatsukawa, "Progression and timing of treatment of zone I retinopathy of prematurity," *American Journal of Ophthalmology*, vol. 146, no. 3, pp. 369–374, 2008.

[58] B. Lorenz, K. Spasovska, H. Elflein, and N. Schneider, "Wide-field digital imaging based telemedicine for screening for acute retinopathy of prematurity (ROP). Six-year results of a multicentre field study," *Graefe's Archive for Clinical and Experimental Ophthalmology*, vol. 247, no. 9, pp. 1251–1262, 2009.

[59] B. A. Berkowitz, R. A. Lukaszew, C. M. Mullins, and J. S. Penn, "Impaired hyaloidal circulation function and uncoordinated ocular growth patterns in experimental retinopathy of prematurity," *Investigative Ophthalmology and Visual Science*, vol. 39, no. 2, pp. 391–396, 1998.

[60] M. Glickstein and M. Millodot, "Retinoscopy and eye size," *Science*, vol. 168, no. 3931, pp. 605–606, 1970.

[61] D. O. Mutti, J. N. Ver Hoeve, K. Zadnik, and C. J. Murphy, "The artifact of retinoscopy revisited: comparison of refractive error measured by retinoscopy and visual evoked potential in the rat," *Optometry and Vision Science*, vol. 74, no. 7, pp. 483–488, 1997.

[62] E. G. de la Cera, G. Rodríguez, L. Llorente, F. Schaeffel, and S. Marcos, "Optical aberrations in the mouse eye," *Vision Research*, vol. 46, no. 16, pp. 2546–2553, 2006.

[63] A. Hughes, "The artifact of retinoscopy in the rat and rabbit eye has its origin at the retina/vitreous interface rather than in longitudinal chromatic aberration," *Vision Research*, vol. 19, no. 11, pp. 1293–1294, 1979.

[64] A. Hughes, "A schematic eye for the rat," *Vision Research*, vol. 19, no. 5, pp. 569–588, 1979.

[65] J. Rymer and C. F. Wildsoet, "The role of the retinal pigment epithelium in eye growth regulation and myopia: a review," *Visual Neuroscience*, vol. 22, no. 3, pp. 251–261, 2005.

[66] M. E. Hartnett, D. Martiniuk, G. Byfield, P. Geisen, G. Zeng, and V. L. Bautch, "Neutralizing VEGF decreases tortuosity and alters endothelial cell division orientation in arterioles and veins in a rat model of ROP: relevance to plus disease," *Investigative Ophthalmology and Visual Science*, vol. 49, no. 7, pp. 3107–3114, 2008.

[67] R. M. Robb, "Increase in retinal surface area during infancy and childhood," *Journal of Pediatric Ophthalmology and Strabismus*, vol. 19, no. 4, pp. 16–20, 1982.

[68] R. Ihaka and R. Gentleman, "R: a language for data analysis and graphics," *Journal of Computational and Graphical Statistics*, vol. 5, no. 3, pp. 299–314, 1996.

[69] J. P. C. Southall, *Mirrors, Prisms and Lenses; a Text-book of Geometrical Optics*, Macmillan Publishing Company, New York, NY, USA, 1918.

[70] A. B. Fulton and B. N. Baker, "The relation of retinal sensitivity and rhodopsin in developing rat retina," *Investigative Ophthalmology and Visual Science*, vol. 25, no. 6, pp. 647–651, 1984.

[71] R. W. Young, "Cell differentiation in the retina of the mouse," *Anatomical Record*, vol. 212, no. 2, pp. 199–205, 1985.

[72] A. B. Fulton, R. M. Hansen, and O. Findl, "The development of the rod photoresponse from dark-adapted rats," *Investigative Ophthalmology and Visual Science*, vol. 36, no. 6, pp. 1038–1045, 1995.

[73] H. Xu and N. Tian, "Pathway-specific maturation, visual deprivation, and development of retinal pathway," *Neuroscientist*, vol. 10, no. 4, pp. 337–346, 2004.

[74] A. Hughes, "The refractive state of the rat eye," *Vision Research*, vol. 17, no. 8, pp. 927–939, 1977.

[75] D. Borja et al., "Distortions of the posterior surface in optical coherence tomography images of the isolated crystalline lens: effect of the lens index gradient," *Biomedical Optics Express*, vol. 1, no. 5, pp. 1331–1340, 2010.

[76] G. E. Meyer and M. C. Salinsky, "Refraction of the rat: estimation by pattern evoked visual cortical potentials," *Vision Research*, vol. 17, no. 7, pp. 883–885, 1977.

[77] J. A. Guggenheim, R. C. Creer, and X. J. Qin, "Postnatal refractive development in the Brown Norway rat: limitations of standard refractive and ocular component dimension measurement techniques," *Current Eye Research*, vol. 29, no. 4-5, pp. 369–376, 2004.

[78] D. L. Mayer, R. M. Hansen, B. D. Moore, S. Kim, and A. B. Fulton, "Cycloplegic refractions in healthy children aged 1 through 48 months," *Archives of Ophthalmology*, vol. 119, no. 11, pp. 1625–1628, 2001.

[79] D. O. Mutti, K. Zadnik, C. A. Johnson, H. C. Howland, and C. J. Murphy, "Retinoscopic measurement of the refractive state of the rat," *Vision Research*, vol. 32, no. 3, pp. 583–586, 1992.

[80] M. G. Harris, and S. E. Heyman, "Ocular albinism: a review of the literature," *Optometric Weekly*, vol. 64, pp. 31–37, 1973.

[81] M. H. Freeman and W. H. A. Fincham, *Optics*, Butterworths, Boston, Mass, USA, 10th edition, 1990.

[82] Y. Geng et al., "Optical properties of the mouse eye," *Biomedical Optics Express*, vol. 2, no. 4, pp. 717–738, 2011.

[83] J. S. Penn, L. A. Thum, and M. I. Naash, "Oxygen-induced retinopathy in the rat: vitamins C and E as potential therapies," *Investigative Ophthalmology and Visual Science*, vol. 33, no. 6, pp. 1836–1845, 1992.

[84] J. S. Penn, B. L. Tolman, L. A. Lowery, and C. A. Koutz, "Oxygen-induced retinopathy in the rat: hemorrhages and dysplasias may lead to retinal detachment," *Current Eye Research*, vol. 11, no. 10, pp. 939–953, 1992.

[85] G. E. Quinn, V. Dobson, R. M. Siatkowski et al., "Does cryotherapy affect refractive error? Results from treated versus control eyes in the cryotherapy for retinopathy of prematurity trial," *Ophthalmology*, vol. 108, no. 2, pp. 343–347, 2001.

[86] G. E. Quinn, V. Dobson, B. V. Davitt et al., "Progression of myopia and high myopia in the early treatment for retinopathy of prematurity study: findings to 3 years of age," *Ophthalmology*, vol. 115, no. 6, pp. 1058–1064, 2008.

[87] D. K. Wallace, J. A. Kylstra, S. J. Phillips, and J. G. Hall, "Poor postnatal weight gain: a risk factor for severe retinopathy of prematurity," *Journal of AAPOS*, vol. 4, no. 6, pp. 343–347, 2000.

[88] J. B. F. Filho, P. P. Bonomo, M. Maia, and R. S. Procianoy, "Weight gain measured at 6 weeks after birth as a predictor for severe retinopathy of prematurity: study with 317 very low birth weight preterm babies," *Graefe's Archive for Clinical and Experimental Ophthalmology*, vol. 247, no. 6, pp. 831–836, 2009.

[89] J. M. Holmes and L. A. Duffner, "The effect of postnatal growth retardation on abnormal neovascularization in the oxygen exposed neonatal rat," *Current Eye Research*, vol. 15, no. 4, pp. 403–409, 1996.

[90] A. Stahl, J. Chen, P. Sapieha et al., "Postnatal weight gain modifies severity and functional outcome of oxygen-induced proliferative retinopathy," *American Journal of Pathology*, vol. 177, no. 6, pp. 2715–2723, 2010.

[91] J. M. Holmes and L. A. Duffner, "The effect of litter size on normal retinal vascular development in the neonatal rat," *Current Eye Research*, vol. 14, no. 8, pp. 737–740, 1995.

[92] S. G. Crewther, H. Liang, B. M. Junghans, and D. P. Crewther, "Ionic control of ocular growth and refractive change," *Proceedings of the National Academy of Sciences of the United States of America*, vol. 103, no. 42, pp. 15663–15668, 2006.

[93] B. A. Berkowitz, M. Gradianu, S. Schafer et al., "Ionic dysregulatory phenotyping of pathologic retinal thinning with manganese-enhanced MRI," *Investigative Ophthalmology and Visual Science*, vol. 49, no. 7, pp. 3178–3184, 2008.

[94] B. T. Chen, M. V. Avshalumov, and M. E. Rice, "H2O2 is a novel, endogenous modulator of synaptic dopamine release," *Journal of Neurophysiology*, vol. 85, no. 6, pp. 2468–2476, 2001.

[95] T. Fujikado, Y. Kawasaki, J. Fujii et al., "The effect of nitric oxide synthase inhibitor on form-deprivation myopia," *Current Eye Research*, vol. 16, no. 10, pp. 992–996, 1997.

[96] T. Fujikado, K. Tsujikawa, M. Tamura, J. Hosohata, Y. Kawasaki, and Y. Tano, "Effect of a nitric oxide synthase inhibitor on lens-induced myopia," *Ophthalmic Research*, vol. 33, no. 2, pp. 75–79, 2001.

Hindawi Publishing Corporation
Journal of Ophthalmology
Volume 2012, Article ID 429387, 4 pages
doi:10.1155/2012/429387

Review Article

In Vivo Molecular Imaging in Retinal Disease

Fang Xie,[1] Wenting Luo,[2] Zhongyu Zhang,[2] and Dawei Sun[2]

[1] *Department of Ophthalmology, First Affiliated Hospital of Harbin Medical University, Harbin 150001, China*
[2] *Department of Ophthalmology, Second Affiliated Hospital of Harbin Medical University, Harbin 150081, China*

Correspondence should be addressed to Dawei Sun, dr.sundw@gmail.com

Received 22 September 2011; Accepted 1 December 2011

Academic Editor: Ofra Benny

There is an urgent need for early diagnosis in medicine, whereupon effective treatments could prevent irreversible tissue damage. The special structure of the eye provides a unique opportunity for noninvasive light-based imaging of ocular fundus vasculature. To detect endothelial injury at the early and reversible stage of adhesion molecule upregulation, some novel imaging agents that target retinal endothelial molecules were generated. *In vivo* molecular imaging has a great potential to impact medicine by detecting diseases or screening disease in early stages, identifying extent of disease, selecting disease and patient-specific therapeutic treatment, applying a directed or targeted therapy, and measuring molecular-specific effects of treatment. Current preclinical findings and advances in instrumentation such as endoscopes and microcatheters suggest that these molecular imaging modalities have numerous clinical applications and will be translated into clinical use in the near future.

1. Introduction

The use of visible light to examine intraocular processes can be considered the traditional form of imaging in ophthalmology. Molecular imaging permits noninvasive visualization and measurement of molecular and cell biology in living subjects, thereby complementing conventional anatomical imaging. Optical molecular imaging technologies use light emitted through fluorescence or bioluminescence. Molecular imaging is defined as the ability to visualize and quantitatively measure the function of biological and cellular processes *in vivo* [1, 2], while anatomical imaging plays a major role in medical imaging for diagnosis, surgical guidance, and treatment monitoring, focused and personalized therapy, and earlier treatment followup. The main advantage of *in vivo* molecular imaging is its ability to characterize pathologies of diseased tissues without invasive biopsies or surgical procedures, and with this information in hand, a more personalized treatment-planning regimen can be applied.

In vivo visualization techniques of the retinal microcirculation, including conventional fundus fluorescein angiography (FFA) and indocyanine green angiography (ICGA) or the experimental laser-targeted angiography [3, 4], are used to investigate the retinal vascular network and hemodynamic conditions [5]. However, these methods do not allow evaluation of leukocyte endothelial interaction in the retinal flow or identification of specific molecular changes during disease. Recently, we introduced a novel technique for detection of endothelial surface molecules in ocular inflammation [6]. Using adhesive molecule-conjugated fluorescent microspheres (MSs) [7] in live animals, we showed early endothelial changes in ocular microvessels at an early stage, which were previously detectable only by the most sensitive *in vitro* techniques, such as immunohistochemistry or PCR [6]. In fluorescence imaging, light of the excitation wavelengths must penetrate tissues to reach a targeted reporter molecule carrying a fluorochrome, resulting in the emission of light of usually lower wavelength that can be registered by a charge-coupled device (CCD) camera. Fluorescent proteins, such as cyan, green, or yellow fluorescent protein, can be introduced into cells of choice by transgenic technology. For accurate *in vivo* detection and measurement, these novel tools provide high specificity for their target.

This paper briefly describes different molecular imaging techniques and devices used in retinal imaging, as well as

potential imaging tools and targets that may be translated into clinical applications in the near future.

2. History of Molecular Imaging

The development of molecular imaging is rooted in radiology and nuclear medicine as well as in molecular biology. Since the 1950s, nuclear imaging of radioactive isotope-labeled biomacromolecule has been an integral part of drug development and diagnostic imaging. The broad clinical significance of such approaches remained restricted until positron emission tomography was introduced in 1979 and became an important tool for the detection of metabolic activities in tissues such as the brain and heart, as well as in cancer. It facilitated a biological imaging readout, albeit with limited specificity. Around the same time, magnetic resonance spectroscopy promoted the evolution of molecular imaging. The ability to collect information about specific endogenous molecules by taking advantage of their intrinsic nuclear spin property represented an early example of molecular imaging. These advances paved the way for pioneering molecular imaging studies by demonstrating *in vivo* imaging of reporter gene expression [8]. Concurrently, optical bioluminescence imaging for *in vivo* detection of the FLuc reporter gene was demonstrated [9]. Taken together, these studies propelled molecular imaging into the scientific spotlight. The introduction of imaging instrumentation dedicated to small animals [10] and the description of enzyme-activated small-molecule probes for optical fluorescence imaging further fueled scientific interest [11]. Recent work has focused on the extension and refinement of molecular imaging technology and its application to the diagnosis of cancer [12] and cardiovascular disease [13]. Molecular imaging has started to emerge as a tool in immunology [14] and microbiology [15].

3. Current Molecular Imaging Strategies and Devices

The use of visible light to examine intraocular processes can be considered the oldest form of imaging in ophthalmology. The unique optical properties of the eye allow direct microscopic observation of the retina. Optical molecular imaging technologies use light emitted through fluorescence or bioluminescence. In fluorescence imaging, light of the excitation wavelengths must penetrate tissues to reach a targeted reporter molecule carrying a fluorochrome, resulting in the emission of light of usually lower wavelength that can be registered by a charge-coupled device (CCD) camera. Fluorescent proteins, such as cyan, green, or yellow fluorescent protein can be introduced into cells of choice by transgenic technology. This technology has greatly facilitated studies on GFP-positive animals. These animals render all cells expressing the fractalkine receptor, such as microglia cells, dendritic cells, and macrophages, intrinsically fluorescent [16]. Certain filters, such as those used by fluorescein or indocyanine green angiography, allow the detection of specifically fluorescent structures. As in fluorescence imaging, numerous transgenic animals have been generated that express various types of luciferase under different promoters whose expression in disease models can be measured after florescence injection. Imaging stations have been developed that allow detection of even faint light emission from within the body of experimental animals. This method is particularly helpful when long emission wavelengths are employed, because these penetrate living tissues much better. Noninvasive time-course analyses have therefore become possible and could theoretically be of great use in ophthalmology as well as in other fields. Inflammation and tracing of inflammatory cells has been a key topic in molecular imaging in recent years. Using an established model of ocular inflammation, endotoxin-induced uveitis, Sun and colleagues visualized the rolling and adhesive interaction of fluorescent microspheres conjugated to recombinant P-selectin glycoprotein ligand-Ig (rPSGL-Ig) in the choriocapillaris by means of SLO. In our recent work [17], we further introduce novel molecular imaging agents that target two distinct types of endothelial surface molecules, a mediator of rolling and one that mediates firm adhesion, and evaluate the success of anti-inflammatory treatment *in vivo*.

Our imaging approach is founded on certain aspects of leukocyte-endothelial interaction, a common component in the pathogenesis of various ocular diseases. Leukocytes normally do not interact with the endothelium of blood vessels, save for occasional tethering. However, at sites of inflammation, endothelial cells express adhesion molecules, such as P-selectin and intercellular adhesion molecule-1 (ICAM-1) which facilitate the multistep leukocyte recruitment cascade [18]. The steps of the recruitment process include tethering, rolling, firm adhesion, and transmigration into the extravascular space [7, 19]. Leukocyte rolling is mediated mainly through transient interaction of selectins with their ligands. Our results show the superior sensitivity of double-conjugated MSs for detection of endothelial injury, compared to MSs that only target one type of endothelial markers. Our previous work showed accumulation of rPSGL-1-conjugated MSs in choroidal microvessels [6]. Here, we also quantitatively compare the rolling of various MSs in retinal and choroidal vessels. The rolling flux of rPSGL-1-conjugated MSs is significantly higher in EIU animals than in controls. In contrast, the rolling flux of anti-ICAM-1-conjugated MSs is not significantly different between EIU and control animals. This finding is in line with the fact that CD18/ICAM-1 is not primarily a rolling ligand pair *in vivo*. The significantly higher rolling interaction of the double-conjugated MSs compared to the rPSGL-1-conjugated MSs indicates that ICAM-1 may contribute to the rolling of the MSs, once the interaction with the endothelium is initiated. Surprisingly, the rolling velocity of the double-conjugated MSs is significantly higher in the choroidal vessels than in the retina. The absolute number of MS interactions in the choriocapillaris is higher than in the retina. This difference might be explained by the higher vascular density in the choriocapillaris compared to the retina. Also, the inflammatory response in the choroid may differ from retina. Another striking qualitative difference between the two vascular beds is that, in the retina, most

rolling initiates from the periphery and continues toward the optic nerve head, suggesting that the rolling interaction mainly occurs in the retinal veins.

Acridine orange digital fluorography revealed leucocyte rolling in the retina of animals with experimental autoimmune uveoretinitis. Acridine orange solution was injected continuously through a tail vein at a proper velocity. Retinal images were generated by an SLO connected to a computer-assisted image analysis system. Acridine orange binds to DNA and RNA, and the spectral properties of acridine orange DNA complexes are very similar to those of sodium fluorescein, with a 502 nm excitation maximum and an emission maximum of 522 nm. Results reveal that leukocyte endothelium interaction and extravascular infiltration in the retinal venous vasculature may play significant roles in the early stages of posterior segment inflammation.

Xu and colleagues reported another method of investigating leucocytes in the retinal vasculature by SLO. They tried to inject calcein-acetoxymethyl ester- (AM-) labeled T cells into the tail vein of rodents [20]. Leucocyte dynamics can also be monitored in the iris stroma, limbus, and choroid using intravital microscopy with an epifluorescent illumination microscope equipped with a black-and-white camera connected to a video capture card. Leucocytes were stained either with rhodamine G66 or carboxy fluorescein diacetate succinimidyl ester (CFSE) to monitor the iris and limbus to visualise leucocytes in the choroid [21]. Interleukin- (IL-) 2, which is expressed upon stimulation of T cells, commonly serves as T-cell activation marker. Becker and colleagues used enhanced GFP as a reporter gene for IL-2 expression. They showed by intravital microscopy that transgenic mice expressing GFP under the control of IL-2 regulatory elements can be used for *in vivo* expression assays that allow detection of activated T cells in the iris at multiple time points within the same animal with experimental uveitis. Transgenic reporter mice for numerous other cytokines exist. Intravital microscopy has also been used for imaging dendritic cells in the cornea using transgenic mice that express YFP under control of the CD11c promoter (CD11c-YFP) [22]. cSLO has also been used to visualise apoptosis of single nerve cells in the retina *in vivo*, in order to perform longitudinal studies of disease processes such as glaucoma [23]. This technique enables direct observation of single nerve cell apoptosis by using Alexa Fluor 488-labelled annexin V and a prototype Zeiss. Further developments in cSLO technique yielded *in vivo* retinal images at a cellular level. Adaptive optics SLO was used to image the retinal pigment epithelial (RPE) cells in patients with rod-cone dystrophy and bilateral progressive maculopathy [24]. "Adaptive optics" denotes a set of methods for measuring and compensating for the aberration of individual eyes, consisting of trial lenses to correct sphere and cylinder, a Shack-Hartmann-based wave front sensor to detect residual aberration, and a deformable mirror to correct this residual aberration. Integrated into an SLO, lateral resolution of 2 mm could be achieved, which enables imaging of RPE cells, cone photoreceptors [25], and the flow of single leucocytes and the lamina cribrosa [26]. Choi and coworkers have integrated adaptive optics into a fundus camera for imaging cone photoreceptors in patients with retinal dystrophies and optic neuropathy [27].

4. Preclinical Developments in Molecular Imaging

Preclinical molecular imaging in small animals is an invaluable part of new molecular targets and contrast agents, as well as developing drugs prior to clinical translation [27]. Research shows that the time intensive and expensive preclinical steps involved in molecular target identification, validation, chemical synthesis, and characterization for new molecular imaging agents. In fact, the majority of current molecular imaging agents used in the clinic were discovered through these exhaustive preclinical experiments at academic institutions [28]. It is estimated that a molecular imaging agent costs about $150 million over 10 years to transfer to the clinic, ending with average double cost per year revenue for successful contrast agents.

To identify a molecular target beginning with understanding and characterizing the biology, the first step is to find the differences between a healthy and diseased state. For instance, since there is an intricate relationship between cancer and inflammation (chronic inflammation maybe promote, cancer, and cancer onset could promote an inflammatory response), the differences between inflammation and cancer states must be characterized. In general, much focus is directed to cancer imaging including retinal and choroidal tumor, and several preclinical studies have identified new molecular targets for imaging cancer. In addition to imaging the cancer phenotype such as increases in metabolism, angiogenesis, proliferation, hypoxia, and apoptosis, agents have been developed to target specific protein markers expressed on cancer cells. Many chemotherapeutic drugs also target these markers; they have been radiolabelled for assessment of biodistribution and pharmacokinetics using noninvasive molecular imaging [27]. Continuing preclinical research has exploded not only in molecular target discovery and imaging probe developments but also in new strategies for imaging methodologies, especially in the areas of optical imaging. With the advent of new, smaller instruments/devices for insertion into the body, molecular imaging strategies with optical devices and specific molecular-targeted contrast agents have great potential for translation into the clinic, which is reviewed in the promising sections.

5. Conclusions

Molecular imaging can be applied to all parts of medical imaging: early detection, screening, diagnosis, therapy delivery, monitoring, and treatment followup. The current status of clinical molecular imaging is limited, with most current applications using visual able imaging and a small number of highly specific applications for MRI and ultrasound. Current demands and trends are calling for new strategies to focus on early disease detection through improved imaging and screening protocols in retina, as well as patient-specific treatment selection delivery and therapy-specific monitoring. It is hoped that these new strategies of early diagnosis and

immediate treatment monitoring will improve success rates for curing diseases with high mortality rates such as retinal disease and some types of cancer, as well as providing more specific treatment for other diseases. Preclinical research has resulted in the identification of a large number of molecular targets and the development of novel molecular imaging contrast agents as well as device, hardware, and software technologies. It is expected that molecular imaging in retina with imaging modalities other than our developed MSs, PET, MRI, molecular ultrasound, and photoacoustic tomography will be integrated into more frequent clinical application in the near future.

Acknowledgments

Support by National Natural Science Foundation of China Grants 81171381, Heilongjiang Science Grant LC2011C27, Ministry of Education Fund 20112307120019 was granted to D. Sun.

References

[1] D. A. Mankoff, "A definition of molecular imaging," *Journal of Nuclear Medicine*, vol. 48, no. 6, pp. 18–21, 2007.

[2] T. E. Peterson and H. C. Manning, "Molecular imaging: ^{18}F-FDG PET and a whole lot more," *Journal of Nuclear Medicine Technology*, vol. 37, no. 3, pp. 151–161, 2009.

[3] P. M. Bischoff, H. J. Niederberger, B. Torok, and P. Speiser, "Simultaneous indocyanine green and fluorescein angiography," *Retina*, vol. 15, no. 2, pp. 91–99, 1995.

[4] Y. Hirata and H. Nishiwaki, "The choroidal circulation assessed by laser-targeted angiography," *Progress in Retinal and Eye Research*, vol. 25, no. 2, pp. 129–147, 2006.

[5] B. Khoobehi, B. Shoelson, Y. Z. Zhang, and G. A. Peyman, "Fluorescent microsphere imaging: a particle-tracking approach to the hemodynamic assessment of the retina and choroid," *Ophthalmic Surgery and Lasers*, vol. 28, no. 11, pp. 937–947, 1997.

[6] S. Miyahara, L. Almulki, K. Noda et al., "In vivo imaging of endothelial injury in choriocapillaris during endotoxin-induced uveitis," *The FASEB Journal*, vol. 22, no. 6, pp. 1973–1980, 2008.

[7] A. Hafezi-Moghadam, K. L. Thomas, A. J. Prorock, Y. Huo, and K. Ley, "L-selectin shedding regulates leukocyte recruitment," *Journal of Experimental Medicine*, vol. 193, no. 7, pp. 863–872, 2001.

[8] J. G. Tjuvajev, R. Finn, K. Watanabe et al., "Noninvasive imaging of herpes virus thymidine kinase gene transfer and expression: a potential method for monitoring clinical gene therapy," *Cancer Research*, vol. 56, no. 18, pp. 4087–4095, 1996.

[9] C. H. Contag, S. D. Spilman, P. R. Contag et al., "Visualizing gene expression in living mammals using a bioluminescent reporter," *Photochemistry and Photobiology*, vol. 66, no. 4, pp. 523–531, 1997.

[10] B. J. Pichler, H. F. Wehrl, and M. S. Judenhofer, "Latest advances in molecular imaging instrumentation," *Journal of Nuclear Medicine*, vol. 49, supplement 2, pp. 5S–23S, 2008.

[11] R. Weissleder, C. H. Tung, U. Mahmood, and A. Bogdanov, "In vivo imaging of tumors with protease-activated near-infrared fluorescent probes," *Nature Biotechnology*, vol. 17, no. 4, pp. 375–378, 1999.

[12] R. Weissleder, "Molecular imaging in cancer," *Science*, vol. 312, no. 5777, pp. 1168–1171, 2006.

[13] F. A. Jaffer, P. Libby, and R. Weissleder, "Molecular imaging of cardiovascular disease," *Circulation*, vol. 116, no. 9, pp. 1052–1061, 2007.

[14] I. J. Hildebrandt and S. S. Gambhir, "Molecular imaging applications for immunology," *Clinical Immunology*, vol. 111, no. 2, pp. 210–224, 2004.

[15] M. Hutchens and G. D. Luker, "Applications of bioluminescence imaging to the study of infectious diseases," *Cellular Microbiology*, vol. 9, no. 10, pp. 2315–2322, 2007.

[16] N. Eter, "Molecular imaging in the eye," *British Journal of Ophthalmology*, vol. 94, no. 11, pp. 1420–1426, 2010.

[17] D. Sun, S. Nakao, F. Xie, S. Zandi, A. Schering, and A. Hafezi-Moghadam, "Superior sensitivity of novel molecular imaging probe: simultaneously targeting two types of endothelial injury markers," *The FASEB Journal*, vol. 24, no. 5, pp. 1532–1540, 2010.

[18] R. C. Garland, D. Sun, S. Zandi et al., "Noninvasive molecular imaging reveals role of PAF in leukocyte-endothelial interaction in LPS-induced ocular vascular injury," *The Journal of the Federation of American Societies for Experimental Biology*, vol. 25, no. 4, pp. 1284–1294, 2011.

[19] K. Suzuma, M. Mandai, J. Kogishi, S. J. Tojo, Y. Honda, and N. Yoshimura, "Role of P-selectin in endotoxin-induced uveitis," *Investigative Ophthalmology and Visual Science*, vol. 38, no. 8, pp. 1610–1618, 1997.

[20] H. Xu, A. Manivannan, K. A. Goatman et al., "Improved leukocyte tracking in mouse retinal and choroidal circulation," *Experimental Eye Research*, vol. 74, no. 3, pp. 403–410, 2002.

[21] D. B. Spencer, E. J. Lee, T. Kawaguchi, and J. T. Rosenbaum, "In vivo imaging of the immune response in the eye," *Seminars in Immunopathology*, vol. 30, no. 2, pp. 179–190, 2008.

[22] R. L. Lindquist, G. Shakhar, D. Dudziak et al., "Visualizing dendritic cell networks in vivo," *Nature Immunology*, vol. 5, no. 12, pp. 1243–1250, 2004.

[23] M. F. Cordeiro, L. Guo, V. Luong et al., "Real-time imaging of single nerve cell apoptosis in retinal neurodegeneration," *Proceedings of the National Academy of Sciences of the United States of America*, vol. 101, no. 36, pp. 13352–13356, 2004.

[24] A. Roorda, Y. Zhang, and J. L. Duncan, "High-resolution in vivo imaging of the RPE mosaic in eyes with retinal disease," *Investigative Ophthalmology and Visual Science*, vol. 48, no. 5, pp. 2297–2303, 2007.

[25] J. A. Martin and A. Roorda, "Direct and noninvasive assessment of parafoveal capillary leukocyte velocity," *Ophthalmology*, vol. 112, no. 12, pp. 2219–2224, 2005.

[26] A. S. Vilupuru, N. V. Rangaswamy, L. J. Frishman, E. L. Smith, R. S. Harwerth, and A. Roorda, "Adaptive optics scanning laser ophthalmoscopy for in vivo imaging of lamina cribrosa," *Journal of the Optical Society of America A*, vol. 24, no. 5, pp. 1417–1425, 2007.

[27] J. K. Willmann, N. van Bruggen, L. M. Dinkelborg, and S. S. Gambhir, "Molecular imaging in drug development," *Nature Reviews Drug Discovery*, vol. 7, no. 7, pp. 591–607, 2008.

[28] E. D. Agdeppa and M. E. Spilker, "A review of imaging agent development," *AAPS Journal*, vol. 11, no. 2, pp. 286–299, 2009.

Hindawi Publishing Corporation
Journal of Ophthalmology
Volume 2012, Article ID 279037, 6 pages
doi:10.1155/2012/279037

Review Article

Leukocyte Adhesion Molecules in Diabetic Retinopathy

Kousuke Noda,[1,2] Shintaro Nakao,[3] Susumu Ishida,[1,2] and Tatsuro Ishibashi[3]

[1] *Laboratory of Ocular Cell Biology and Visual Science, Hokkaido University Graduate School of Medicine, N-15, W-7, Kita-ku, Sapporo 060-8638, Japan*
[2] *Department of Ophthalmology, Hokkaido University Graduate School of Medicine, N-15, W-7, Kita-ku, Sapporo 060-8638, Japan*
[3] *Department of Ophthalmology, Graduate School of Medical Sciences, Kyushu University, Fukuoka 812-8582, Japan*

Correspondence should be addressed to Kousuke Noda, nodako@med.hokudai.ac.jp

Received 13 August 2011; Accepted 24 September 2011

Academic Editor: Ofra Benny

Diabetes is a systemic disease that causes a number of metabolic and physiologic abnormalities. One of the major microvascular complications of diabetes is diabetic retinopathy (DR), a leading cause of blindness in people over age 50. The mechanisms underlying the development of DR are not fully understood; however, extensive studies have recently implicated chronic, low-grade inflammation in the pathophysiology of DR. During inflammation leukocytes undergo sequential adhesive interactions with endothelial cells to migrate into the inflamed tissues, a process known as the "leukocyte recruitment cascade" which is orchestrated by precise adhesion molecule expression on the cell surface of leukocytes and the endothelium. This paper summarizes the recent clinical and preclinical works on the roles of leukocyte adhesion molecules in DR.

1. Introduction

Inflammation is a nonspecific, defensive response of the body to tissue injury in which leukocytes are recruited to inflamed tissues. In acute inflammation, leukocytes clear away invading agents and degrade necrotized tissue components, generally contributing to tissue repair. However, if inflammation persists chronically, leukocytes can damage tissues by prolonged secretion of chemical mediators and toxic oxygen radicals. There is an accumulating body of evidence showing that leukocytes play a significant role in the pathogenesis of a number of vision-threatening retinal diseases, such as glaucoma, age-related macular degeneration, and diabetic retinopathy (DR) [1]. This paper will present important findings from the growing amount of research on inflammation specifically in relation to DR.

DR is one of the main microvascular complications of diabetes and one of the most common causes of blindness in people over age 50. Recent studies have elucidated that chronic, low-grade inflammation underlies much of the vascular complications of DR [2, 3]. Microscopic inflammatory responses, such as vessel dilation, vascular leakage, and leukocyte recruitment, occur in the diabetic retina and are implicated in the development of DR [4].

For instance, leukocyte adhesion molecules are upregulated in the vessels of the diabetic retina and choroid, and consequently inflammatory cells accumulate in the chorioretinal tissues [5]. Indeed, extensive accumulation of polymorphonuclear leukocytes has been observed in the lumen of microaneurysms, a cause of retinal vascular leakage, in human type 1 diabetic subjects [6, 7]. Correlations between elevated numbers of accumulated leukocytes and capillary damage have been shown in postmortem DR patients [6] and in spontaneously diabetic monkeys [8]. Preclinical studies using animal models of early DR have also revealed that leukocytes adhering to the endothelium damage endothelial cells and increase the vascular permeability of retinal vessels [9, 10]. Leukocytes have also been shown to be present in fibrovascular membranes, a characteristic feature of the pathologic changes associated with proliferative diabetic retinopathy (PDR) [11]. It has been furthermore reported that T lymphocytes infiltrate the fibrovascular membrane [12] and that this infiltration correlates well with the severity of retinopathy and poor visual prognosis [13]. Taken together, these lines of evidence indicate that leukocytes disrupt the homeostasis of the vasculature and facilitate proliferative damage in DR.

The following sections describe the leukocyte recruitment cascade, which is regulated by a series of adhesion molecules, and present the emerging findings regarding the adhesion molecules specifically involved in DR.

2. Leukocyte Recruitment Cascade

The recruitment of leukocytes from circulating blood into tissues is crucial for the inflammatory response. During the process, a number of well-studied adhesion molecules on the endothelium sequentially interact with their ligands expressed on the cell surface of leukocytes. The interaction between adhesion molecules and ligands occurs in a cascade-like fashion, guiding leukocytes from the circulation to the extravascular space, that is, through the steps of leukocyte rolling, firm adhesion, and transmigration (Figure 1).

The selectin family of adhesion molecules mediates the capture and rolling steps of leukocytes along the endothelial cells. The selectins consist of three members of C-type lectins: P-, E-, and L-selectin [14]. P-selectin, stored in the granules of endothelial cells and platelets, translocates rapidly to the cell surface in response to several inflammatory stimuli. Whereas all of the selectins bind to sialyl-Lewis X carbohydrate ligands, such as P-selectin glycoprotein ligand-1 (PSGL-1), interaction between P-selectin and PSGL-1 is responsible for a major part of the leukocyte rolling in inflammation [15]. E-selectin, a heavily glycosylated transmembrane protein, is present exclusively in endothelial cells and is increased by stimulation of representative inflammatory cytokines, such as tumor necrosis factor- (TNF-) α and interleukin- (IL-) 1β [16]. These inflammatory cytokines are also reported to induce the expression of P-selectin on the endothelium [17, 18]. L-selectin is expressed on many subclasses of leukocytes [14] and binds to endothelial ligands containing sulfated sialyl Lewis X [19].

After the selectins have initiated leukocyte rolling along the surface of the endothelium, a different set of adhesion molecules comes into play to reduce the leukocyte-rolling velocity and allow the leukocytes to firmly adhere to the endothelial surface. This firm adhesion step is largely mediated by molecules of the immunoglobulin superfamily, such as intercellular adhesion molecule- (ICAM-) 1 and vascular cell adhesion molecule- (VCAM-) 1, expressed on endothelial cells and by those of the integrin family expressed constitutively on leukocytes as well as on many other types of cells. The principal integrins that bind to endothelial ICAM-1 are LFA-1 (CD11a/CD18) and Mac-1 (CD11b/CD18), while VLA-4 (CD49d/CD29) is the integrin that binds to endothelial VCAM-1 [20]. Recent studies have revealed that the binding of selectins to PSGL-1 increase the affinity of LFA1 to ICAM-1, indicating that rolling step facilitates the next events, leukocyte adhesion to the endothelial surface [21].

Upon achievement of stable adhesion to the endothelial surface, the leukocytes extravasate between endothelial cells along the intercellular junctions. Platelet endothelial cell adhesion molecule- (PECAM-)1 is an immunoglobulin superfamily member expressed at endothelial cell-cell junctions that mediates this leukocyte transmigration, particularly that of monocytes and neutrophils. In addition, vascular adhesion protein- (VAP-) 1, a 170 kDa homodimeric sialylated glycoprotein, is an endothelial adhesion molecule regulating the transmigration step of lymphocytes, monocytes, and polymorphonuclear leukocytes. VAP-1 was originally discovered in inflamed synovial vessels [22], and; thereafter, it was revealed that it is also expressed on the vascular endothelial cells in tissues such as skin, brain, lung, liver, and heart [23–26]. In ocular tissues, VAP-1 was detected on the endothelial cells of retinal and choroidal vessels [27–29].

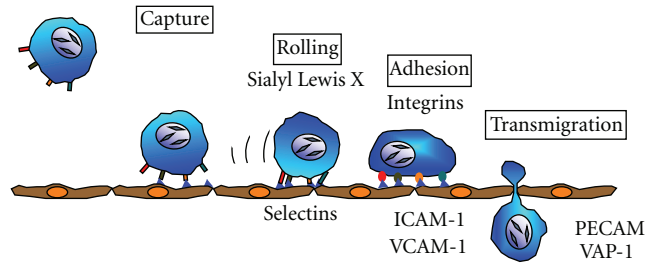

Figure 1: Leukocyte recruitment to the vessel wall.

3. Leukocyte Adhesion Molecules in Diabetic Retinopathy

Clinically, DR is divided into two stages based on the proliferative status of the retinal vasculature: the non-proliferative stage (NPDR) and the proliferative stage (PDR). In NPDR, the early stage of DR, the development of retinopathy begins with vascular lesions that involve pericyte loss, basement membrane thickening, capillary microaneurysms, and obliteration of capillaries [11]. The obliterated capillaries reduce the amount of retinal perfusion and, therefore, lead to ischemic changes in the diabetic retina. This ischemia causes neovascularization in the retina and/or the optic disk. PDR, the later stage of DR, is characterized by retinal neovascularization associated with the formation of a fibrovascular membrane at the vitreoretinal interface. Tractional change against the fibrovascular membrane leads to further severe complications, such as vitreous hemorrhage and tractional and/or rhegmatogenous retinal detachments. Clinical and preclinical studies have provided evidence that leukocyte adhesion molecules play a significant role during both stages of DR.

4. Selectins

The data regarding the role of the selectin family specifically in the retinal vessels in DR turns out to be rather intriguing, especially in light of the selectin family's generally known responsibility for leukocyte rolling as described above. Reports show, for instance, that P-selectin is upregulated in

the choroidal vessels of diabetic patients, but it is not upregulated in their retinal vessels [5]. Moreover, E-selectin has not been detected in the chorioretinal tissues of either diabetic or nondiabetic patients [5]. On the leukocyte side, a significant decrease in the amount of surface L-selectin expression has been observed in patients with diabetic microangiopathy in comparison with diabetic patients without microangiopathic complications and healthy controls [30].

The reason for this pattern of diminished selectin expression on the leukocytes and endothelial cells in DR might be due to the specific nature of the inflammation in DR, that is, in its chronic, low-grade nature. It is known, for instance, that selectins are removed from the cell surface of leukocytes and endothelia through proteolytic shedding during inflammation [31], and this seems to be what is occurring under the longstanding and subclinical inflammatory conditions of DR. Indeed, elevated serum levels of soluble adhesion molecules have been reported in patients with DR; the serum level of soluble E-selectin, for example, is reportedly increased in patients with diabetes [32, 33] and correlates with the progression of DR [34, 35]. It has also been demonstrated that patients with PDR show higher serum levels of soluble P-selectin [36].

As for the mechanisms, it has been reported that a disintegrin and metalloproteinase (ADAM) 8, one of the major ectodomain shedding proteinases, is upregulated during pathological neovascularization, and its overexpression facilitates the shedding of E-selectin [37]. Similarly, during inflammation, L-selectin is shed by ADAM17, which is upregulated in response to inflammatory stimulation [38, 39].

In the vitreous, the level of soluble E-selectin was considerably higher in subjects with PDR [40]. Furthermore, vitreous levels of soluble E-selectin in eyes with PDR complicated by traction retinal detachment were significantly increased in comparison with the eyes with vitreous hemorrhage alone [41]. Interestingly, it has been shown that soluble E-selectin stimulates retinal capillary endothelial cell migration [42] and promotes angiogenesis through a sialyl-Lewis-X-dependent mechanism [43].

Accordingly, these various lines of evidence indicate that the shedding of selectins is enhanced on the endothelium during the progression of diabetes and that the soluble form of selectin proteins has the potential to be a clinically useful biomarker of the severity of DR; E-selectin, in particular, may also serve as a proangiogenic factor.

5. ICAM-1

While the selectin expression on leukocytes and endothelial cells appears low in DR, other molecules may be compensating for the adhesion gaps. Several studies, for instance, suggest that ICAM-1 and its binding partners are operative in DR and may serve as potential targets for therapeutic interventions. Indeed, ICAM-1 is found to be highly expressed in the blood vessels of the retina, choroid and fibrovascular membrane in patients with diabetes [5, 44], and its expression correlates with the number of migrated neutrophils in the retina and choroid of these patients [5], indicating that elevated ICAM-1 facilitates leukocyte recruitment and the vascular complications in DR. In accord with these clinical observations, ICAM-1 is increased in the retinal vessels in an animal model of DR, and blockade of ICAM-1 attenuated leukostasis, endothelial cell death, and vascular leakage in the retinal vessels of the diabetic animals [10].

Not only ICAM-1 but also LFA-1 (CD11a/CD18) and Mac-1 (CD11b/CD18) ligands for ICAM-1 are upregulated in patients with diabetes. The β-integrin subunit CD18 is increased in patients with DR [45], and likewise significant increases in α-integrin subunits CD11a [46] and CD11b [30] are found in these patients. Consequently, these data indicate that ICAM-1 and its ligands are important and interruption of either component of the integrin-ICAM-1 interaction may be beneficial in preventing the deterioration of DR. However, it was also reported that the effect of ICAM-1 depletion was limited to prevent angiogenesis in oxygen-induced retinopathy model [47]. Further investigation is still required to elucidate the role of integrin-ICAM-1 interaction in DR.

6. VCAM-1

Similar to ICAM-1, a role for endothelial VCAM-1 in DR is also emerging, although there has not been as much research conducted on VCAM-1 as with ICAM-1. Before its potential role in DR was examined, it first came to light that VCAM-1 had been involved in the macrovascular complications of diabetes [48]; however, it has since been revealed that the interaction of VCAM-1 with its ligand, integrin VLA-4, is important in the development of DR. For instance, it has been demonstrated in an animal model of DR that hyperglycemia upregulates VCAM-1 expression in the retinal vessels [49]. Also, in an animal model of early DR, it has been found that VLA-4-mediated leukocyte adhesion to the retinal vessels is significantly increased, and blockade of VLA-4 attenuates vascular leakage and production of inflammatory cytokines [50].

In addition, increased serum levels of soluble VCAM-1 have been found in type 2 diabetic patients with microvascular complications, similar to E-selectin [32], and levels of soluble VCAM-1 are elevated in the vitreous of DR patients as well [40, 41]. Notably, it has been shown that soluble VCAM-1 acts on endothelial cells as an angiogenic factor through a VLA-4-dependent mechanism, in common with E-selectin [42, 43], suggesting that blockade of both soluble adhesion molecules, soluble forms of E-selectin and VCAM-1, could have a beneficial effect on DR.

7. VAP-1

Along with ICAM-1, VAP-1 seems also to be a key player in the inflammation associated with DR, as demonstrated through several lines of evidence. Blockade of VAP-1, for example, significantly reduces the transmigration and/or capillary entrapment of leukocytes in the retina in an

animal model of DR [51]. Transmigrated leukocytes under pathological conditions are thought to play an important role in neovascularization through secretion of VEGF [52]. Furthermore, leukocytes firmly adhering to capillary endothelial cells induce apoptotic changes in the endothelial cells [53]. Therefore, VAP-1 seems to be locally involved in the pathogenesis of DR by mediating leukocyte recruitment.

In further support of this conclusion, VAP-1 also exists as a soluble form in plasma, and much attention has recently been paid to the elevated serum concentration of soluble VAP-1 in patients with diabetes [54, 55]. Interestingly, besides its role as an adhesion molecule, VAP-1 has also an enzymatic function as a semicarbazide-sensitive amine oxidase (SSAO), which converts aliphatic primary monoamines to the corresponding aldehydes with the release of hydrogen peroxide and ammonia [56]. Metabolites generated by VAP-1/SSAO, for example, hydrogen peroxide and methylglyoxal from aminoacetone are known to be involved in cellular oxidative stress and advanced glycation end-product formation, both of which are crucial for the pathogenesis of diabetic retinopathy [57, 58]. Therefore, it seems likely that soluble VAP-1 in the serum and vitreous may promote vascular complications in DR. In fact, patients with DR display significantly higher plasma VAP-1/SSAO activities compared to patients without DR [55]. Further investigation using human ocular samples may aid in a better understanding of the role of VAP-1 in DR.

8. Conclusions

The pathogenesis of DR is not entirely known. However, based on the preceding discussion, growing evidence supports a role for leukocytes and their adhesion molecules in the development of DR. In addition, soluble adhesion molecules may contribute to DR by acting as angiogenic factors or enzymes. Specific inhibition of leukocyte adhesion molecules could be of therapeutic value for diabetic patients.

References

[1] H. Xu, M. Chen, and J. V. Forrester, "Para-inflammation in the aging retina," *Progress in Retinal and Eye Research*, vol. 28, no. 5, pp. 348–368, 2009.

[2] D. A. Antonetti, A. J. Barber, S. K. Bronson et al., "Diabetic retinopathy: seeing beyond glucose-induced microvascular disease," *Diabetes*, vol. 55, no. 9, pp. 2401–2411, 2006.

[3] T. W. Gardner, D. A. Antonetti, A. J. Barber, K. F. LaNoue, and S. W. Levison, "Diabetic retinopathy: more than meets the eye," *Survey of Ophthalmology*, vol. 47, supplement 2, pp. S253–S262, 2002.

[4] A. P. Adamis and A. J. Berman, "Immunological mechanisms in the pathogenesis of diabetic retinopathy," *Seminars in Immunopathology*, vol. 30, no. 2, pp. 65–84, 2008.

[5] D. S. McLeod, D. J. Lefer, C. Merges, and G. A. Lutty, "Enhanced expression of intracellular adhesion molecule-1 and P-selectin in the diabetic human retina and choroid," *American Journal of Pathology*, vol. 147, no. 3, pp. 642–653, 1995.

[6] G. A. Lutty, J. Cao, and D. S. McLeod, "Relationship of polymorphonuclear leukocytes to capillary dropout in the human diabetic choroid," *American Journal of Pathology*, vol. 151, no. 3, pp. 707–714, 1997.

[7] A. W. Stitt, T. A. Gardiner, and D. B. Archer, "Histological and ultrastructural investigation of retinal microaneurysm development in diabetic patients," *British Journal of Ophthalmology*, vol. 79, no. 4, pp. 362–367, 1995.

[8] S. Y. Kim, M. A. Johnson, D. S. McLeod, T. Alexander, B. C. Hansen, and G. A. Lutty, "Neutrophils are associated with capillary closure in spontaneously diabetic monkey retinas," *Diabetes*, vol. 54, no. 5, pp. 1534–1542, 2005.

[9] A. M. Joussen, V. Poulaki, N. Mitsiades et al., "Suppression of Fas-FasL-induced endothelial cell apoptosis prevents diabetic blood-retinal barrier breakdown in a model of streptozotocin-induced diabetes," *The FASEB Journal*, vol. 17, no. 1, pp. 76–78, 2003.

[10] K. Miyamoto, S. Khosrof, S. E. Bursell et al., "Prevention of leukostasis and vascular leakage in streptozotocin-induced diabetic retinopathy via intercellular adhesion molecule-1 inhibition," *Proceedings of the National Academy of Sciences of the United States of America*, vol. 96, no. 19, pp. 10836–10841, 1999.

[11] M. Yanoff and B. S. Fine, *Ocular Pathology*, Mosby-Wolfe, London, UK, 1996.

[12] S. Tang and K. C. Le-Ruppert, "Activated T lymphocytes in epiretinal membranes from eyes of patients with proliferative diabetic retinopathy," *Graefe's Archive for Clinical and Experimental Ophthalmology*, vol. 233, no. 1, pp. 21–25, 1995.

[13] S. Kase, W. Saito, S. Ohno, and S. Ishida, "Proliferative diabetic retinopathy with lymphocyte-rich epiretinal membrane associated with poor visual prognosis," *Investigative Ophthalmology & Visual Science*, vol. 50, no. 12, pp. 5909–5912, 2009.

[14] K. Ley, "Functions of selectins," *Results and Problems in Cell Differentiation*, vol. 33, pp. 177–200, 2001.

[15] R. P. McEver, "Selectins: lectins that initiate cell adhesion under flow," *Current Opinion in Cell Biology*, vol. 14, no. 5, pp. 581–586, 2002.

[16] C. W. Wyble, K. L. Hynes, J. Kuchibhotla, B. C. Marcus, D. Hallahan, and B. L. Gewertz, "TNF-α and IL-1 upregulate membrane-bound and soluble E-selectin through a common pathway," *Journal of Surgical Research*, vol. 73, no. 2, pp. 107–112, 1997.

[17] N. A. Essani, M. A. Fisher, C. A. Simmons, J. L. Hoover, A. Farhood, and H. Jaeschke, "Increased P-selectin gene expression in the liver vasculature and its role in the pathophysiology of neutrophil-induced liver injury in murine endotoxin shock," *Journal of Leukocyte Biology*, vol. 63, no. 3, pp. 288–296, 1998.

[18] A. Weller, S. Isenmann, and D. Vestweber, "Cloning of the mouse endothelial selectins. Expression of both E- and P-selectin is inducible by tumor necrosis factor α," *Journal of Biological Chemistry*, vol. 267, no. 21, pp. 15176–15183, 1992.

[19] N. C. Kaneider, A. J. Leger, and A. Kuliopulos, "Therapeutic targeting of molecules involved in leukocyte-endothelial cell interactions," *FEBS Journal*, vol. 273, no. 19, pp. 4416–4424, 2006.

[20] H. Ulbrich, E. E. Eriksson, and L. Lindbom, "Leukocyte and endothelial cell adhesion molecules as targets for therapeutic interventions in inflammatory disease," *Trends in Pharmacological Sciences*, vol. 24, no. 12, pp. 640–647, 2003.

[21] N. Hogg, I. Patzak, and F. Willenbrock, "The insider's guide to leukocyte integrin signalling and function," *Nature Reviews Immunology*, vol. 11, no. 6, pp. 416–426, 2011.

[22] M. Salmi and S. Jalkanen, "A 90-kilodalton endothelial cell molecule mediating lymphocyte binding in humans," *Science*, vol. 257, no. 5075, pp. 1407–1409, 1992.

[23] E. Akin, J. Aversa, and A. C. Steere, "Expression of adhesion molecules in synovia of patients with treatment-resistant lyme arthritis," *Infection and Immunity*, vol. 69, no. 3, pp. 1774–1780, 2001.

[24] K. Jaakkola, S. Jalkanen, K. Kaunismäki et al., "Vascular adhesion protein-1, intercellular adhesion molecule-1 and P-selectin mediate leukocyte binding to ischemic heart in humans," *Journal of the American College of Cardiology*, vol. 36, no. 1, pp. 122–129, 2000.

[25] M. Salmi, K. Kalimo, and S. Jalkanen, "Induction and function of vascular adhesion protein-1 at sites of inflammation," *Journal of Experimental Medicine*, vol. 178, no. 6, pp. 2255–2260, 1993.

[26] B. Singh, T. Tschernig, M. Van Griensven, A. Fieguth, and R. Pabst, "Expression of vascular adhesion protein-1 in normal and inflamed mice lungs and normal human lungs," *Virchows Archiv*, vol. 442, no. 5, pp. 491–495, 2003.

[27] L. Almulki, K. Noda, S. Nakao, T. Hisatomi, K. L. Thomas, and A. Hafezi-Moghadam, "Localization of vascular adhesion protein-1 (VAP-1) in the human eye," *Experimental Eye Research*, vol. 90, no. 1, pp. 26–32, 2010.

[28] K. Noda, S. Miyahara, T. Nakazawa et al., "Inhibition of vascular adhesion protein-1 suppresses endotoxin-induced uveitis," *The FASEB Journal*, vol. 22, no. 4, pp. 1094–1103, 2008.

[29] K. Noda, H. She, T. Nakazawa et al., "Vascular adhesion protein-1 blockade suppresses choroidal neovascularization," *The FASEB Journal*, vol. 22, no. 8, pp. 2928–2935, 2008.

[30] K. Mastej and R. Adamiec, "Neutrophil surface expression of CD11b and CD62L in diabetic microangiopathy," *Acta Diabetologica*, vol. 45, no. 3, pp. 183–190, 2008.

[31] D. M. Smalley and K. Ley, "L-selectin: mechanisms and physiological significance of ectodomain cleavage," *Journal of Cellular and Molecular Medicine*, vol. 9, no. 2, pp. 255–266, 2005.

[32] K. Matsumoto, Y. Sera, Y. Ueki, G. Inukai, E. Niiro, and S. Miyake, "Comparison of serum concentrations of soluble adhesion molecules in diabetic microangiopathy and macroangiopathy," *Diabetic Medicine*, vol. 19, no. 10, pp. 822–826, 2002.

[33] S. S. Soedamah-Muthu, N. Chaturvedi, C. G. Schalkwijk, C. D. Stehouwer, P. Ebeling, and J. H. Fuller, "Soluble vascular cell adhesion molecule-1 and soluble E-selectin are associated with micro- and macrovascular complications in Type 1 diabetic patients," *Journal of Diabetes and its Complications*, vol. 20, no. 3, pp. 188–195, 2006.

[34] M. Nowak, T. Wielkoszyński, B. Marek et al., "Blood serum levels of vascular cell adhesion molecule (sVCAM-1), intercellular adhesion molecule (sICAM-1) and endothelial leucocyte adhesion molecule-1 (ELAM-1) in diabetic retinopathy," *Clinical and Experimental Medicine*, vol. 8, no. 3, pp. 159–164, 2008.

[35] A. M. Spijkerman, M. A. Gall, L. Tarnow et al., "Endothelial dysfunction and low-grade inflammation and the progression of retinopathy in Type 2 diabetes," *Diabetic Medicine*, vol. 24, no. 9, pp. 969–976, 2007.

[36] C. Gustavsson, E. Agardh, B. Bengtsson, and C. D. Agardh, "TNF-α is an independent serum marker for proliferative retinopathy in type 1 diabetic patients," *Journal of Diabetes and its Complications*, vol. 22, no. 5, pp. 309–316, 2008.

[37] V. H. Guaiquil, S. Swendeman, W. Zhou et al., "ADAM8 is a negative regulator of retinal neovascularization and of the growth of heterotopically injected tumor cells in mice," *Journal of Molecular Medicine*, vol. 88, no. 5, pp. 497–505, 2010.

[38] A. Chalaris, N. Adam, C. Sina et al., "Critical role of the disintegrin metalloprotease ADAM17 for intestinal inflammation and regeneration in mice," *Journal of Experimental Medicine*, vol. 207, no. 8, pp. 1617–1624, 2010.

[39] J. Scheller, A. Chalaris, C. Garbers, and S. Rose-John, "ADAM17: a molecular switch to control inflammation and tissue regeneration," *Trends in Immunology*, vol. 32, no. 8, pp. 380–387, 2011.

[40] J. Adamiec-Mroczek, J. Oficjalska-Młyńczak, and M. Misiuk-Hojło, "Proliferative diabetic retinopathy-The influence of diabetes control on the activation of the intraocular molecule system," *Diabetes Research and Clinical Practice*, vol. 84, no. 1, pp. 46–50, 2009.

[41] G. A. Limb, J. Hickman-Casey, R. D. Hollifield, and A. H. Chignell, "Vascular adhesion molecules in vitreous from eyes with proliferative diabetic retinopathy," *Investigative Ophthalmology and Visual Science*, vol. 40, no. 10, pp. 2453–2457, 1999.

[42] J. A. Olson, C. M. Whitelaw, K. C. McHardy, D. W. Pearson, and J. V. Forrester, "Soluble leucocyte adhesion molecules in diabetic retinopathy stimulate retinal capillary endothelial cell migration," *Diabetologia*, vol. 40, no. 10, pp. 1166–1171, 1997.

[43] A. E. Koch, M. M. Halloran, C. J. Haskell, M. R. Shah, and P. J. Polverini, "Angiogenesis mediated by soluble forms of E-selectin and vascular cell adhesion molecule-1," *Nature*, vol. 376, no. 6540, pp. 517–519, 1995.

[44] H. P. Heidenkummer and A. Kampik, "Intercellular adhesion molecule-1 (ICAM-1) and leukocyte function-associated antigen-1 (LFA-1) expression in human epiretinal membranes," *Graefe's Archive for Clinical and Experimental Ophthalmology*, vol. 230, no. 5, pp. 483–487, 1992.

[45] H. Song, L. Wang, and Y. Hui, "Expression of CD18 on the neutrophils of patients with diabetic retinopathy," *Graefe's Archive for Clinical and Experimental Ophthalmology*, vol. 245, no. 1, pp. 24–31, 2007.

[46] A. Kretowski, J. Myśliwiec, and I. Kinalska, "The alterations of CD11A expression on peripheral blood lymphocytes/monocytes and CD62L expression on peripheral blood lymphocytes in Graves' disease and type 1 diabetes," *Roczniki Akademii Medycznej w Bialymstoku (1995)*, vol. 44, pp. 151–159, 1999.

[47] N. Kociok, S. Radetzky, T. U. Krohne et al., "ICAM-1 depletion does not alter retinal vascular development in a model of oxygen-mediated neovascularization," *Experimental Eye Research*, vol. 89, no. 4, pp. 503–510, 2009.

[48] J. L. Wautier and M. P. Wautier, "Blood cells and vascular cell interactions in diabetes," *Clinical Hemorheology and Microcirculation*, vol. 25, no. 2, pp. 49–53, 2001.

[49] C. Gustavsson, C. D. Agardh, A. V. Zetterqvist, J. Nilsson, E. Agardh, and M. F. Gomez, "Vascular cellular adhesion molecule-1 (VCAM-1) expression in mice retinal vessels is affected by both hyperglycemia and hyperlipidemia," *PLoS One*, vol. 5, no. 9, Article ID e12699, pp. 1–12, 2010.

[50] E. Iliaki, V. Poulaki, N. Mitsiades, C. S. Mitsiades, J. W. Miller, and E. S. Gragoudas, "Role of α4 integrin (CD49d) in the pathogenesis of diabetic retinopathy," *Investigative Ophthalmology and Visual Science*, vol. 50, no. 10, pp. 4898–4904, 2009.

[51] K. Noda, S. Nakao, S. Zandi, V. Engelstädter, Y. Mashima, and A. Hafezi-Moghadam, "Vascular adhesion protein-1 regulates

leukocyte transmigration rate in the retina during diabetes," *Experimental Eye Research*, vol. 89, no. 5, pp. 774–781, 2009.

[52] S. Tazzyman, C. E. Lewis, and C. Murdoch, "Neutrophils: key mediators of tumour angiogenesis," *International Journal of Experimental Pathology*, vol. 90, no. 3, pp. 222–231, 2009.

[53] A. M. Joussen, T. Murata, A. Tsujikawa, B. Kirchhof, S. E. Bursell, and A. P. Adamis, "Leukocyte-mediated endothelial cell injury and death in the diabetic retina," *American Journal of Pathology*, vol. 158, no. 1, pp. 147–152, 2001.

[54] H. Garpenstrand, J. Ekblom, L. B. Bäcklund, L. Oreland, and U. Rosenqvist, "Elevated plasma semicarbazide-sensitive amine oxidase (SSAO) activity in Type 2 diabetes mellitus complicated by retinopathy," *Diabetic Medicine*, vol. 16, no. 6, pp. 514–521, 1999.

[55] J. L. Grönvall-Nordquist, L. B. Bäcklund, H. Garpenstrand et al., "Follow-up of plasma semicarbazide-sensitive amine oxidase activity and retinopathy in Type 2 diabetes mellitus," *Journal of Diabetes and its Complications*, vol. 15, no. 5, pp. 250–256, 2001.

[56] D. J. Smith and P. J. Vainio, "Targeting vascular adhesion protein-1 to treat autoimmune and inflammatory diseases," *Annals of the New York Academy of Sciences*, vol. 1110, pp. 382–388, 2007.

[57] M. Bourajjaj, C. D. Stehouwer, V. W. Van Hinsbergh, and C. G. Schalkwijk, "Role of methylglyoxal adducts in the development of vascular complications in diabetes mellitus," *Biochemical Society Transactions*, vol. 31, no. 6, pp. 1400–1402, 2003.

[58] E. A. Ellis, D. L. Guberski, M. Somogyi-Mann, and M. B. Grant, "Increased H_2O_2, vascular endothelial growth factor and receptors in the retina of the BBZ/WOR diabetic rat," *Free Radical Biology and Medicine*, vol. 28, no. 1, pp. 91–101, 2000.